Heliyon 10 (2024) e26254

Contents lists available at ScienceDirect

Heliyon

journal homepage: www.cell.com/heliyon

Research article

# Techno-economic and environmental assessments of optimal planning of waste-to-energy based CHP-DG considering load growth on a power distribution network

Moshood Akanni Alao *, Olawale Mohammed Popoola

*Department of Electrical Engineering & Centre for Energy and Electric Power, Tshwane University of Technology, Pretoria, South Africa*

ARTICLE INFO

*Keywords:*
Biogas
Food waste
Distributed generation planning
Improved PSO
Internal combustion engine
Fuel cells

ABSTRACT

Load growth puts pressure on existing electric infrastructure and impacts on the system's performance parameters which may necessitate network expansion. Conventionally, electric network expansion is done by building new substations or reinforcing the existing ones with new transformers and upgrading the network feeders. However, optimal allocation of combined heat and power distributed generators (CHP-DGs) on distribution networks (DNs) can be adopted for network expansion planning problem. Optimal DG allocation is an optimisation problem which requires an efficient optimisation approach. In this paper, an improved particle swarm optimisation (IPSO) based on weighted randomised acceleration coefficient and adaptive inertia weight is proposed for optimal DG allocation problem. The considered CHP-DGs include internal combustion engine (ICE) and fuel cells (FCs) powered by biogas obtained from anaerobic digestion of food wastes. The proposed IPSO is tested on IEEE 69 bus radial distribution network under single and multi-objectives considering constant and mixed seasonal voltage-dependent load models. Some of the key findings show that integrating ICE-based CHP-DGs operating at optimal power factor in winter day mixed voltage dependent load in base year achieves 97.63 % active power loss reduction in comparison to 77.14 % loss reduction for unity power factor operating FC-based CHP-DG. Economic and environmental evaluation indicate that FC-based CHP-DG records a net present value of over 29.29 million $, levelised cost of energy of 0.0493 $/kWh and zero pollutant emission in comparison with 28.40 million $, 0.0501 $/kWh and 0.2817 million kg pollutant emission for ICE-based CHP-DG over the planning horizon. In comparison with the standard PSO, the proposed IPSO performs better in terms of solution quality, convergence speed and statistical results.

## 1. Introduction

Reserve's depletion and fluctuating prices of fossil fuels as well as emissions of greenhouse gases from their combustion are serious environmental and sustainability issues for thermal power plants. Another fundamental issue of local and global concern is the proliferation of municipal solid wastes (MSW). Conventional MSW management such as open burning, dumping and centralised landfill sites are environmentally and socially unfriendly as a lot of health-related issues occur due to air, water, and land pollution. In the face of these environmental issues, countries worldwide are looking forward to using more efficient and environmentally friendly

* Corresponding author.
*E-mail addresses:* 220417476@tut4life.ac.za (M. Akanni Alao), popoolao@tut.ac.za (O. Mohammed Popoola).

https://doi.org/10.1016/j.heliyon.2024.e26254
Received 9 September 2023; Received in revised form 2 February 2024; Accepted 8 February 2024
Available online 16 February 2024

**Nomenclature**

| | |
|---|---|
| AD | Anaerobic digestion |
| MSW | Municipal solid waste |
| EDSEP | Electric distribution system expansion program |
| DISCOs | Distribution companies |
| DGs | Distributed generators |
| EDNs | Electric distribution networks |
| CHP | Combined heat and power |
| DER | Distributed energy resource |
| ICE | Internal combustion engine |
| FCs | Fuel cells |
| NPV | Net present value ($) |
| LCOE | Levelised cost of energy ($/kWh) |
| MC | Unit maintenance cost ($/kWh) |
| $OC^{CHP}$ | Operating cost ($) |
| IC | Unit investment cost ($/kW) |
| PSO | Particle swarm optimisation |
| FW | Food waste |
| HPR | Heat-to-power ratio |
| $V_{CH_4}$ | Gross volume of methane extractable per kg of FW ($m^3$) |
| $\not{c}$ | Fraction of FW that does not decompose in the digester |
| $F_{ORG(t)}$ | Amount of FW (kg) treated in year |
| $V_{CH_4A(t)}$ | Actual quantity of methane (biogas) produced in a specific year t ($m^3$) |
| $V_{CH_4P(t)}$ | Purified biogas (bio-methane) ($m^3$) |
| $\Omega$ | Extent of biogas purification (%) |
| $D_{bio-methane}$ | Density of purified biogas ($kg/m^3$) |
| $\dot{m}_{H_2(t)}$ | Mass of hydrogen gas produced through reforming process (kg) |
| $\eta_{sys}$ | Total efficiency of reforming process (%) |
| $\eta_{comp}$ | Compression efficiency (%) |
| $H_{2d}$ | Density of compressed hydrogen ($kg/m^3$) |
| $LHV_{H_2}$ | Lower heating value of hydrogen (MJ/kg) |
| $\eta_{FC}$ | Electrical efficiency of fuel cell (%) |
| $\theta$ | Conversion factor from MJ to kWh |
| $P_{gFC(t)}$ | Gross capacity of FC (kW) in year t |
| $P_{FC(t)}$ | Actual capacity of FC (kW) in year t |
| $\eta_{inverter}$ | Inverter efficiency (%) |
| $\eta_{ICE}$ | Electrical efficiency of ICE (%) |
| $LHV_{CH_4}$ | Lower heating value of methane ($MJ/m^3$) |
| $P_{ICE(t)}$ | Capacity of ICE (kW) |
| $\alpha$ | Load growth rate (%) |
| $p_{Di,t}$ | Active load demands at bus in year t (kW) |
| $q_{Di,t}$ | Reactive load demands at bus in year t (kVar) |
| $p_{D0i}$ | Initial active load demand at bus of the distribution network in 0th year (kW) |
| $q_{D0i}$ | Initial reactive load demand at bus of the distribution network in 0th year (kVar) |
| $\beta$ | Percentage population growth rates (%) |
| $\gamma$ | Percentage GDP growth rates (%) |
| $\mu$ | Load growth rate controlling factor |
| $dl$ | Demand (load) level |
| $p_{Di,t,dl,s}$ | Active power demand at bus *i* in year t for load level dl and season s (kW) |
| $q_{Di,t,dl,s}$ | Reactive power demand at bus *i* in year t for load level dl and season s (kVar) |
| $P_{Di,t,dl,s}$ | Mixed seasonal voltage dependent active demand at bus *i*, in year t at dl, season s (kW) |
| $Q_{Di,t,dl,s}$ | Mixed seasonal voltage dependent reactive demand at bus *i*, in year t at dl season s (kVar |
| $PL^{CHP}$ | Power loss with CHP allocated (kW) |
| $PL^0$ | Power loss without CHP (kW) |
| $VD^{CHP}$ | Voltage deviation with CHP allocated (p.u) |
| $VD^0$ | Voltage deviation without CHP (p.u) |
| $VSI_{i+1}^{CHP}$ | Voltage stability index with CHP allocated (p.u) |

technologies to produce energy and ~~for~~ managing MSW. Waste-to-energy (WtE) system such as anaerobic digestion (AD) has been acclaimed as a veritable avenue for harvesting renewable energy from wastes. As a renewable energy source (RES), the biogas obtained from AD system can be fed into a prime mover (engine) for firm electrical power generation. The growing trend in technological advancement and rigorous exploitation of renewable energy (RE) resources have made small-scale power generation practicable, and their integration into the distribution networks is now prevalent.

One critical issue of concern to distribution companies (DISCOs) is electric distribution system expansion planning (EDSEP) due to load growth. Conventionally, EDSEP is done by building new substations or reinforcing the existing ones with new transformers and upgrading the network feeders. This additional cost may impose significant financial burdens on the DISCOs. However, the integration of distributed generation (DG) to the present-day electric distribution networks (EDNs) has the capability of addressing the EDSEP problem. The benefits of integrating DGs to the distribution networks span across technical, economic and environmental. Some of the technical benefits are reduction of the system power losses, improvement of the system voltage profile, enhancement of the power quality as well as the system's reliability improvement [1]. Due to their location being close or at the load centre, DGs can reduce the cost of transmitting or distributing power to the consumers, lessen the load demand on the network and enable deferment or removal of network upgrade investment [2,3]. They also ensure reduction in the operation and maintenance costs of the distribution network [4] as well as environmental emission and noise pollution curtailment [5].

Despite the laudable benefits of using DGs for electric distribution expansion problem, maximum achievement of these merits is subject to optimal planning. An optimal planning scheme involves finding the optimal position, operation, type and size of DG [6] to be connected to EDN, considering various consumer types such as residential, commercial and industrial [7], load growth, and seasonal variation in load consumption while satisfying and maintaining the network constraints.

| | |
|---|---|
| $VSI_{i+1}^{0}$ | Voltage stability index without CHP allocated (p.u) |
| $V_{min}$ | Minimum bus voltage (p.u) |
| $V_{max}$ | Maximum bus voltage (p.u) |
| $P_{t,k}^{CHP}$ | Total optimal active power allocated CHP units k in year t (kW) |
| $Q_{k,t}^{CHP}$ | Total optimal reactive power allocated CHP units k in year t (kVar) |
| $P_{Li,t}$ | Active power loss in the distribution system (kW) |
| $Q_{Li,t}$ | Reactive power loss in the distribution system (kVar) |
| $\lambda$ | Penetration level ratio |
| $P_{\min\ t,k}^{CHP}$ | Minimum active power generated in year t (kW) |
| $P_{\max\ t,k}^{CHP}$ | Maximum active power generated in year t (kW) |
| $Q_{\min\ t,k}^{CHP}$ | Minimum reactive power generated in year t (kVar) |
| $Q_{\max\ t,k}^{CHP}$ | Maximum reactive power generated in year t (kVar) |
| $H_{t,k}^{CHP}$ | Thermal capacity of CHP unit k in year t (kW) |
| $H_{Rk(t)}$ | Thermal power recovered (kW) |
| $\xi$ | Heat recovery efficiency (%) |
| $\eta_{bCHP}$ | Boiler efficiency (%) |
| $\delta_e^{s,dl}$ | Retail cost of electrical energy in season s and load level dl ($/kWh) |
| $\tau_{s,dl}$ | Operating time in season s and load level dl (h) |
| $d$ | Discount rate (%) |
| $\varepsilon_{s,dl}$ | Wholesale price of electricity in season s and load level dl ($/kWh) |
| $\Delta S_{D,t}$ | Yearly apparent load growth (kVA) |
| $UG$ | Yearly upgrade value ($/kVA) |
| $UGC_t$ | Discounted cost of system upgrade in year t ($) |
| $EMC_t^{NoCHP}$ | Emission cost without CHP allocation ($) |
| $EP_p^{grid}$ | Emission potential of pollutants from the upstream grid (kg/kWh) |
| $C_p$ | Cost implication (penalty) for the pollutants ($/kg) |
| $Rev_1^{CHP}$ | Revenue from the sale of electricity ($) |
| $Rev_2^{CHP}$ | Revenue from the sale of heat ($) |
| $Rev^{CHP}$ | Total discounted revenue ($) |
| $C_T^{CHP}$ | Total discounted cost ($) |
| $H_{Sup,t,dl,s}$ | Heat supplied by the CHP after passing through heat recovery system |
| $\delta_h^{s,dl}$ | Retail price of heat energy ($/kWh) |
| $C_P^{CHP}$ | Cost of power purchased from the grid with CHP allocation ($) |
| $C_P^{0}$ | Cost of power purchased without CHP ($) |
| $\Delta P_{CHP}$ | Yearly incremental capacity of CHP added (kW) |
| $F_c$ | Unit fuel cost ($/m$^3$) |
| $\delta^{CHP}$ | Parameter which indicates the mode of operation of the DG |

### 1.1. Literature survey

Based on literature survey, the EDSEP problem in the presence of DG allocation has been investigated by considering timing, problem formulation, solution method, load models, and DG types and numbers. From the standpoint of timing, static and dynamic planning approaches are commonly used. With load growth, DG planning need to incorporate mechanism to handle load growth over the planning horizon. Most importantly is the investment cost of the DG which is expected to change due to the need to increase DG capacity to trail the load growth. Static planning approach involves finding the optimal location and size as well as type of the DG technology to be installed at one instant in time [4,8]. In static planning, the investment cost of DG is determined at the beginning of the project up to the last year of the planning horizon as a one-time cost. Some previous researchers such as [7,9–11] adopted static approach to determine the techno-economic assessment of DG allocation. It is believed that this approach might not be cost effective due to waste of resources at the beginning to few years into the planning period. On the other hand, in dynamic planning approach apart from determining the optimal location and size of the DG technology to be installed, DG's installation year is also optimised [12]. Also in dynamic planning, the investment costs of the DGs changes gradually in a manner according to the load growth until the end of the planning horizon. A few of the previous studies such as [13,14] have applied dynamic approach for optimal planning of DG allocation problem. This approach is deemed to have investment savings and better technical responses [13].

On the part of problem formulation, single and multiple objective functions have been formulated for solving EDSEP. Most commonly used objective functions are minimisation of network power losses, minimisation of DG operating cost, minimisation of environmental emission as well as improvement of voltage profile and reliability of the network. These objective functions can be singly (individually) or simultaneously optimised to create a single or multi-objective problem. From the viewpoint of solution methods for solving the formulated objective function in EDSEP, analytical approaches [15,16], mathematical programming methods [17,18], heuristic, and meta-heuristic [4,19–22] have been adopted. The analytical approach requires short computation time and is easy to apply but requires a lot of assumptions. It is also limited in terms of objective function optimisation as majority of them are applied for single-objective problem such as minimisation of power loss [9]. Mathematical programming techniques, such as linear and non-linear mixed programming require many variables and linearization to simplify the problem formulation. They also have a high computational cost making their application in EDSEP limited especially for large scale network. Heuristic methods and meta-heuristic algorithms on the other hand such as genetic algorithm (GA), particle swarm optimisation (PSO) require few parameters, no simplification of the problem and can guarantee global or near global solutions with relatively limited computation time. Therefore, researchers have taken delight in applying them to solve EDSEP problem.

From the perspective of load models, EDSEP problem has been investigated using different load models such as constant [2,8], voltage dependent [23,24] and time-varying voltage dependent [25] load models. Load model plays an important role in the reliability of results and decisions made for EDSEP. The load demands (active and reactive) at the utility grid are time varying (i.e., hourly or seasonal variation) and dependent on the voltage profile of various consumer types (i.e., residential, commercial and industrial) connected to it. A constant load model is that which assumes that the active and reactive powers of the utility grid to be always constant and independent of the bus voltages. When considering only the voltage dependency of load demands without considering the time-varying nature of load, it is referred to as voltage dependent load model. However, a small modification in voltage dependent load model by incorporating the instantaneous time varying characteristics of loads results in time-varying voltage dependent (TVVD) load models [26]. Since distribution system is the closest to the consumers, it is characterised by non-constant but rather voltage dependent behaviour of consumer loads. Therefore, decisions and results based on the constant load model assumptions for distribution system studies could not be technically feasible. Further explanation is presented in subsequent section. Based on this premise, voltage dependent load model is the most appropriate when solving problems related to EDSEP.

Some researchers have considered single and multiple renewable and non-renewable based DGs for integration into DNs. It has been pointed out that multiple DGs placement is more advantageous compared with single location DG placement in EDSEP [27]. Of note is the use of combined heat and power (CHP) as a DG technology due to its efficiency and resiliency and the capability to produce both electric and heat powers simultaneously. The application of CHP in EDSEP planning has been gaining traction in recent times [28]. Based on the above-mentioned perspectives, some recently published studies in EDSEP involving CHP distributed energy resources (DER) or DGs are briefly discussed in the following paragraphs.

In Ref [29], a modified PSO (MPSO) algorithm is applied to find the optimal size of the CHP-based distributed generation in order to improve the technical and economic constraints of the network for an industrial area. The main objective is to maximise the profit-to-cost ratio of system. A multi-objective GA II (MOGA II) is adopted by Ref. [30] to determine the optimal size and number of CHP equipment with storage facilities for a typical hospital with the view to maximizing the primary energy saving and minimising the payback period. In Ref. [31], grey wolf optimisation algorithm is adopted to optimally determine the size of the components of a hybrid CHP system with energy storage for residential buildings with an objective of reliability assessment. In Ref. [32] investigated the impact of carbon tax on the optimal size of an internal combustion engine (ICE) in a medium scale CHP system. The capacity of a cogeneration or CHP plant is determined by Ref. [33] based on MINLP for minimising the annual total cost of the plant. In another work by Ref. [34], an optimisation technique based on MILP approach is applied to find the optimal size of thermal energy storage systems (TES) for coal-powered CHP plants considering specific investment costs with the major objective of optimizing the annual operation scheduling of the CHP-TES system. A multi-linear regression model is formulated and applied by Ref. [17] to optimally size CHP units in urban distribution network. It could be inferred from the above-mentioned papers that their focus was to find only the optimum size of CHP systems.

The optimal location and capacity of three CHP equipment such as fuel cells (FC), internal combustion engine (ICE), and micro-turbine (MT) were determined by Ref. [35] based on the environmental costs of pollutants. The focus of the work is profit

**Table 1**
Summary of previous studies on optimal planning of CHP- DGs.

| Ref. | Decision variable | Planning method | Network | Load model | Load growth | Fuel | Objective function | Optimisation algorithm |
|---|---|---|---|---|---|---|---|---|
| [6] | site + size | S | P and H | CL | X | NG | max profit | IPSO |
| [7] | site + size + power factor | S | P | VDL | ✓ | NG | max profit | GA |
| [18] | site + size | S | P and H | CL | ✓ | NG | max profit | MILP |
| [30] | size | S | P | X | X | NG | max energy | GA |
| [31] | size | S | P | X | X | NG | min NPC | GWO |
| [36] | size + site | S | P | CL | ✓ | NG | Max profit | PSO |
| [35] | site + size | S | P and H | CL | ✓ | NG | Max profit | MILP |
| [38] | site + size | S | P | CL | X | NG | Min cost, min power loss | GA |
| [39] | site + size | S | P and H | CL | X | NG | Min loss, min cost | PSO |
| [40] | site + size | S | P | CL | X | NG | Min cost, min VD, min emission | θ-SAGSA |
| [41] | site + size | S | P | CL | X | NG | Min power loss | Graph theory |
| [42] | site + size | S | P | CL | X | NG | Min loss, max reliability | PSO |
| [43] | site + size | S | P and H | CL | X | NG | Min losses | E-ICA |
| [45] | site + size | S | P and H | CL | X | NG | min loss, cost | IGA |
| [50] | site + size | S | P | X | X | NG | min losses | LR |
| This study | site + size + power factor | D | P | SVDL | ✓ | Biogas | Min loss, VD, max VSI, profit | IPSO |

S = static, D = dynamic, P = power, H = heat, CL = constant load, VDL = voltage dependent load, SVDL = seasonal voltage dependent load, pf = power factor, X = not applied, IPSO = improved particle swarm optimisation, GA = genetic algorithm, LR = Linear regression, MILP = mixed linear integer programming, GWO = grey wolf optimisation, θ-SAGSA = θ-Self Adaptive Gravitational Search Algorithm, E-ICA = enhanced imperialist competitive algorithm, IGA = improved genetic algorithm, NG = natural gas.

maximisation for the CHP owners while considering the load and energy price increase over the planning horizon. In Ref. [18], optimal CHP planning was conducted using a risk-averse approach with the view to maximise the CHP owner's profits and minimise the system operation costs while considering the load and energy price increase and network voltage stability issue.

In the work of [7], genetic algorithm (GA) was adopted for optimal planning of CHP distributed generation considering time-varying voltage dependent load demand, increased load demands and energy prices with the aim of maximizing the present value profit of the distribution network operator (DNOs) as against the supplying costs. As a component of revenue generation, the sale of heat energy to consumers was left out in their study which may reduce the profitability (revenue stream) and make the results non-optimal. The stochastic placement and sizing of CHP systems are determined by Ref. [36] using PSO for maximizing the profit-to-cost ratio of the system. Although stochastic demand and energy prices are considered. In the work of, a selective PSO is adopted for network reconfiguration. Also, Ref [37] applied fuzzy logic for optimal placement of capacitors in a distribution system.

In Ref [38] optimal place, size, and operation of CHP equipment in multi-carrier energy networks has been carried out with the goal of maximizing network reliability, reducing power loss, and improving the voltage profile of the network. In the work of [39], the optimal location and size of tri-generation equipment to be deployed in an autonomous community microgrid considering uncertainties of renewable energy sources was conducted using the PSO algorithm with the sole of aim of minimising the total heat and power losses of the microgrid. A long-term planning of various CHP-DGs, including FC, ICE, and MT is investigated by Ref. [6] using PSO by considering the environmental emission costs of pollutants with the aim of maximizing the profit in an integrated heat and electricity network. In Ref. [40], θ-Self Adaptive Gravitational Search Algorithm was adopted for optimal placement of FC-based CHP in IEEE 69 bus system. In a research conducted by Ref. [41], a graph method is applied to optimally allocate CHP equipment for power loss reduction and capacity release of DN. A multi-objective-based PSO algorithm was used by Ref. [42] to optimally allocate CHP system to improve technical performance of the distribution network.

In the work of [43], a new enhanced imperialist competitive algorithm (E-ICA) was applied for optimal allocation of CHP systems in an interconnected heat and electricity distribution network with the objective of minimising electric and heat transfer losses. Only power loss minimisation was considered. In all the aforementioned references [6,7,18,35,37,39,41–44], no cognisance is taken of simultaneous consideration of load growth and seasonal voltage dependent load model in their planning approaches. In Ref. [45], the optimal CHP placement in an integrated heat and electricity systems was carried out using an improved GA method. Although load demand levels were applied, consumer types and load growth were neglected.

Economic and environmental assessments were equally not accounted for in their work.

In CHP allocation problem, operating the equipment at an optimal power factor could guarantee the optimum power generation and minimum loss when connected to the distribution network. Several previous studies have undertaken optimal location and sizing of DGs using fixed power factor which has been pre-set prior to the optimisation process [8,20,46,47]. Others have used the combined power factor of the connected loads as the optimal power factor of the DGs [9,25,26]. In both cases, this assumption may lead to a non-optimal global result in the optimisation algorithm [48,49]. Therefore, finding optimal operating power factor for CHP-DG when connected to the distribution network should be further investigated.

### *1.2. Research gap and contributions*

In most of these aforementioned previous works, the authors assumed the connected loads were constant and did not consider the variability around the required loads in distribution systems. In addition, the load growth and voltage dependent load models were not simultaneously considered in their optimisation procedure. As previously mentioned, fixed power factors were mostly considered in previous works. In the above-reviewed studies, few of them investigated the economic and environmental assessment of CHP [6,7,18] using static planning method. Another important observation from the literature is that most of the CHP plants are natural gas-fired. Although natural gas is more environmentally friendly than diesel or gasoline, its combustion still emits some greenhouse gases thereby having environmental and sustainability issues. The use of biogas obtained from food waste (FW) components of the municipal solid waste (MSW) obtained from the area where the CHP plants are located could be an important substitute for natural gas in powering CHP equipment. Although the reviewed studies provide important insights into the CHP-DG planning problem, to the best of the authors' knowledge none of them has considered a dynamic planning framework incorporating voltage-dependent load models, load growth, demand variability and optimal power factor simultaneously for biogas powered CHP-DG in a distribution network.

It is observed from the previous study that PSO algorithm has been frequently employed for optimal sizing and placement of CHP-based DG. The popularity in the usage of PSO could be attributed to its simplicity, very few parameter selections, and that it does not require any good initial solution to start the algorithm iteration process [11]. It can also generate high-quality solutions within less calculation time and has a more stable convergence characteristics than other stochastic methods [21]. However, PSO is bedevilled with a major problem of premature convergence and being trapped in local optimum. In a bid to handle these problems, an improved PSO is proposed which is capable of ensuring a balance in the exploration and exploitation phases, hence improving the performance for better output. Table 1 shows the summary of the reviewed papers concerning the optimal planning of CHP-DGs.

Therefore, to address the shortcomings identified in the reviewed studies, this paper proposes an improved PSO for dynamic planning of CHP-DG in DNs. The main contributions of this paper are.

- The proposed approach considers the impact of the practical voltage-dependent load models in power flow calculations during different seasons of the year.
- The proposed approach also incorporates load growth and seasonal load demand level variability.

- An improved PSO (IPSO) algorithm is presented to find the optimal locations, sizes and power factor of CHP-DG under single and multiple objectives.
- Formulate a dynamic approach to investigate the economic and environmental impact of the CHP-DG integration.
- The proposed method is tested on a standard radial power distribution network (i.e., IEEE 69 bus system)
- Results obtained with the proposed methodology are compared with the standard PSO and other state-of-the-art methods found in the literature to show its performance.
- Statistical analysis is performed to demonstrate the robustness and effectiveness of the proposed algorithm.

## 2. CHP-based distributed generation description

Based on active and reactive power generation capabilities, DGs are categorised into four types. Type 1 DGs are those that generate only active power such as solar PV and fuel cells. They are inverter-based DGs and operate at unity power factor (*pf*) (i.e., $pf = 1$). Type 2 DGs are those that generate only reactive power such as shunt capacitors, synchronous condensers, and static var compensators (SVC). They operate at zero *pf* (i.e., $pf = 0$). Type 3 DGs are those that inject both active and reactive powers into the power system. Synchronous generator such as gas turbine (GT) and internal combustion engines (ICE) are examples of Type 3 DGs and operate at lagging power factor [46] with values ranging from 0 to 1 (i.e. $0 \leq pf \leq 1$). Type 4 DGs are those that inject active but consume reactive power from the network. Wind turbine-based squirrel cage induction generators are examples of Type 4 DG [51] and they operate at a leading *pf* [8] with value ranging from 0 to 1 (i.e. $0 \leq pf \leq 1$). CHP is a firm or constant power generation technology that produces multiple energy services (such as electricity and heat) simultaneously from a single equipment and fuel source. The prime movers such as FCs, ICE, MT, gas turbines (GT) and steam turbines (ST) are used as equipment for CHP-based DGs [52]. Taking a cue from the work conducted by Ref. [53], FCs and ICE are considered as the best and second best equipment for biogas powered CHP-based DG due to their complementary environmental, economic, and technical advantages. In this study, FCs as a type 1 DG (i.e., that produces only active power and operates at unity power factor) and ICE as a type 3 DG (i.e., that produces both active and reactive powers and operates at power factor between 0 and 1) will be considered as CHP equipment for placement on the distribution network.

It should be noted that ICE is run by biogas and FC is powered by hydrogen gas derived from biogas. The biogas is produced from the AD process using the food waste (FW) of the community where the CHP-DGs are to be installed. As the capacity of a DG is inherently limited by the energy resources of the location it is meant to be sited, it is therefore, important to calculate the amount of biogas from the FW and the electrical energy generated by the FC and ICE.

### 2.1. Determination of biogas production

Biogas is a mixture of methane and carbon dioxide produced from microbial decomposition of organic wastes such as FW under an anaerobic environment. The actual quantity of methane $V_{CH_4A(t)}$ ($m^3$) that can be derived from FW is determined theoretically according to Eqn. (1).

$$V_{CH_4A(t)} = V_{CH_4} \times F_{ORG(t)}(1 - \not{\ell}) \tag{1}$$

where, $V_{CH_4}$ ($m^3$) is the gross methane extractable per kg of FW, $\not{\ell}$ is the fraction of FW that does not decompose whose value is taken as 0.15 [54], $F_{ORG(t)}$ is the amount of FW (kg) treated in year *t*. The detailed process and procedure for determining $V_{CH_4A(t)}$ can be found in Ref. [55].

In order to enhance the energy quality of methane, the recovered methane is purified by removing impurities such as hydrogen sulphide, and carbon dioxide. Carbon dioxide does not support combustion while hydrogen sulphide gives a pungent and obnoxious odour. It also poisons the catalyst in the FC while causing corrosion in the ICE which may lessen the useful lifetime of this equipment. Therefore, the amount of purified methane $V_{CH_4P(t)}$ ($m^3$) is obtained using Eqn. (2).

$$V_{CH_4P(t)} = V_{CH_4A(t)} \times \Omega \tag{2}$$

where Ω is the extent of purification whose value is assumed as 87 % [56].

### 2.2. Determination of power generation from FC and ICE

This section provides the mathematical relations for determining the power outputs of FC and ICE.

#### 2.2.1. Power generation for FC

FC is a device that converts the chemical energy in fuels (usually hydrogen) into direct current (DC) power with zero or near-zero emissions. The main by-product of FC's chemical reaction is water vapour which portends no danger to the environment. The main fuel for FCs is hydrogen gas which can be obtained through water electrolysis or steam reforming process. In the works presented by Refs. [54,55], an analytical approach was adopted to determine the mass of hydrogen ($\dot{m}_{H_2(t)}$) in (kg) extractable from biogas ($CH_4$) via biogas steam reforming process according to Eqn. (3).

$$\dot{m}_{H_2(t)} = 0.5 \times D_{bio-\text{methane}} \times V_{CH_4P(t)} \times \eta_{sys} \tag{3}$$

where, $D_{bio-methane}$ is the density of bio-methane at room temperature (taken as 0.717 (kg/m$^3$)) [57], $V_{CH_4P(t)}$ (m$^3$) is the volume of purified biogas (bio-methane), $\eta_{sys}$ is the combined system efficiencies ($\eta_{sys} = \eta_B \times \eta_R$) where $\eta_B$ and $\eta_R$ are boiler and biogas reformer efficiencies, respectively and their values are both taken as 80% [58].

Due to low density of hydrogen at room temperature 0.089886 kg/m$^3$, its storage is very crucial. It will require a large volume capacity container to store it in this form. Therefore, compression at high pressure is usually done. The hydrogen gas is stored in a compressed gas cylinder (hydrogen tank) at a high pressure in the range of 200–800 bar [59]. When compressed, the density of hydrogen gas at 35.0 MPa is about 23 kg/m$^3$ and at 70.0 MPa is about 38 kg/m$^3$ [60]. Based on this information, the volume (m$^3$) of the compressed hygrogen gas is determined as shown in Eqn. 4

$$H_{2vol(t)} = \frac{\dot{m}_{H_2(t)}\eta_{comp}}{H_{2d}} \tag{4}$$

where $\dot{m}_{H_2}$, $\eta_{comp}$ and $H_{2d}$ are the mass of hydrogen gas obtained from biogas reforming (see Eqn. (3)), compression efficiency (taken as 95 % [54,59]) and the compressed density of hydrogen gas (taken as 36 kg/m$^3$ [54]), respectively. The number of the tank ($H_{\text{tank}}$) can be calculated as in Eqn. (5).

$$H_{\text{tank}} = \frac{H_{2vol(t)}}{A_{size}} \tag{5}$$

where $A_{size}$ available hydrogen gas storage tank capacity in the market. There are a varieties of compressed hydrogen storage tank types (i.e., Types 1, 2, 3 and 4) [61]. Type I storage tanks usually made of steel are mature and mostly used in industrial and commercial applications; and are available with a net volume of 2.5–50 m$^3$ at a pressure of 200–300 bar and can also withstand pressure up to 500 bar [62]. However, improvement in material technology and development have led to the production of lightweight materials such as aluminium and composite.

The compressed hydrogen gas is fed to FCs for energy generation. The amount of electrical energy (kWh) produced from the FC is determined as in Eqn. (6).

$$E_{FC(t)} = \frac{\left(LHV_{H_2} \times \eta_{FC} \times \dot{m}_{H_2(t)} \times \eta_{comp}\right)}{\theta} \tag{6}$$

$LHV_{H_2}$ is the lower heating value of $H_2$ (taken as 119.9 MJ/kg [63]), $\theta$ is the conversion factor from MJ to kWh taken as 3.6 while $\eta_{FC}$ is the electrical efficiency of FC.

The gross capacity ($P_{gFC(t)}$) of the FC in (kW) is determined as in Eqn. (7).

$$P_{gFC(t)} = \frac{E_{FC(t)}}{T} \tag{7}$$

The operating time (T) is assumed to be 8760 h. It should be noted that this is an idealistic assumption to determine the maximum capacity of FC it were to be operated year-round. Since the electrical power generated by FC is direct current (DC), an inverter is required to convert it to alternating current (AC) before feeding it to the distribution network. Therefore, the actual capacity of the FC is given as in Eqn. 8

$$P_{FC(t)} = P_{gFC(t)} \times \eta_{inverter} \tag{8}$$

The inverter efficiency $\eta_{inverter}$ is assumed as 95 % [64].

### 2.2.2. Power generation for ICE

An ICE is another piece of equipment for CHP application that can be powered by biogas/methane.

An ICE is a synchronous based electrical machine that generates electrical power from the combustion of fuels. In the course of electrical power generation, heat energy is equally emitted from the exhaust pipe, making ICE a good candidate for CHP equipment. Being a synchronous machine, the ICE generates active and reactive power depending on the operating *pf*. The active power generated by an ICE is determined according to Eqn. 9

$$P_{ICE(t)} = \frac{\left(V_{CH_4P(t)} \times LHV_{CH_4} \times \eta_{ICE}\right)}{\theta \times T} \tag{9}$$

Where, $V_{CH_4P(t)}$ is the purified biogas (m$^3$) produced in year t, $\eta_{ICE}$ is the electric efficiency of the ICE with a value taken as 35% [65] after subtracting the self-consumption for the plant. $LHV_{CH_4}$ is taken as 37.2 MJ/m$^3$ [65]. Similar to FC, the operating time is assumed to be 8760 h. Based on operating, the reactive power generation capacity (kVAr) of the ICE is determined as follows according to Eqn. (10) [66].

$$Q_{ICE(t)} = P_{ICE(t)} \times \tan\left(\cos^{-1} pf\right) \tag{10}$$

The apparent power capacity (kVA) of the ICE is determined as in Eqn. (11).

$$S_{ICE(t)} = \sqrt{P_{ICE(t)}^2 + Q_{ICE(t)}^2} \tag{11}$$

## 3. Load growth and load demand variability modelling

Electrical load growth has been on the increase in recent times and varies from place to place. The rate of increase depends on population growth, improved economic status of individuals, and industrialisation among others. People tend to increase their energy demand when they are economically buoyant and vice versa.

### 3.1. Determination of yearly load growth

The yearly load growth for a distribution load bus is modelled according to Eqns. (12) and (13) [24].

$$p_{Di,t} = p_{D0i}(1+\alpha)^t \tag{12}$$

$$q_{Di,t} = q_{D0i}(1+\alpha)^t \tag{13}$$

where, $p_{Di,t}$ and $q_{Di,t}$ are the active and reactive load demands at bus $i$ in year t, $p_{D0i}$ and $q_{D0i}$ are the initial active and reactive load demand at bus $i$ of the distribution network in the reference (base) year (0th year), respectively. The parameter ($\alpha$) is the load growth rate.

#### 3.1.1. Determination of load growth rate (α)

According to Ref. [67], the electric load growth rate on the power distribution network is related to the connection of new customers and the need to meet the increasing demands of existing customers. The first factor could be traced to increase in population and urban development while the second can be attributed to industrialisation and improved income levels for consumers. Industrialisation and improved income of the populace is a direct manifestation of favourable gross domestic product (GDP) of a country. Premised on this, electric load growth rate can be said to have a direct correlation with population growth and economic (GDP) growth rates. Therefore, the parameter $\alpha$ can be determined using Eqns. (14) and (15)

$$\alpha = \mu(\beta+\gamma) - \beta\gamma \tag{14}$$

$$\mu = \begin{Bmatrix} 1 & (\beta+\gamma) \geq 0 \\ 0 & \text{otherwise} \end{Bmatrix} \tag{15}$$

where, $\mu$ is the load growth rate controlling factor, $\beta$ and $\gamma$ are respectively percentage population and GDP growth rates of a particular society or country. Depending on the economic status of the country, $\gamma$ can be positive or negative. Positive $\gamma$ implies economic prosperity and good income for the energy consumers while negative $\gamma$ means economic recession and poor income for the populace. Similarly, positive $\beta$ signifies population increase while negative $\beta$ shows population decline. In this paper, it is assumed that the economic situation is favourable and the population growth rate is envisaged to increase in the future, therefore the values of $\beta$ and $\gamma$ are assumed positive.

### 3.2. Load demand variability and voltage dependent load model

As previously stated, the load demands (active and reactive) at the utility grid are time varying (i.e., hourly or seasonal variation) and are dependent on the voltage profile of various consumer types (i.e., residential, commercial and industrial) connected to it.

#### 3.2.1. Load demand variability model

Loading of the distribution system varies daily (hour-to-hour variation) and in different seasons such as summer, winter, spring and autumn day and night of the year due to changes in some atmospheric conditions such as temperature and humidity. It is expected that a decrease in temperature as experienced on winter day will introduce significant increase in power consumption as consumers use their heating and other equipment to keep themselves warm. However, for long term planning that involves multiple years of study, considering an hour-to-hour load will be computationally demanding. In this case, one of the best approaches for modelling this seasonal/time-varying load is using three different load levels, including off-peak, normal and heavy load levels [68] such that the load pattern and the price of electricity have specific values in each load level. Therefore, the active and reactive load demands at each load level ($dl$) in each season ($s$) in year (t) is determined as shown in Eqns. (16) and (17), respectively.

**Table 2**
Load levels.

| Load level | Low load | Base load | High load |
|---|---|---|---|
| Magnitude | 0.75 | 1.0 | 1.25 |

$$p_{Di,t,dl,s} = dl,s \times p_{Di,t} \tag{16}$$

$$q_{Di,t,dl,s} = dl,s \times q_{Di,t} \tag{17}$$

Based on seasonal load variation, the network loading in each season of the year is discretised into three loading levels (*dl*) such as low, moderate (base) and high-load levels. The discretised values for *dl* are depicted in Table 2.

### 3.2.2. Voltage dependent load model

For a real practical situation, the distribution network is penetrated with a mixture of different load types such as residential, commercial and industrial whose active and reactive power requirements are dependent on supply voltage and frequency of the system [24]. Depending on the nature of the area being supplied, different load types may be connected to different load buses or every bus of the system has different load types connected to it. The first approach reflects a well-organised area in which DISCOs have pre-allocated different buses for different load types. The second approach signifies a situation when DISCOs may not be aware of the load types connected to the distribution network. Since practical distribution system loads are not completely residential, industrial, and commercial, the best approach to model distribution loads should be in a mixed-type form. This study considers a mixed load model in which every bus of the system has a mixture of these load types connected to it. Therefore, considering the voltage dependent load and the seasonal load variability, the mixed seasonal voltage dependent load model is mathematically formulated as in Eqns. 18 and 19 [49].

$$P_{Di,t,dl,s} = p_{Di,t,dl,s}\left(\alpha_{p1}\left(\frac{V_i}{V_0}\right)^{\sigma_r} + \alpha_{p2}\left(\frac{V_i}{V_0}\right)^{\sigma_c} + \alpha_{p3}\left(\frac{V_i}{V_0}\right)^{\sigma_{in}}\right) \tag{18}$$

$$Q_{Di,t,dl,s} = q_{Di,t,dl.s}\left(\beta_{q1}\left(\frac{V_i}{V_0}\right)^{\omega_r} + \beta_{q2}\left(\frac{V_i}{V_0}\right)^{\omega_c} + \beta_{q3}\left(\frac{V_i}{V_0}\right)^{\omega_{in}}\right) \tag{19}$$

where $P_{Di,t,dl,s}$ and $Q_{Di,t,dl,s}$ are the mixed seasonal voltage dependent active and reactive power demands at bus *i* in year t, demand level dl and season s, respectively. The parameters $p_{Di,t,dl,s}$ and $q_{Di,t,dl,s}$ are the active and reactive powers at operating point in bus *i* in year t, demand level dl and season s. $V_i$ is the voltage at bus *i* and $V_0$ (usually assumed as unity) is the nominal voltage at the operating point.

According to Eqns. 18 and 19, $\sigma$ and $\omega$ are the active and reactive power exponents of the voltage-dependent load model such as, residential, commercial and industrial load models with subscript *r*, *c* and *in*, respectively. The values of the load power exponents for typical representation of summer and winter day and night of a year are presented in Table 3 [69].

The coefficient $\alpha_{p1}$, $\alpha_{p2}$ and $\alpha_{p3}$ indicate the weight of active power and, $\beta_{q1}$, $\beta_{q2}$ and $\beta_{q3}$ are for reactive powers of each load type. These values are assigned by the DISCOs (utility) or the design engineer based on the active and reactive power consumptions of each load type with respect to the actual load demands of the network. For a completely residential load model, $\alpha_{p1} = \beta_{q1} = 1$ while other coefficients are zero. For a distribution network connected to a commercial centre, the load model has $\alpha_{p2} = \beta_{q2} = 1$ while other coefficient parameters are equal to zero. Lastly, for only industrial load, the $\alpha_{p3} = \beta_{q3} = 1$ whereas other coefficients are zero. Therefore, the summation of coefficients of the active and reactive power consumptions relating to real practical distribution network (i.e., a mixture of residential, commercial, and industrial) are $\alpha_{p1} + \alpha_{p2} + \alpha_{p3} = 1$ and $\beta_{p1} + \beta_{p2} + \beta_{p3} = 1$, respectively.

## 3.3. Load flow computation

Due to the radial structure of distribution network with high resistance to reactance ratio, the traditional load flow techniques such as Gauss-Seidel (GS), Newton Raphson (NR) and fast decoupled methods are not suitable due to formulation of Jacobian matrix or Y-admittance matrix which could be computational demanding and may lead to non-convergence. A straightforward iterative method called forward-backward sweep (FBS) based on direct approach for distribution system load flow model developed by Ref. [70] is used due to the elimination of Jacobian matrix and matrix decomposition [71] and the capability to cope with the topological structure of the distribution network thereby leading to simplicity, robustness, and computational efficiency [72]. The FBS load model works based on three matrices namely bus injection to branch current (BIBC), branch current to bus voltage (BCBV) and direct load flow (DLF) formed by fundamental circuit laws of Kirchhoff's current law (KCL) and Kirchhoff's voltage law (KVL). A detailed explication of this approach can be found in Refs. [20,73]. It is assumed that the three-phase radial distribution network is balanced and can be

**Table 3**
Seasonal load models and their power exponent value.

| Season | Load duration | Load models | | | | | |
|---|---|---|---|---|---|---|---|
| | | Residential | | Commercial | | Industrial | |
| | | $\sigma_r$ | $\omega_r$ | $\sigma_c$ | $\omega_c$ | $\sigma_{in}$ | $\omega_{in}$ |
| Summer | Day | 0.72 | 2.96 | 1.25 | 3.50 | 0.18 | 6.00 |
| | Night | 0.92 | 4.04 | 0.99 | 3.95 | 0.18 | 6.00 |
| Winter | Day | 1.04 | 4.19 | 1.50 | 3.15 | 0.18 | 6.00 |
| | Night | 1.30 | 4.38 | 1.51 | 3.40 | 0.18 | 6.00 |

represented by their equivalent single-line diagram. Figs. 1 and 2 show a simple electrical equivalent of a typical radial distribution feeder and its branch, respectively.

## 4. Problem formulation

In this paper, single and multi-objective based optimal placement of CHP-based DG have been formulated considering two types of CHP technologies subject to system constraints. In this study, three technical objectives are considered which are individually and simultaneously optimised. The cost-benefit in terms of the economic and environmental analysis of the connected CHP to the system is also dwelled on.

### 4.1. Single objective function

The power loss in a distribution network is a function of the current drawn by the connected loads and the line impedance. Since most distribution networks are radial or weakly meshed, significant power loss is experienced due to high resistance of the line conductors and low operating voltage. Mostly, active power loss minimisation forms the major goal of DISCOs due to its criticality in determining their annual revenue and maximizing their profit. Therefore, this objective is singly minimised by applying the following formula as indicated in Eqns. (20) and (21) [74].

$$F_1 = \min\left(\frac{PL^{CHP}}{PL^0}\right) \tag{20}$$

$$P_{Loss}{}^0 = \sum_{i=1}^{Nbr} \left(I_{i+1}^0\right)^2 \times R_{i+1} \tag{20a}$$

$$P_{Loss}{}^{CHP} = \sum_{i=1}^{Nbr} \left(I_{i+1}^{CHP}\right)^2 \times R_{i+1} \tag{20b}$$

$$\left(I_{i+1}^{CHP}\right)^2 = \frac{P_i^{\,2} + Q_i^{\,2}}{\left|V_i^{CHP}\right|^2} \tag{21}$$

where $P_i$ and $Q_i$ are the real and reactive powers injected in the $i$ th bus, while $\left|V_i^0\right|$ and $\left|V_i^{CHP}\right|$ are the magnitude of the $i$ th bus voltage of the distribution network without and with CHP. $\left(I_{i,i+1}^{CHP}\right)^2 \times R_{i,i+1}$, $\left(I_{i,i+1}^0\right)^2 \times R_{i,i+1}$ are the active power loss at the line section between bus $i$ and $i+1$ without and with CHP equipment, $I_{i,i+1}^0$ and $I_{i,i+1}^{CHP}$ are the line current that flows between bus $i$ and $i+1$ without and with CHP while $R_{i,i+1}$ is the resistance of the line (conductor) connecting bus $i$ and $i+1$ while *Nbr* is the branch number. The load flow algorithm described in subsection 3.3 will be adopted to determine the bus voltages of the network with and without CHP-DG.

It should be noted that when a DG is installed at bus $i$, the active power generated from DG will change active power injections from $P_i$ in the load bus $i$ to $P_i = P_{D,i} - P_{DG,i}$ while the reactive power generated from DG will change reactive power injections from $Q_i$ in the load bus $i$ to $Q_i = Q_{D,i} - Q_{DG,i}$. Where, $Q_{DG,i} = sign(P_{DG,i} \times \tan(\cos^{-1} pf))$. For DG supplying both active and reactive powers, *sign* is positive and operates at a lagging power factor between 0 and 1 while for a DG that supplies active power and absorbs reactive power, the *sign* is negative and operates at a leading power factor between 0 and 1.

### 4.2. Multi-objective function

The integration of DG into the distribution network improves the technical performance of the system. Most of the technical performance parameters of the distribution system have conflicting attribute. For example, the system power losses and the deviation

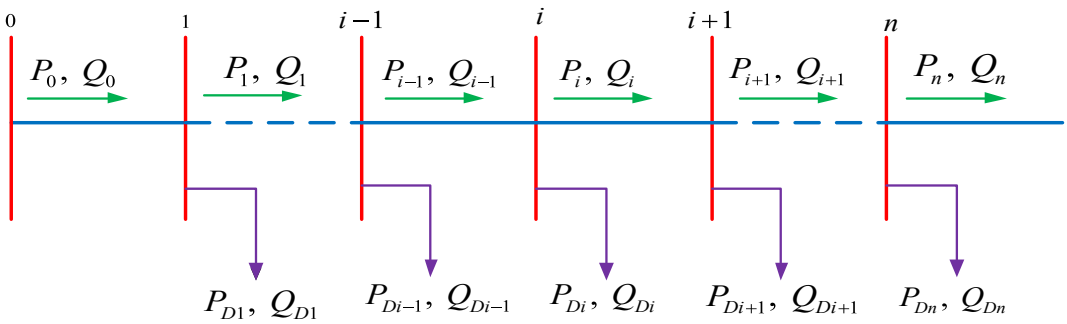


**Fig. 1.** A simple representation of the radial distribution network.

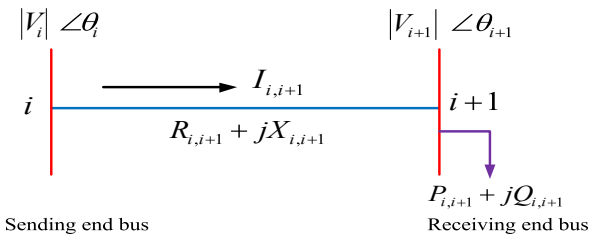


**Fig. 2.** A simplified illustration of a branch of an RDS.

in the buses' voltage are expected to reduce while the voltage stability for each bus's voltage is expected to increase while improving voltage profile of the system. To maximise the technical benefit and achieve a trade-off among these conflicting parameters, simultaneous optimisation is necessary. Therefore, a multi-objective function comprising three technical parameters of total active power loss, total voltage deviation and total voltage stability of the network are simultaneously taken into consideration while maintaining various operational constraints. Because of the divergent characteristics of the evaluation indices, an index-based approach is applied to normalise the conflicting attributes and make them unit-less. To solve this multi-objective problem, the weighted sum method is used due to its simplicity and wide acceptability and its ability to avoid the dominance of one objective over another [46].

#### 4.2.1. Voltage deviation index (VDI)

In practice, there is voltage deviation (VD) at each voltage bus from the nominal voltage because of voltage drop along the radial distribution network due to the line impedance. This effect usually determines the quality of power supply and is mostly pronounced at buses far away from the substation. Therefore, to ensure better quality power and improved voltage profile of the radial distribution network, this effect should be minimised. This objective function is formulated as shown in Eqns. (22)–(24) [46].

$$F_2 = \min\left(\frac{\mathrm{VD}^{\mathrm{CHP}}}{\mathrm{VD}^0}\right) \tag{22}$$

$$VD^{CHP} = \sum_{i=1}^{nb} \left(V_i^{CHP} - V_0\right)^2 \tag{23}$$

$$VD^0 = \sum_{i=1}^{nb} \left(V_i^0 - V_0\right)^2 \tag{24}$$

where, $V_i^0$ p.u. is the reference voltage (no CHP-DG) value which is taken as 1.0 p.u. and $V_i^{CHP}$ is the bus voltage after the placement of CHP-DG on the network and *nb* is the bus number.

#### 4.2.2. Voltage stability index (VSI)

Stability and security of the distribution system under varying operating and loading conditions are anchored on the capability of maintaining the bus voltages within the statutory limit. To ensure this, the VSI of all the buses must be determined in order to identify the weakest and sensitive buses to voltage collapse and instability. Usually, a bus that has VSI close to zero is more liable to voltage collapse and those having VSI close to unity are very viable nodes or buses. Therefore, to ensure the stability of the radial distribution network, VSI must be maximised by minimising the inverse of the ratio of the sum of VSI before DG integration to that when DG is integrated. This objective function is formulated according to Eqns. (25)–(27) [75].

$$F_3 = \max\left(\frac{\sum_{i=1}^{nb} \mathrm{VSI}_{i+1}^{\mathrm{CHP}}}{\sum_{i=1}^{nb} \mathrm{VSI}_{i+1}^{0}}\right) \tag{25}$$

$$VSI_{i+1}^0 = \left|V_i^0\right|^4 - 4(P_{i+1}X_{i+1} - Q_{i+1}R_{i+1})^2 - (P_{i+1}R_{i+1} - Q_{i+1}X_{i+1})\left|V_i^0\right|^2 \tag{26}$$

$$VSI_{i+1}^{CHP} = \left|V_i^{CHP}\right|^4 - 4(P_{i+1}X_{i+1} - Q_{i+1}R_{i+1})^2 - (P_{i+1}R_{i+1} - Q_{i+1}X_{i+1})\left|V_i^{CHP}\right|^2 \tag{27}$$

where, $VSI_{i+1}^0$ is the voltage stability index at bus receiving end when CHP-DG is not connected and $VSI_{i+1}^{CHP}$ is the voltage stability index at the receiving end when CHP-DG is connected while $\left|V_i^0\right|$ and $\left|V_i^{CHP}\right|$ are the voltage magnitude at sending end bus *i* without and with CHP-DG, respectively. $R_{i,i+1}$ and $X_{i,i+1}$ are the resistance and reactance of the line between the sending and receiving end buses, respectively.

#### 4.2.3. Overall multi-objective function

The overall multi-objective function (MOF) is formulated as a weighted sum of all the objective functions. The total MOF is minimised and is formulated as shown in Eqn. (28).

$$MOF = \min\left(\mathrm{k_p}F_1 + \mathrm{k_v}F_2 + \mathrm{k_s}{F_3}^{-1}\right) \tag{28}$$

where $\mathrm{k_p}$, $\mathrm{k_v}$ and $\mathrm{k_s}$ are the weighting factors of each objective function. The sum of these factors must equal unity (i.e., $\mathrm{k_p} + \mathrm{k_v} + \mathrm{k_s} = 1$). In this paper, $k_p$, $k_v$ and $k_s$ have been determined using fuzzy best worst multi-criteria decision-making method and the results are 0.4332, 0.2937 and 0.2731, respectively. Based on the assigned value, the power loss is a major factor that influences the technical and economic viability of power system and a major contributor to the DISCO's revenue. By virtue of its importance, it is ranked first with a weighting factor of 0.4332 while voltage deviation (VD) and voltage stability index (VSI) are second and third with weighting coefficients of 0.2937 and 0.2731, respectively to maintain the power quality and voltage profile of the system. The FBS is applied to compute the total active power loss, the system bus voltage, and voltage deviation index and voltage stability prior to installing CHP-DG and after while ensuring that the system constraints are not violated.

### 4.3. Constraint of the optimisation

The optimisation of these objectives is subject to both equality and inequality constraints.

#### 4.3.1. Power balance constraint

To ensure steady state operation of the system, power conservation in the system must be maintained. That is the algebraic sum of the incoming power to the distribution system must equal the outgoing power from the system. This implies that the total power supplied from the grid (slack) bus and the power delivered by the CHP equipment should satisfy the total power demand and the network losses. Therefore, the power balance constraint is formulated as shown in Eqns. (29) and (30).

$$P^{grid} + \sum_{k=1}^{K} {P_{t,k}}^{CHP} = \sum_{i=1}^{Nb} P_{Li,t} + \sum_{i=1}^{Nb} P_{Di,t} \tag{29}$$

$$Q_{grid} + \sum_{k=1}^{K} {Q_{k,t}}^{CHP} = \sum_{i=1}^{Nb} Q_{Li,t} + \sum_{i=1}^{Nb} Q_{Di,t} \tag{30}$$

where, ${P_{t,k}}^{CHP}$ is the total active power produced by the CHP units k, $P_{grid}$ is the input active power of the main bus, $P_{Di,t}$ is active connected electrical loads in the distribution system and $P_{Li,t}$ is the active power loss in the distribution system while $Q_{grid}$ is the input reactive power of the main bus, $Q_{Di,t}$ is reactive connected electrical loads in the distribution system and $Q_{Li,t}$ is the reactive power loss in the distribution system ${Q_{k,t}}^{CHP}$ is the reactive power injected by the CHP unit into the network.

#### 4.3.2. Inequality constraint

The inequality constraints considered in this paper are described as follows.

*4.3.2.1. Voltage limit constraint.* Under normal operating conditions, the voltage $V_i$ of each bus of the system must be kept within the statutory limit according to Eqn. 31

$$V_{\min} \le V_i \le V_{\max} \tag{31}$$

where, $V_{\min}$ and $V_{\max}$ are the lowest and highest allowable values of voltage. In this study, $V_{\min}$ is set at 0.95 p.u and $V_{\max}$ is set to 1.05 p.u [74].

*4.3.2.2. Total active and reactive power constraints.* To prevent reverse power flow, the total active and reactive power injected into the distribution network by the CHP-DGs must be less than the total active and reactive load demand of the network at any load level. This constraint is formulated as Eqns. (32) and (33).

$$\sum_{k=1}^{K} {P_{t,k}}^{CHP} \le \sum_{i=1}^{Nb} P_{Di} \tag{32}$$

$$\sum_{k=1}^{K} {Q_{t,k}}^{CHP} \le \sum_{i=1}^{Nb} Q_{Di} \tag{33}$$

*4.3.2.3. DG capacity limit constraint.* The active and reactive power injected by each CHP-DG must fall within their predetermined limit as presented in Eqns. (34) and (35), respectively. The minimum and maximum limit of the CHP-DG active and reactive powers are described according to Eqns. (36) and (37), respectively

$$\sum_{k=1}^{K} P_{t,k}^{CHP} \leq P_{CHPk}^{\max} \tag{34}$$

$$\sum_{k=1}^{K} Q_{t,k}^{CHP} \leq Q_{CHPk}^{\max} \tag{35}$$

$$P_{\min\ t,k}^{CHP} \leq P_{t,k}^{CHP} \leq P_{\max\ t,k}^{CHP} \tag{36}$$

$$Q_{\min\ t,k}^{CHP} \leq Q_{t,k}^{CHP} \leq Q_{\max\ t,k}^{CHP} \tag{37}$$

where $P_{CHPk}^{\max}$ is determined according to Eqns. (8) and (9). $P_{\min\ t,k}^{CHP}$ and $P_{\max\ t,k}^{CHP}$ are the minimum and maximum active power generated by CHP k at year t while $Q_{\min\ t,k}^{CHP}$ and $Q_{\max\ t,k}^{CHP}$ are respectively the minimum and maximum reactive powers of each DG. The maximum power limit is determined according to Eqn. (38).

$$P_{\max\ t,k}^{CHP} = \lambda \times \sum_{i=1}^{nb} P_{Di} \tag{38}$$

Where the parameter $\lambda$ is the penetration level of the DG into the network which is determined based on Eqn. (39).

$$\lambda = \begin{cases} \dfrac{P_{\max\ t,k}^{CHP}}{\sum_{i=1}^{nb} P_{Di}} & \text{if} \quad P_{CHPk}^{\max} \leq \sum_{i=1}^{nb} P_{Di} \\ \dfrac{\sum_{i=1}^{nb} P_{Di}}{P_{\max\ t,k}^{CHP}} & \text{if} \quad P_{CHPk}^{\max} \geq \sum_{i=1}^{nb} P_{Di} \end{cases} \tag{39}$$

The value of $\lambda$ varies between 0 and 1.

*4.3.2.4. Power factor limit.* For effective power delivery of a CHP equipment, it should be operated at optimal power factor ($pf^{opt}$) according to the following Eqn. (40)

$$0.8 \leq pf^{opt} \leq 1 \tag{40}$$

### 4.4. Heat energy generation

The thermal capacity of each CHP equipment is a function of its active power output and the heat-to-power ratio (HPR). Recovering heat from the CHP prime movers enhances the overall efficiency of the system. The thermal capacity of FC and ICE is calculated as in Eqn. (41) [6,57].

$$H_{t,k}^{CHP} = P_{t,k}^{CHP} HPR_k \tag{41}$$

Since not all heat generated can be recovered due to losses, therefore the actual heat recovered would depend on the efficiency of the heat recovery equipment system. There are a variety of heat recovery systems such as fixed plate, heat pipe, rotary wheel and round around [76]. Each of them has different heat recovery efficiencies (see Table 4).

Therefore, the actual recovered heat ($H_{Rk(t)}$) by CHP k at year t could be determined according to Eqn. (42).

$$H_{Rk(t)} = H_{t,k}^{CHP} \xi \tag{42}$$

The parameter $\xi$ is the heat recovery efficiency.

## 5. Economic and environmental analysis

This section focuses on the economic and environmental evaluation of the integration of the CHP-DGs in the distribution network.

**Table 4**
Heat recovery system and their efficiencies [76].

| Heat recovery system | Efficiency of the system |
|---|---|
| Fixed plate | 50–80 % |
| Heat pipe | 45–55 % |
| Rotary wheel | Above 80 % |
| Round around | 45–65 % |

### 5.1. Economic analysis

For long-term planning of distributed generation implementation, economic assessment of the project is very essential in order to give the investor (private or utility) an idea of the cost-effectiveness of investing in the project. This is because economic evaluation is the major driving force for an effective investment decision. In this paper, the economic evaluation is based on two economic metrics i.e., net present value (NPV) of profit and levelised cost of energy (LCOE).

#### 5.1.1. Net present value of profit

Since the fundamental intention of an investor is to maximise their yearly economic profit, the annual economic savings in terms of the economic profit are used to express the overall economic performance of the distribution network. All the future costs and revenues obtained from the project are discounted to the present time (with a discount rate) to yield a net present value (NPV). Therefore, the overall NPV of the economic profit is determined according to Eqn. (43).

$$NPV(\text{Pr } ofit) = NPV(\text{Re}venue) - NPV(Costs) \tag{43}$$

Two economic scenarios are investigated (1) when CHP-DGs are operated in power-only mode and (2) in CHP mode. The revenue and cost components of Eqn. (43) are defined in detail in the subsequent section.

*5.1.1.1. Revenue stream before CHP integration.* Before the CHP installation, the revenue of the DISCOs comes mainly from the sales of electricity to retail consumers of various types. The revenue made from the sale of electricity for various consumer types is determined according to Eqn. 44

$$\text{Rev}_0{}^{NoCHP} = \sum_{t=0}^{T} \frac{1}{(1+d)^t} \sum_{i=1}^{N} \sum_{dl=1}^{K} \sum_{s=1}^{S} \left(P_{Di,t,dl,s} \times \delta_e{}^{s,dl} \times \tau_{s,dl}\right) \tag{44}$$

$P_{Di,t,dl,s}$ is the active power demand of the network in year t at load level dl and season s, $\tau_{s,dl}$ is the time period in each demand level dl for season $s$, and $\delta_e{}^{s,dl}$ ($/kWh) is the retail prices of electricity in season $s$ at load level dl and $d$ is discount rate.

*5.1.1.2. Costs stream before the installation of CHP.* Before CHP installation, the costs incurred by the DISCOs are in three folds but not limited. The first one is the cost of purchasing active power from the main upstream grid, the second one is the cost of system upgrade to meet up with load growth and lastly the cost of environmental emission incurred due to power purchased from the grid.

*5.1.1.2.1. Cost of power purchased from the grid before CHP.* The cost of buying power at a wholesale price from the grid and selling to the retail consumers is estimated according to Eqn. 45

$$C_P{}^{NoCHP} = \sum_{t=0}^{T} \frac{1}{(1+d)^t} \sum_{i=1}^{N} \sum_{dl=1}^{K} \sum_{s=1}^{S} \left(P_{Di,t,dl,s} + P_{Loss,t,dl,s}{}^{NoCHP}\right) \times \varepsilon_{s,dl} \times \tau_{s.dl} \tag{45}$$

$P_{Di,t,dl,s}$ (kW) is the active power demand in year $t$ in demand level $dl$ and season s while $P_{Loss,t,dl,s}{}^{NoCHP}$ (kW) is the total active power loss in the case (no CHP) in demand level $dl$ dl in year t and season s, $\varepsilon_{s,dl}$ ($/kWh) is the wholesale price of electricity purchased from the upstream grid at demand level $dl$ in season s and $\tau_{s.dl}$ (h) is the operating time in season s and demand level dl.

*5.1.1.2.2. Cost of system upgrade.* Yearly load growth has a major impact on the distribution network. Apart from the technical effects such as increased line losses, voltage profile depreciation and system stability issue, there is also structural and infrastructural implications. With load growth, the DISCOs have two options to keep their systems working: Load shedding (load rationing) and system expansion (upgrade). The first approach implies removing some loads from the network at specific interval(s) (time) to relieve the network and prevent overloading. This approach is simple but is not technically good as it will incur reliability issue and is not economically wise on the part of the DISCOs and consumers as it will impact their business and reduce their revenue base. The second approach entails spending extra money on purchase and installation of new equipment and devices such as transformers and cables to build additional substations and feeders with a view to cater for the load growth. The value of this cost depends on the topology and distribution network structure, the type and size of feeder lines as well as load growth rate [6,18]. To quantify this cost, an annual value is considered which depends on the yearly total load growth of the distribution network. Therefore, the discounted cost of system upgrade is determined according to Eqn. (46).

$$UGC_t = \sum_{t=0}^{T} \frac{1}{(1+d)^t} \left(UG \times \Delta S_{D,t}\right) \tag{46}$$

where, $UG$ ($/kVA) and $\Delta S_{D,t}$ (kVA) are the yearly upgrade value and apparent load growth, respectively. The apparent load growth rate is determined as the difference between the present and the previous year's apparent load demand. It should be noted that at t = 0 (i.e., no load growth), the value of $\Delta S_{D,t}$ is equal to zero. A value of 120 $/kVA is assumed for $UG$ [6,77]

*5.1.1.2.3. Cost of environmental emission before CHP placement.* Among the costs that DISCOs pay due to energy purchased from the upstream grid are various environmental costs like pollution cost and cost of pollution control. There are various forms of air pollutants released from the combustion of fuels during power generation. Most of these pollutants are greenhouse gases (GHGs). The most critical among them are $CO_2$, $SO_2$ and $NO_X$. The DISCOs are required to pay for these emissions even though they are not the ones generating them. This cost is evaluated as given below in Eqn. 47

$$\mathrm{EMC_t}^{\mathrm{NoCHP}} = \sum_{t=0}^{T} \frac{1}{(1+d)^t} \sum_{i=1}^{N} \sum_{dl=1}^{K} \sum_{p=1}^{P} \sum_{s=1}^{S} \left( \left( P_{Di,t,dl,s} + {P_{Loss,t,dl,s}}^{NoCHP} \right) \times {EP_p}^{grid} \times C_p \times \tau_{s.dl} \right. \tag{47}$$

where ${EP_p}^{grid}$ (kg/kWh) and $C_p$ ($/kg) are respectively the amount of pollutant p emitted from the fuel during power generation and cost implication (penalty) for the pollutant p. In this study, a coal power plant supplies power to the main grid. The total discounted net present value of the costs before CHP integration is obtained as in Eqn. 48

$${C_T}^{NoCHP} = {C_{P,t}}^{NoCHP} + UGC_t + \mathrm{EMC_t}^{\mathrm{NoCHP}} \tag{48}$$

*5.1.1.3. Revenue stream for DISCOs after installation of CHP-DGs.* The revenue streams are the various channels of income for investing in CHP installation. As previously mentioned, the CHP facility is owned and operated by a DISCO. In this study, the sources of income for the DISCO for owning and operating CHP include the sale of electricity to the consumers and the sale of heat to the nearby consumers around the bus where the CHP is located. The total discounted revenue from the sale of electricity and heat are defined as in Eqns. (49) and (50).

$$\mathrm{Rev_1}^{CHP} = \sum_{t=0}^{T} \frac{1}{(1+d)^t} \sum_{i=1}^{N} \sum_{dl=1}^{K} \sum_{s=1}^{S} \left( P_{Di,t,dl,s} \times {\delta_e}^{s,dl} \times \tau_{s,dl} \right) \tag{49}$$

$$\mathrm{Rev_2}^{CHP} = \sum_{t=0}^{T} \frac{1}{(1+d)^t} \sum_{dl=1}^{K} \sum_{s=1}^{S} \left( H_{Sup,t,dl,s} \times {\delta_h}^{s,dl} \times \tau_{s.dl} \right) \tag{50}$$

where $\mathrm{Rev_1}^{CHP}$ and $\mathrm{Rev_2}^{CHP}$ are the revenue from the sale of electricity and heat, respectively $P_{Di,t,dl,s}$ (kW) and $H_{Sup,t,dl,s}$ (kW) are respectively the active power demand and heat power supplied in year t at load level dl and season s. $\tau_{s,dl}$ is the time period in each demand level dl for season $s$. ${\delta_e}^{s,dl}$ and ${\delta_h}^{s,dl}$ in ($/kWh) are respectively the retail prices of electricity and heat in season $s$ at load level dl. Since the heat recovered has to be transported through pipeline, the thermal resistance of the pipeline characteristics (either buried or above ground) as well as environmental conditions may cause thermal losses along the pipeline [43]. Therefore, the thermal power that may eventually be supplied to consumers for use will be a fraction of the heat recovered due to heat loss which can be mathematically quantified as in Eqn. (51).

$$H_{Sup,t,dl,s} = (1-\upsilon) H_{Rk(t)} \times dl, s \tag{51}$$

where, $H_{Sup,t,dl,s}$, $H_{Rk(t)}$ and $\upsilon$ are the heat supplied, heat recovered and heat loss factor, respectively. In separate works by Refs. [43,78], prudential values ranging from 0.05 to 0.15 per km of pipeline have been assumed for the heat loss factor taking into consideration the low and high heat loss rates, respectively. Since the CHP-DG sites are to be located close to the consumers, then the heat loss is expected to be minimal, and therefore, $\upsilon$ is taken as 0.05 in this study. The overall discounted net present value of the revenues is obtained according to Eqn. (52).

$$\mathrm{Rev}^{CHP} = \mathrm{Rev_1}^{CHP} + \mathrm{Rev_2}^{CHP} \tag{52}$$

*5.1.2. Costs stream for the DISCO*

The total operating costs for the implementation of CHP integration by the DISCO comprise of various cash outflow channels including the cost of the purchase of power from the upstream grid, investment, operation, and maintenance costs as well as cost due to environmental emission penalty incurred.

*5.1.2.1. Cost of power purchased from the grid.* To ensure security and avoid reverse power flow in the network, the total installed capacity (size) of the CHP-based DG should be less than the total connected load power at every loading condition. Therefore, to ensure the reliability of power to consumers, the shortfall in the energy demand should be purchased from the upstream grid. The cost of energy purchased is determined as in Eqn. 53

$${C_P}^{CHP} = \sum_{t=0}^{T} \frac{1}{(1+d)^t} \sum_{i=1}^{N} \sum_{dl=1}^{K} \sum_{s=1}^{S} \left( P_{Di,t,dl,s} - P_{CHP,t,dl,s} + {P_{Loss,t,dl,s}}^{CHP} \right) \times \varepsilon_{s,dl} \times \tau_{s.dl} \tag{53}$$

where, $P_{CHP,t,dl,s}$ (kW) is the active power generated by the CHP in year $t$ in demand level $dl$ and season s, $P_{D,t,dl}$ (kW) is the active power demand in year $t$ in demand level $dl$ while ${P_{Loss,t,dl,s}}^{CHP}$ is the total active power loss in demand level $dl$ in year t, $\varepsilon_{s,dl}$ ($/kWh) is the wholesale price of electricity purchased from the upstream grid at demand level $dl$ in season s and $\tau_{s.dl}$ (h) is the operating time in season s and demand level dl.

*5.1.2.2. Investment cost.* The investment cost ($IC^{CHP}$) includes the capital cost for the purchase and installation of the energy generating equipment such as ICE, FC stack, inverter, heat exchanger and other accessories. It also entails the investigation fee, site preparation, construction and monitoring equipment [10]. In static DG planning, the whole investment is made at the commencement of the project. However, when considering DG planning with load growth, it is expected that new DG must be added to take care of the

load growth. Considering the addition of new DG, it is worth noting that the investment cost will be dynamically and gradually increasing with load growth. For DGs that have their lifetime greater than the planning period, a salvage value for the newly added DGs must be included in the calculation. The initial investment cost is determined according to Eqn. (54). At the beginning of the planning horizon (with no load growth (i.e., t = 0)), the incremental investment cost $\Delta IC_t^{CHP}$ is equal to zero (see Eqn. (55)) and all the investment made is equal to the initial investment cost. In the subsequent years, the value of $\Delta IC_t^{CHP}$ is determined as the product of the newly added CHP and the CHP's unit investment cost ($/kW) (see Eqn. (55)). The newly added CHP ($\Delta P_{CHP}$) is determined as the difference between the total previous year's DG capacity and the total present year's DG capacity. With little salvage value of DG units after their lifetime, the DG's initial cost is uniformly distributed through the years of economic life and by considering the planning period these costs are summed and converted to the present value using the discount rate. The total discounted investment costs are determined as in Eqn. (56).

$$IC_0^{CHP} = \left(\frac{d(1+d)^{LT}}{(1+d)^{LT}-1}\right) \times (P_{CHP} \times IC) \tag{54}$$

$$\Delta IC_t^{CHP} = \left(\frac{(1+d)^{t}-1}{d(1+d)^{t}}\right) \times (\Delta P_{CHP} \times IC) \times \left(\frac{d(1+d)^{LT}}{(1+d)^{LT}-1}\right) \tag{55}$$

$$IC^{CHP} = IC_0^{CHP} + \sum_{t=0}^{T} \Delta IC_t^{CHP} \tag{56}$$

where $P_{CHP}$ (kW) and $\Delta P_{CHP}$ (kW) are the total capacity of CHP units in the initial (base) year and the yearly incremental capacity of CHP added, $IC$ ($/kW) is the unit investment cost of CHP and $d$ is the prevailing discount rate, $LT = 20$ (years) is the lifetime of the DG and $t$ is the operating horizon ranging from 0 to 5 (years) where zero stands to the base year.

For the CHP application, it is assumed that the generated heat will be transported to the heat customer through existing water pipes, therefore there is no need for constructing or installing new water pipelines.

*5.1.2.3. Maintenance cost.* Maintenance cost $MC^{CHP}$ is a yearly cost that includes annual mechanical and electrical, inquiry and renovation costs. This cost is a function of the energy generation capability (output) of the DG and the extent (time frame) of DG usage. It changes throughout the planning horizon due to economic factors of the country where the equipment is being used. The total discounted maintenance cost is determined according to Eqn. (57).

$$MC^{CHP} = \sum_{t=0}^{T} \frac{1}{(1+d)^{t}} \sum_{s=1}^{N} \sum_{dl=1}^{K} \left(P_{CHP,t,dl,s} \times MC \times \tau_{s.dl}\right) \tag{57}$$

where $MC$ ($/kWh) is the unit maintenance cost of the CHP-DG.

*5.1.2.4. Operation cost.* The output power of a generator (such as CHP-DGs) depends on its input source (fuel). Therefore, the operation cost $OC^{CHP}$ of CHP-DG is equivalent to fuel cost. The FC stack has an in-built reformer for biogas to hydrogen conversion. The cost of fuel for the CHP is based on the consumption rate due to capacity of the DG as well as the mode of operation. Therefore, the discounted operation cost is determined according to Eqn. (58).

$$OC^{CHP} = \sum_{t=0}^{T} \frac{1}{(1+d)^{t}} \sum_{dl=1}^{K} \sum_{s=1}^{S} \left(\frac{P_{CHP,t,dl,s} \times F_c \times \tau_{s.dl} \times \delta^{CHP}}{\eta_{eCHP} \times \theta \times LHV_f}\right) \tag{58}$$

where $F_c$ is the unit cost of the fuel ($/m$^3$), $LHV_f$ is the lower heating value of the fuel in MJ/m$^3$; $\theta$ is the conversion factor from MJ to kWh (3.6 kWh/MJ); and $\eta_{eCHP}$ is the electrical efficiency of the CHP-DG while $\delta^{CHP}$ is a parameter which indicates the mode of operation of the DG (i.e., power-only or CHP operation mode). The value of this parameter is taken as 1 when operating in power-only mode. However, when the mode of operation is in CHP, this parameter is calculated according to Eqn. (59) [79].

$$\delta^{CHP} = 1 - \frac{\xi \times (\eta_{tCHP} - \eta_{eCHP})}{\eta_{bCHP}} \tag{59}$$

where $\eta_{bCHP}$ is the thermal efficiency of the replaced heat source such as a fossil-fuelled boiler; $\eta_{tCHP}$ is the overall (electrical and

**Table 5**
Economic parameters for CHP equipment.

| CHP type | IC ($/kW) [18] | MC ($/kWh) [18] | HPR (average) [6,52] |
|---|---|---|---|
| FC | 6500 | 0.038 | 1.50 |
| ICE | 2900 | 0.025 | 0.95 |

thermal) efficiency (i.e., $\eta_{eCHP} + \eta_{hCHP}$), and $\xi$ is the heat recovery efficiency. Table 5 contains the economic unit investment and maintenance costs as well as the HPR while Table 6 shows the adopted values for each of these parameters.

*5.1.2.5. Cost due to emission penalty incurred.* The environmental aspect of renewable-based DG planning could be viewed as a benefit or penalty depending on the ownership of the DG. If the DG is owned and operated by an individual investor, the emission abatement is rewarded with carbon credit. Among the costs that DISCOs pay due to energy purchased from the upstream grid are various environmental costs like pollution cost and cost of pollution control. With the inclusion of renewable based DG such as biogas/biomass CHP-DG, the environmental emission costs (EMC) incurred by the DISCOs is reduced due to limited energy purchased as well as reduction of emissions from biogas/biomass-based DGs. The total discounted annual emission (environmental) costs incurred by DISCOs due to environmental impact reduction with the biogas CHP-DG is determined according to Eqn. (60).

$$\mathrm{EMC_t}^{\mathrm{CHP}} = \sum_{t=0}^{T} \frac{1}{(1+d)^t} \sum_{i=1}^{N} \sum_{dl=1}^{K} \sum_{p=1}^{P} \sum_{s=1}^{S} \left( \left( P_{Di,t,dl,s} - P_{CHP,t,dl,s} \right) \times {EP_p}^{grid} + \left( P_{CHP,t,dl,s} \times EP_p \right) \right) \times C_p \times \tau_{s.dl} \tag{60}$$

where $EP_p$ (kg/kWh) is the emission factor of biogas combustion for each pollutant p of the CHP plant and $C_p$ ($/kg) is the emission penalty for each pollutant.

*5.1.2.6. Total cost ($).* The total cost is the summation of all costs incurred in the project over the planning horizon. It is determined as in Eqn. (61).

$${C_T}^{CHP} = {C_P}^{CHP} + {IC_P}^{CHP} + {MC_P}^{CHP} + {OC_P}^{CHP} + {EMC_P}^{CHP} \tag{61}$$

## 5.2. Levelised cost of energy ($/kWh) (LCOE)

The LCOE is a crucial economic indicator applied to assess and compare cost effectiveness of different energy generation facilities. It is determined as the ratio of the total costs spent to the useful energy generated over the planning horizon and is calculated as in Eqns. 62 [57].

$$LCOE = \frac{{C_T}^{CHP}}{E + H} \tag{62}$$

$$E = \sum_{t=0}^{T} \frac{1}{(1+d)^t} \sum_{dl=1}^{K} \sum_{s=1}^{S} \left( P_{CHP,t,dl,s} \times \tau_{s.dl} \right) \tag{63}$$

$$H = \sum_{t=0}^{T} \frac{1}{(1+d)^t} \sum_{dl=1}^{K} \sum_{s=1}^{S} \left( H_{Sup,t,dl,s} \times \tau_{s.dl} \right) \tag{64}$$

Where E (see Eqn. (63)) and H (see Eqn. (64)) are the total electric and thermal energy supplied by the CHP units in year t, season s and demand level dl. For power only, H becomes zero.

## 5.3. Environmental analysis

The cumulated emission of greenhouse gases over the planning period during power generation from the CHP-DGs are quantified and determined according to Eqn. (65). It should be noted that the carbon dioxide emitted from the combustion of biogas during power and heat production process is considered biogenic and is carbon neutral with no effect on climate change. So, the emission factor for $CO_2$ is disregarded and assumed zero. However, there are other pollutants emitted from the combustion of biogas such as sulphur dioxide ($SO_2$) and nitrogen oxide ($NO_x$).

$$\mathrm{EM_t}^{\mathrm{CHP}} = \sum_{t=0}^{T} \sum_{dl=1}^{K} \sum_{p=1}^{P} \sum_{s=1}^{S} \left( P_{CHP.t,dl,s} \times EP_p \times \tau_{s,dl} \right) \tag{65}$$

The $EP_p$ (kg/kWh) of these pollutants and their corresponding penalty $C_p$ ($/kg) values are given in the following Table 7.

**Table 6**
Performance parameters for the CHP equipment.

| | ($\eta_{eCHP}$) [52] | | ($\eta_{tCHP}$) [52] | | $\eta_{bCHP}$ [79] | $\xi$ [76] |
|---|---|---|---|---|---|---|
| CHP equipment | FC | ICE | FC | ICE | – | – |
| Range value | 30–63 % | 27–41 % | 55–80 % | 77–80 % | – | 45–80 % |
| Adopted value | 60 % | 35 % | 75 % | 80 % | 60 % | 60 % |

**Table 7**
Emission potentials and penalty values.

| Pollutants (p) | | $CO_2$ | $NO_x$ | $SO_2$ |
|---|---|---|---|---|
| $EP_p$ (kg/kWh) | Grid [80] | 0.9212461 | 0.00230 | 0.00526 |
| | CHP [81] | – | 0.00194 | 0.00009 |
| $C_p$ ($/kg) [8] | | 0.0147400 | 0.94438 | 1.56096 |

## 6. Particle swarm optimisation algorithm (PSO)

This section describes the particle swarm optimisation algorithm.

### 6.1. The particle swarm optimisation PSO

The PSO is a population-based nature inspired swarm intelligence computational technique proposed by Kennedy and Eberhart in 1995 [82] to solve complex optimisation problems. The philosophy behind PSO follows the social and cooperative activities among some creatures such as birds and fishes that search for their food in flocks. This cooperative activity enables the birds or fishes to expend less effort in search of food as there is information sharing among them during the search process. In PSO, each particle has a position and it moves with a velocity in a particular direction in the search space. Therefore, there are vector components that identify *ith* particle $(i = 1, 2, ...., N)$ velocity and position. In short in a D-dimensional search space, velocity vector $v_i = (v_{i1}, v_{i2}, v_{i3}, ..., v_{iD})$, while the position vector $x_i = (x_{i1}, x_{i2}, x_{i3}, ..., x_{iD})$. The value N represents the particle population number or swarm size. During the search process, each particle updates its position using its previous position and new information about the velocity. During this position update, two best positions (i.e., personal best (*pbest*) and global best (*gbest*)) emerge among the particles. The best position found for a particle *i* in the search space so far is called *pbest* while the best position found for all the particles in the swarm is called *gbest*. After identifying these two best values, the particle updates its velocity and position according to Eqns. 66 and 67, respectively.

$$v_{iD}{}^{(k+1)} = w \times v_{iD}{}^{(k)} + c_1 \times r_1 \times \left(pbest_{iD}{}^{(k)} - x_{iD}{}^{(k)}\right) + c_2 \times r_2 \times \left(gbest^{(k)} - x_{iD}{}^{(k)}\right) \tag{66}$$

$$x_{iD}{}^{(k+1)} = x_{iD}{}^{(k)} + v_{iD}{}^{(k+1)} \tag{67}$$

where, $v_{iD}{}^{(k)}$ is the velocity of the *ith* particle at *Dth* dimension in *kth* iteration, $x_{iD}{}^{(k)}$ is the previous position of *ith* particle at *Dth* dimension, *w* is the inertia weight while $r_1$ and $r_2$ are random numbers uniformly generated in the range [0,1]. The particle position is bounded by the upper and lower limits of the decision variables while the velocity is bounded with the range of minimum ($v_{\min}$) and maximum ($v_{\max}$) $[v_{\min}\ v_{\max}]$ to reduce the possibility of the particle not leaving the search space, where $v_{\min}$ is usually taken as a negative fraction (such as 0.1) of $v_{\max}$. The parameters $c_1$ and $c_2$ represent the acceleration coefficients (i.e., cognitive and social, respectively). It is clear from the above equations that the flight process of a particle in every iteration depends on three control parameters such as inertia weight, acceleration coefficient and random numbers. Therefore, performance of PSO is highly dependent on these parameters. The acceleration coefficient influences the movement of the particle towards its *pbest* and the *gbest* of the swarm, the two random numbers $r_1$ and $r_2$ influence the convergence of a swarm [83] while the inertia weight ensures a trade-off between the local search ability (exploitation) and global search ability (exploration) during the optimisation process [84]. It is known that PSO suffers from local optima and premature convergence problems therefore adequate selection of the control parameters (inertia weight and acceleration coefficients) can play a significant role in achieving a global or near-global optimal solution.

In standard PSO, linearly decreasing inertia weight is applied while the acceleration coefficients are taken as constant values i.e., $c_1 = c_2 = 2$. It been argued that in order to accelerate the convergence, the acceleration coefficients may be unequal as a larger value should be assigned to $c_2$ than $c_1$ such that the new position of a particle will be closer to the global best position *gbest* [85]. The acceleration coefficient could also be selected randomly since randomisation can enable the search process to prevent the solution from being stuck in local optima [86]. In 2002, Ref [87] introduced a constriction factor $\kappa$ ($\kappa = 0.7298$) as a multiplier to the velocity equation in the standard PSO in order to enhance the convergence rate. Based on this premise, an improved PSO is formulated with adaptively decreasing inertia weight and a randomised acceleration coefficient with a constriction factor and applied to solve the EDSEP problem.

### 6.2. Proposed improved particle swarm optimisation (IPSO)

As previously mentioned, the proposed IPSO combines an adaptive inertia weight with a randomised acceleration coefficient in order to avoid local optima entrapment and achieve global search ability.

#### 6.2.1. Adaptive decreasing inertia weight (ADIW)

The approaches for selecting inertia weight (*w*) fall into linear time varying [21], non-linear time varying [88], and adaptively adjusted methods [89]. Generally, a larger inertia weight is applied at the beginning of the search process to ensure global exploration and the value is reduced towards the end of the search process for local exploitation. However, the success rate of the particle in each iteration is not captured. Therefore, taking a cue from Nickabadi et al. [89], an adaptive inertia weight that combines the success rate

and the decreasing inertia weight for local search is adopted. According to Ref. [89], high value of success rate implies that there is the possibility that the particles have converged to a point that is far from the optimum and the whole particle population is gradually moving towards the optimal solution. However, when there is low success rate, the particles tend to swing within the area of the optimum point with little or no success rate. For a minimisation problem, the rate of success of the $i$ th particle at the $k$ th iteration is expressed as Eqn. (68).

$$\theta_i(k) = \begin{cases} 1, f(pbest_i(k)) < f(pbest_i(k-1)) \\ 0, f(pbest_i(k)) = f(pbest_i(k-1)) \end{cases} \tag{68}$$

where $pbest_i(k)$ is the personal best position of the $i$th particle so far until the $k$th generation, $pbest_i(k-1)$ the previous personal best position until $pbest_i(k)$ is found, $f(\cdot)$ is the fitness of the objective function being optimised. Hence, the success rate of the entire population is given by Eqn. (69).

$$\psi(k) = k_{\max}^{-1} \times \sum_{i=1}^{n} \theta_i(k) \tag{69}$$

where, $k_{\max}$ is the maximum value of the iteration, $n$ the population size, and $\psi(k) \in [0\ 1]$ is the ratio of the number of particles numbers which have produced better fitness values in the previous generation. According to the success rate the inertia weight is linearly and adaptively changing as the iteration progresses according to Eqn. (70).

$$w_{new}(k) = w_{\max} - (\psi(k) \times (w_{\max} - w_{\min})) \tag{70}$$

where, $w_{\max}$ and $w_{\min}$ are the maximum and minimum inertia weights, $k$ and $k_{\max}$ are the current iteration and maximum iteration, respectively

### 6.2.2. Random acceleration co-efficient

In this paper, a weight randomised acceleration coefficient factor like the randomisation parameter in firefly algorithm is applied. The proposed weighted randomised acceleration coefficients are presented as in Eqns. (71) and (72), respectively

$$c_{1new} = \alpha_1 \times (r_3(0,1) - 0.5) \tag{71}$$

$$c_{2new} = \alpha_2 \times (r_4(0,1) - 0.5) \tag{72}$$

Where, $\alpha_1$ and $\alpha_2$ are respectively non-negative randomisation weights while $r_3$ and $r_4$ are two independent uniformly generated random numbers in the range of [0, 1].

Therefore, the new equation for velocity and position updates are shown in Eqns. (73) and (74), respectively.

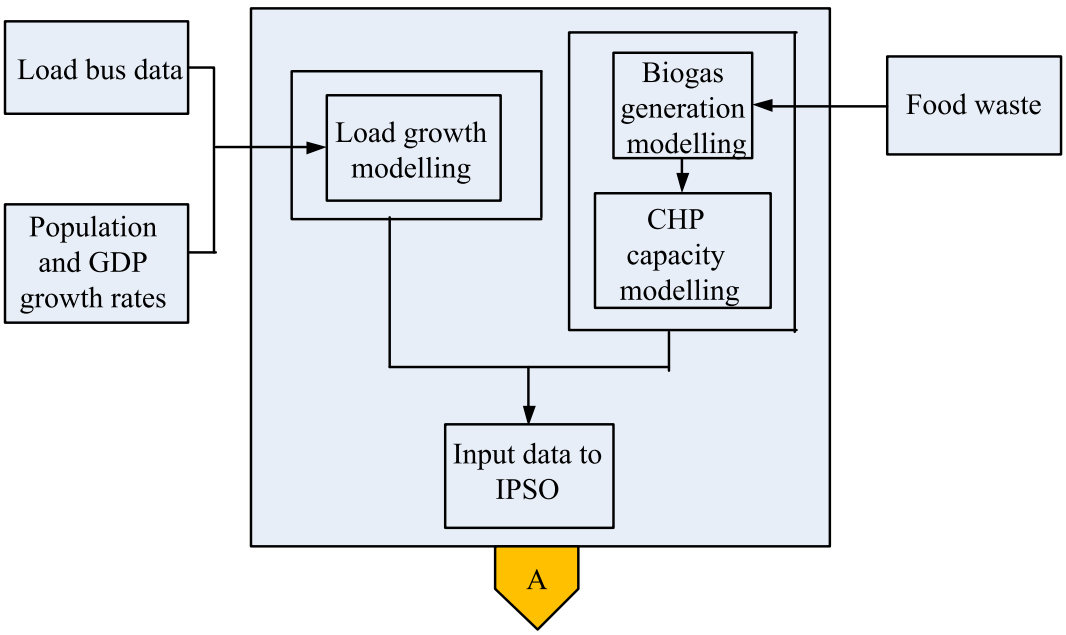


**Fig. 3.** Input data generation for the IPSO algorithm.

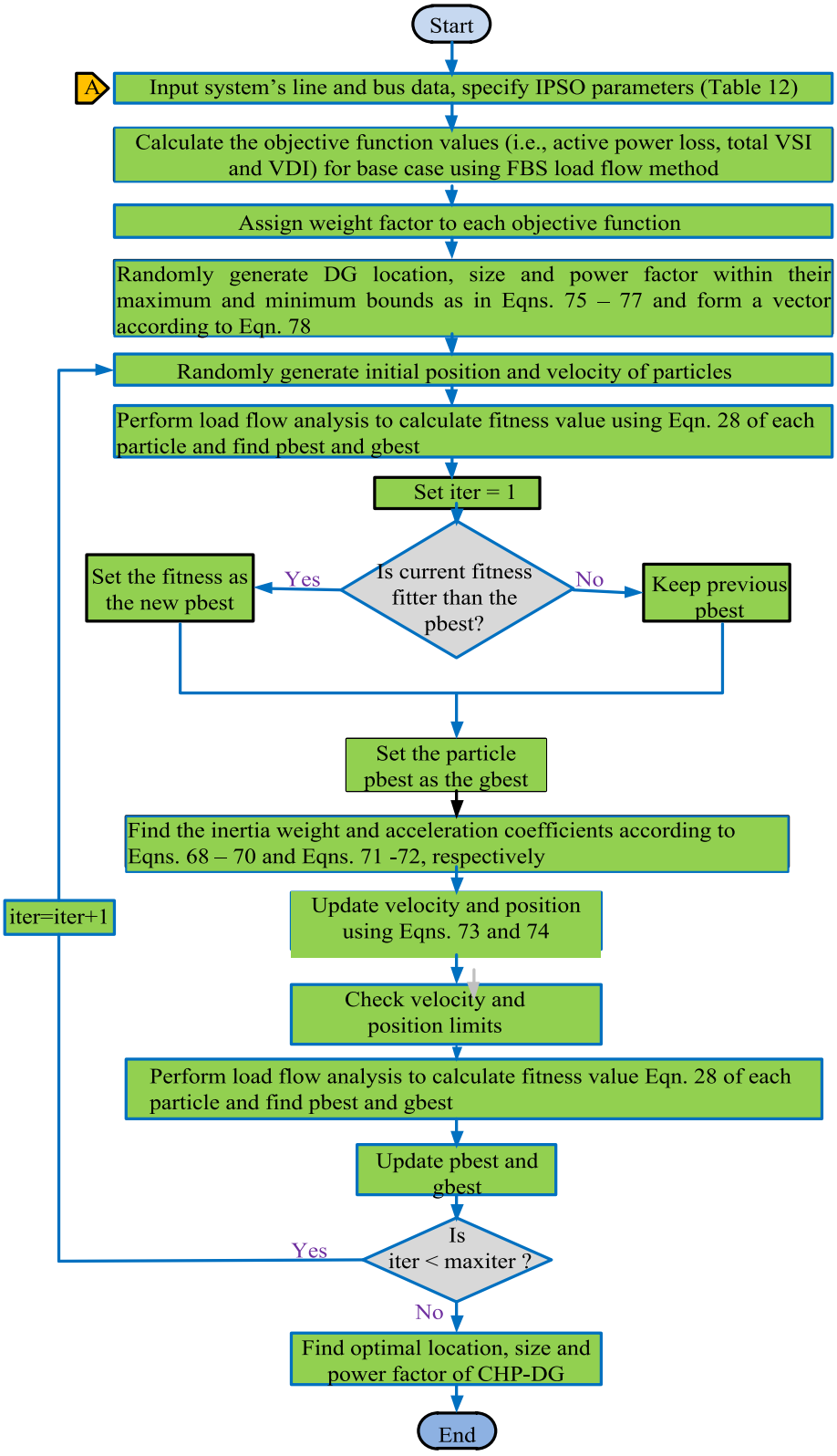


**Fig. 4.** Flowchart of the proposed IPSO for optimal location and capacity determination of biogas CHP-DG.

$$v_{iD}^{(k+1)} = \kappa \times \left[ w_{new} \times v_{iD}^{(k)} + c_{1new} \times r_1 \times \left( pbest_{iD}^{(k)} - x_{iD}^{(k)} \right) + c_{2new} \times r_2 \times \left( gbest^{(k)} - x_{iD}^{(k)} \right) \right] \tag{73}$$

$$x_{iD}^{(k+1)} = x_{iD}^{(k)} + v_{iD}^{(k+1)} \tag{74}$$

## 7. Application of the proposed method to a case study

Due to the mixed integer nature of the problem, active power capacity (size) ($P_{CHP-DG(i)}$), location ($Loc_{CHP-DG(i)}$) and power factor ($pf_{CHP-DG(i)}$) of the CHP-DGs are initially randomly generated within their upper and lower limits according to Eqns. (75)–(77).

$$P_{CHP-DG(i)} = P_{CHP-DG(i)}^{\min} + rand\left( P_{CHP-DG(i)}^{\max} - P_{CHP-DG(i)}^{\min} \right) \tag{75}$$

$$Loc_{CHP-DG(i)} = round\left( Loc_{CHP-DG(i)}^{\min} + rand\left( Loc_{CHP-DG(i)}^{\max} - Loc_{CHP-DG(i)}^{\min} \right) \right) \tag{76}$$

$$pf_{CHP-DG(i)} = pf_{CHP-DG(i)}^{\min} + rand\left( pf_{CHP-DG(i)}^{\max} - pf_{CHP-DG(i)}^{\min} \right) \tag{77}$$

A vector comprising these three parameters will be formed according to Eqn. 78

$$X = \left[ P_{CHP-DG1}, P_{CHP-DG2}, ...., P_{CHP-DG(NDG)}, Loc_{CHP-DG1}, Loc_{CHP-DG2}, ...., Loc_{CHP-DG(NDG)}, pf_{CHP-DG1}, pf_{CHP-DG1}, ...., pf_{CHP-DG(NDG)} \right] \tag{78}$$

The reactive power component is determined as shown in Eqn. (79).

$$Q_{CHP-DG(i)} = P_{CHP-DG(i)} \tan\left( \cos^{-1} pf_{CHP-DG(i)} \right) \tag{79}$$

Fig. 3 shows the block diagram for the generation of input data for the CHP equipment while Fig. 4 presents the flowchart for IPSO implementation.

### 7.1. Case study

The proposed IPSO was applied to determine the optimal location and capacity of FC and ICE for a medium-scale distribution network considering typical townships in South Africa called South-western townships (Soweto). The coordinates of Soweto are 26°15′58″ South and 27°57′37″ East. It is located in the City of Johannesburg and is about 43 % of the population of Johannesburg [90]. The population of Johannesburg is estimated to be 5.783 million [91]. Soweto is the largest township in the whole of South Africa and its estimated population was about 1.9 million as of 2019 [90]. Due to the presence of mining activities, it receives influxes of people for business and industrial means, the present population must have surpassed that of 2019. It is dominated by blacks with the tradition of eating cooked food. The huge population of this township is a plus for its food waste potential which is the feedstock for biogas production. Of note is the proximity of Soweto to one of the four functional landfill sites (LSs) in Johannesburg which is an important factor for setting up a biogas plant facility and a major element for selecting Soweto as the case study in this paper. Table 8 shows the data for determining the food and biogas generation potentials as well as the electric capacity of FC and ICE units.

The IEEE 69 bus distribution network is employed to test the applicability of the proposed method. Although real network of Soweto would have been more appropriate to be applied, due to a lack of detailed network data that could serve the purpose of this study, the IEEE 69 bus system being an established universal medium scale distribution network for any location is employed. In this system, bus 1 is considered as a slack (reference) bus from where the external grid is connected, and the rest buses are considered as candidate buses for DG integration. The base voltage of this network is 12.66 kV, base apparent power is 100 MVA while the total active and reactive load demands are 3.8019 MW and 2.6941 MVAr, respectively. The technical data of this network can be found in Ref. [93].

Due to metropolitan nature of Soweto, the load demands are modelled as a mixture of residential, commercial, and small-scale industrial loads. The active and reactive load exponents presented in Table 3 represent a typical seasonal load model for a medium voltage distribution network in South Africa. The load demand varies due to seasonal variations. Van der Walt and Fitchett [94] have statistically classified South African seasons into four seasonal brackets such as summer (October to March), early autumn (April) and late autumn (May), winter (June to August), and spring (September). The load demand differs along the time-of-use periods (TOU) -

**Table 8**
Data for calculating the biogas potential and capacity of each DG.

| Population size | Population growth rate | GDP growth rate | Per capita food waste (kg/capita/week) | Waste collection rate |
|---|---|---|---|---|
| 2.487[a] million [55] | 2.63 % [55] | 2.26 % [55] | 0.22 [92] | 69 % [55] |

[a] is determined as $(0.43 \times 5.783)$ million.

peak, the standard and the off-peak periods based on the variability of utilisation as a result of activity and appliance usage as well as seasonal impact. Considering a typical day and night in each season and based on the seasonal classification made by Ref. [94] as well as seasonal load demand, it is assumed that the distribution network is lightly (low load level) loaded in the summer night, moderately loaded (base load level) in the summer day and winter night, and highly loaded (high load level) especially in winter day. The autumn and spring are transitional seasons between summer and winter. According to Table 3, autumn and spring seasons are not separately considered. The reason may be due to their transitional characteristics in which autumn has a feature of winter (i.e., mild coldness) while spring has a feature of summer (i.e., mild warmth). Therefore, it is assumed that the distribution network in autumn is subjected to a loading equivalent to low-load level in winter night. Similarly, in spring season, the distribution network loading is assumed to be equivalent to lightly-loaded summer day. The discrete values of the loading levels (i.e., *dl*) are presented in Table 2. According to the recent release by National Energy Regulator of South Africa (NERSA) and the main electricity utility (i.e., ESKOM), the wholesale and retail energy tariff for a typical province in South Africa are depicted in Tables 9 and 10, respectively.

Again, the biogas, being the fuel for powering the CHP equipment, is assumed to have been purified to the standard of natural gas. The price of biogas is taken as 0.15 $/m$^3$ an equivalent of natural gas price [79]. The heating value of purified biogas is taken as 37.2 MJ/m$^3$ while the conversion factor is 3.6 kWh/MJ.

The cost of heat is mostly considered as a fraction of the electricity cost. In Ref. [6], the heat cost is taken as 40 % of electricity cost while [18] assumed 60 % of electricity cost. In this paper, 50 % of electricity cost is considered for heat selling price at all seasons and load levels. Also, 15 h (i.e., 4.00–19.00 h) are considered for the daytime while 9 h (i.e., 19.00–4.00 h) make up the night-time, and are repeated for all days and nights of the seasons. Table 11 depicts the breakdown of seasonal hours for days and nights in a year.

The proposed algorithm was implemented in self-written codes in MATLAB 2021b software and the simulation is done on Intel core i5-4200U 1.6 GHz 8 GB RAM Laptop computer.

### 7.2. General assumptions and limitation

The following assumptions and limitations are made for this study.

1) The CHP-DGs are implemented mathematically as a negative load.
2) The test RDN is examined under balance operating conditions.
3) The effect of harmonics injected by inverter-based DG such as FC on the test network is neglected.
4) The heat generated by CHP units is considered as a by-product of energy conversion system for the CHP-DGs
5) Prior to CHP installation, no heat is bought from external boiler and the DISCO does not have any boiler to sell heat to the consumers and heat demand utilisation at the consumer end is not considered.
6) Only electric distribution network is considered.
7) DGs are installed at the PQ buses for load flow purposes.
8) The ICE is operated at an optimal power factor in the range of 0.8–1 while FC is operated at unity power factor.
9) Maximum of three CHP- DGs are to be connected to the distribution system
10) The CHP-DG capacity is limited within 100 kW and $\lambda \sum_{i=1}^{nb} P_{Di}$ kW (see section 4.3.2.3).
11) A discount rate of 12 % is assumed for the economic analysis.
12) All the heat power demand after pipeline losses is sold to the consumers.
13) The biogas plant is located in the study area and is owned and operated by an independent investor, therefore the cost of biogas production is not included.
14) The information regarding the setting of parameters for the IPSO and PSO is given in Table 12

## 8. Results and discussion

The results for the biogas and CHP-DG (i.e., ICE and FCs) capacity for the selected study area as well as the impact of integrating these DGs on the distribution network are presented. The impact on the distribution network is in two cases: mono and multi-objective optimisation. In the first case, only total active power loss is minimised for constant and seasonal voltage dependent mixed load model while in the second case the total active power losses, voltage stability and voltage deviation are simultaneously minimised.

### 8.1. DG electric capacity potential determination

Using data presented in Table 6, Eqns. (1)–(7), and Ref [55], the food waste potential, biogas potential and electric power capacities of FC and ICE over the operating time horizon of five years for Soweto townships are estimated and the results are presented in

**Table 9**
Seasonal wholesale electricity rates ($/kWh) [95].

| Low demand (Summer) | | | High demand (Winter) | | |
|---|---|---|---|---|---|
| Low (Off peak) | Base (Standard) | High (Peak) | Low (Off peak) | Base (Standard) | High (Peak) |
| 0.02617 | 0.03664 | 0.06517 | 0.03617 | 0.03925 | 0.15703 |

R 19.231 to 1 $ as at 23/05/23.

**Table 10**
Seasonal retail electricity rates ($/kWh) for various customers [96].

| Load type | Summer | | | Winter | | |
|---|---|---|---|---|---|---|
| | Low | Base | High | Low | Base | High |
| Residential | 0.0688 | 0.0875 | 0.1106 | 0.0736 | 0.1042 | 0.2544 |
| Commercial | 0.1523 | 0.1523 | 0.1523 | 0.1567 | 0.1567 | 0.1567 |
| Industrial | 0.0626 | 0.0814 | 0.1081 | 0.0673 | 0.0982 | 0.2573 |
| Mixed (average) | 0.0946 | 0.1071 | 0.1237 | 0.0992 | 0.1197 | 0.2228 |

R 19.231 to 1 $ as at 23/05/23.

**Table 11**
Seasonal time duration.

| Time duration | Seasons | | | |
|---|---|---|---|---|
| | Summer | Autumn | Spring | Winter |
| Day (hours) | 2730 | 915 | 450 | 1380 |
| Night (hours) | 1638 | 549 | 270 | 828 |

**Table 12**
The parameters for the IPSO and PSO.

| Methods | Population size | $k_{max}$ | $w_{min}$ | $w_{max}$ | $v_{max}$ | $v_{min}$ | $\alpha_1$ | $\alpha_2$ |
|---|---|---|---|---|---|---|---|---|
| IPSO | 50 | 100 | 0.4 | 0.9 | 1.125 × range | $-0.8v_{max}$ | 1.5 | 2.5 |
| PSO | 50 | 100 | 0.4 | 0.9 | range | $-0.1v_{max}$ | – | – |

**Table 13**
Estimated food waste, biogas potential and electric and heat power capacity of FC and ICE for Soweto Township.

| Year | Base | 1 | 2 | 3 | 4 | 5 |
|---|---|---|---|---|---|---|
| FW potential (kilotons/annum) | 19.6289 | 20.6005 | 21.6201 | 22.6901 | 23.8132 | 24.9918 |
| Biogas potential (x $10^6$ $m^3$/annum) | 6.9094 | 7.2514 | 7.6103 | 7.9870 | 8.3823 | 8.7972 |
| CHP type | Maximum power capacity of each CHP per year ($P_{max\ t,k}^{CHP}$) (kW) | | | | | |
| ICE | 3123.64 | 3278.24 | 3440.49 | 3610.78 | 3789.49 | 3977.05 |
| FC | 3573.25 | 3750.11 | 3935.72 | 4130.51 | 4334.95 | 4549.51 |

Table 13.

It is observed from Table 13 that both CHP-DGs have the potential capacities to feed the load buses of the selected network. Since the maximum active power capacity of each CHP-DG is comparable to the total active power demand (i.e., 3801.9 kW) of the IEEE 69 bus network. Therefore, the capacity limit of the DG is rated between 100 kW and the values in rows 5 and 6 of Table 13 for each year of the planning horizon.

### 8.2. Network performance analysis

In this section, two categories are investigated. Each category has two scenarios and each scenario has two cases. In category one, constant power load model is investigated under single objective optimisation scenario for case (a) FC-based CHP operating at unity power factor and case (b) ICE-based CHP operating at optimal power factor. In scenario 2 of category one, multi-objective optimisation for constant load model for case (a) and case (b). In Category 2, the seasonal mixed voltage dependent load model considering single and multi-objective optimisation scenarios as stated in category 1 are investigated.

**Table 14**
Results for load demand and system performance parameters for constant load without DGs.

| Year | $P_{Di(t)}$ (MW) | $Q_{Di(t)}$ (MW) | $PL^0$ (kW) | $VSI^0$ (pu) | $VD^0$ p.u | $V_{min}$ (bus) |
|---|---|---|---|---|---|---|
| Base (0) | 3.801890 | 2.694100 | 224.960628 | 61.224136 | 0.0995772 | 0.9090065 (65) |
| 1 | 3.985543 | 2.824241 | 249.469320 | 60.898899 | 0.1103917 | 0.9041291 (65) |
| 2 | 4.178067 | 2.960666 | 276.813583 | 60.557992 | 0.1224506 | 0.8989568 (65) |
| 3 | 4.379890 | 3.103684 | 307.354625 | 60.200628 | 0.1359109 | 0.8934674 (65) |
| 4 | 4.591464 | 3.253609 | 341.506874 | 59.825973 | 0.1509528 | 0.8876359 (65) |
| 5 | 4.813258 | 3.410777 | 379.747546 | 59.433133 | 0.1677829 | 0.8814349 (65) |

*8.2.1. Category 1: Constant power load model*

Here performance of the system before and after the installation of FCs and ICE-based DGs to the distribution network under constant load models with an estimated load growth of 4.83 % over a five-year operation horizon is investigated. Before optimisation with no CHP-DG, the performance metrics of the system over an operating time of five years are displayed in Table 14.

A look at Table 14 shows that as the load increases from 3.80189 MW to 4.813258 MW, all the network parameters keeps deteriorating and the impact on the network indicates a decrease in total voltage stability, an increase in voltage deviation and a decline in voltage profile from the acceptable limit of 0.95 p.u. Since the line parameters (i.e., resistance and reactance) remain the same, the increase in load demand will cause an increase in the line current $I$ drawn by the connected loads thereby increasing the active power loss $I^2R$ of the line over the years. Active power loss is the major cause of revenue loss to the DISCOs. However, the integration of DG can adequately ameliorate this issue which is investigated in the following scenarios and cases.

*8.2.1.1. Scenario 1: CHP-DG placement for active power loss minimisation only.* Due to the stochastic nature of the proposed optimisation algorithm, the algorithm is subjected to twenty (20) runs with 100 iterations for each run. The run with minimum fitness value is taken as the best result. In this scenario, the proposed optimisation algorithm is applied to determine the site and size of CHP-DG by singly minimising the total active power loss under two operating cases: Case 1 (FC–CHP) and Case 2 (ICE-CHP). The optimised results for both cases are reported as tabulated in Table 15.

According to Table 15, the allocation of FCs (i.e., Case 1) at buses **61, 11, 18** is able to reduce the total active power loss from the initial 224.960628 kW before CHP-DG integration to 69.4100178 kW in the base year prior to load growth which is about 69.15 % reduction. As the load grows, and with the integration of the FC, the power loss reduction improved from 69.15 % to 70.41 % in the final year. Similarly, when the ICEs (i.e., Case 2) are located in buses **61, 11, 18** and operated at optimal factors of 0.8139, 0.8135, and 0.8333, respectively, the total active power loss is reduced to 4.26668492 kW in the base year in comparison with 224.960628 kW prior to the integration of the DG which is 98.10 % loss reduction. Other network parameters such as the total voltage deviation (VD) and total voltage stability index (VSI) are equally improved with the integration of both CHP-DGs into the network. For FC and ICE -based CHP-DG, the total VD records about 94.40–94.64 % and 99.871–99.877 % improvement, respectively from base year till fifth year. Similarly, the total VSI increases from 8.183 to 10.693 % for FC based CHP-DG and 10.647–13.869 % for ICE based CHP-DG between the base year and the last year of planning horizon. It is clear from these results that operating DG at optimal power factor reduces the network losses and improves the performance of system parameters better than operating the DG at unity.

To test the effectiveness of the proposed IPSO, the results obtained for the base year (no load growth) are used to compare with standard PSO and other optimisation techniques found in literature. The comparison results are tabulated in Table 16 and Table 17 for Case 1 and Case 2, respectively.

A look at Table 16 shows that for FC based CHP-DG operating at unity pf (i.e., Case 1), the total active power loss is reduced to 69.4100 kW (69.15 %) which is less than that from SOS-NNA [49], Heuristic [2], APSO [72], MGSA [72], LSF-SCA [97], WOA [4], OCDE [98], Hybrid-PSO [99], DE [48], ALO [100], HFEO [101], and BWO [8] but has an approximate value to that from IHHO [22]. Similarly, from Table 17 for ICE based CHP-DG operating at optimal pf (i.e., Case 2), the proposed IPSO finds the optimal locations, sizes, and optimal PFs with a reduced total active power loss of 4.2667 kW (98.10% reduction), which is lower than most of other reported methods such as SOS-NNA [49], APSO [72], MGSA [72], IHHO [22], LSF-SCA [97], DE [48], I-GWO [104] and PSO except for I-GWOPSO [104] which gives a slightly better power loss reduction than the proposed IPSO. However, for other parameters (i.e., VSI and VD) the proposed method returns better results than other methods. By and large, it could be inferred that the results achieved by the proposed IPSO technique in this study, are highly competitive, effective, and more efficient in comparison with the standard PSO and other state-of-the-art algorithms reported in literature. This thereby validates the novelty and the capability of the proposed IPSO to find optimal locations and sizes for FC and ICE based CHP-DG as well as the optimal pf with the objective of minimising the total active power loss while improving the voltage profile and other system parameters of the distribution network.

**Table 15**
Results for optimal location, power factor and capacity of FC and ICE for constant load model for loss minimisation only.

| Year | $PL^{DG}$ (kW) | $VSI^{DG}$ (p.u) | $VD^{DG}$ (p.u) | $V_{min}$ (bus) | Capacity/location | | |
|---|---|---|---|---|---|---|---|
| Case 1: Allocation of 3 FC @ unity power factor | | | | | FC (kW)/bus/pf | FC (kW)/bus/pf | FC (kW)/bus/pf |
| Base | 69.410018 | 66.234227 | 0.0055754 | 0.97794695 (65) | 1718.9659/**61**/1.0 | 526.8271/**11**/1.0 | 380.0522/**18**/1.0 |
| 1 | 76.414124 | 66.152485 | 0.0061343 | 0.97685335 (65) | 1804.4600/**61**/1.0 | 554.0489/**11**/1.0 | 398.5127/**18**/1.0 |
| 2 | 84.132706 | 66.068345 | 0.0067439 | 0.97570080 (65) | 1894.1412/**61**/1.0 | 582.9305/**11**/1.0 | 418.3197/**18**/1.0 |
| 3 | 92.639841 | 65.978103 | 0.0074271 | 0.97449610 (65) | 1988.8411/**61**/1.0 | 613.0908/11/1.0 | 438.1845/18/1.0 |
| 4 | 102.019126 | 65.831185 | 0.0081746 | 0.97322633 (65) | 2088.2206/61/1.0 | 644.9171/11/1.0 | 459.6768/18/1.0 |
| 5 | 112.356588 | 65.788276 | 0.0089945 | 0.97189138 (65) | 2192.7459/**61**/1.0 | 678.9174/**11**/1.0 | 481.8331/**18**/1.0 |
| Case 2: Allocation of 3 ICE @ optimal power factor | | | | | ICE (kW)/bus/pf | ICE (kW)/bus/pf | ICE (kW)/bus/pf |
| Base | 4.26668492 | 67.742803 | 0.000128685 | 0.99426198 (50) | 1674.3294/**61**/0.8139 | 494.5437/**11**/0.8135 | 378.7676/**18**/0.8333 |
| 1 | 4.69057046 | 67.730584 | 0.000141376 | 0.99398259 (50) | 1755.3008/**61**/0.8139 | 518.4682/**11**/0.8135 | 397.0999/**18**/0.8333 |
| 2 | 5.15666088 | 67.717795 | 0.000155318 | 0.99368949 (50) | 1840.1930/**61**/0.8139 | 543.5528/**11**/0.8135 | 416.3202/**18**/0.8333 |
| 3 | 5.67124178 | 67.704123 | 0.000170874 | 0.99338199 (50) | 1929.1958/**61**/0.8139 | 569.6786/**11**/0.8135 | 436.6518/**18**/0.8333 |
| 4 | 6.23274576 | 67.690402 | 0.000187454 | 0.99305937 (50) | 2022.5092/**61**/0.8139 | 597.4285/**11**/0.8135 | 457.6030/**18**/0.8333 |
| 5 | 6.85248646 | 67.675746 | 0.000205930 | 0.99272087 (50) | 2120.3423/**61**/0.8139 | 626.3406/**11**/0.8135 | 479.7587/**18**/0.8333 |

**Table 16**
Comparative results of DG allocation for active power loss minimisation for unity factor (such as FC-DG).

| Method | Bus No | DG capacity (kW) | Total DG size (kW) | RPL (kW) | % Loss Reduction | VDI (p.u) | min (VSI) (p.u) |
|---|---|---|---|---|---|---|---|
| Base case | – | – | – | 224.9606 | – | 0.0995772 | 0.6833 |
| SOS-NNA [49] | 11, 18, 61 | 526.80, 380.30, 1719.00 | 2626.10 | 69.4284 | 69.14 | **0.0052010** | 0.9185 |
| Heuristic [2] | 61, 21, 12 | 1689.00, 312.00, 471.00 | 2472.00 | 69.7000 | – | – | – |
| APSO [72] | 17, 61, 64 | 536.27, 1173.75, 522.81 | 2232.83 | 71.7100 | – | – | – |
| MGSA [72] | 15, 61, 63 | 562.65, 1190.11, 523.31 | 2275.64 | 71.9000 | – | – | – |
| LSF-SCA [97] | 11, 18, 61 | 522.22, 396.24, 1711.40 | 2629.86 | 69.4200 | – | – | – |
| WOA [4] | 66, 18, 61 | 459.80, 399.60, 1727,00 | 2586.40 | 69.6900 | – | – | – |
| OCDE [98] | 11, 18, 61 | 525.93, 380.18, 1718.96 | 2625,07 | 69.4360 | – | – | – |
| Hybrid-PSO [99] | 11, 17, 61 | 510.00, 380.00, 1670.00 | 2560.00 | 69.5400 | 69.09 | – | – |
| IHHO [22] | 11, 17, 61 | 527.20, 382.50, 1719.40 | 2629.10 | 69.4100 | – | – | – |
| DE [48] | 61, 18, 11 | 1718.70, 381.10, 525.20 | 2625.00 | 69.4230 | 69.15 | – | – |
| ALO [100] | 61,17, 65 | 1324.90, 451.60, 270.30 | 2046.80 | 70.5100 | 68.67 | – | – |
| HFEO [101] | 66, 19,61 | 770.20, 530.50, 1748.30 | 3049.00 | 72.9450 | – | – | – |
| BWO [8] | 11, 17, 61 | 502.00, 404.00, 1751.00 | 2657.00 | 69.4500 | 69.13 | – | – |
| TSO [102] | 9, 22, 61 | 825.09, 405.14, 1050.10 | 2280.33 | 70.2500 | – | | |
| OTCDE [103] | 11, 18, 61 | 526.84, 380.35, 1718.97 | 2626.16 | 69.4280 | 69.14 | – | – |
| IPSO [85] | 11, 18, 61 | 526.80, 380.00, 1718.90 | 2625.70 | 69.4020 | 69.16 | – | – |
| Standard PSO | 18, 11, 61 | 382.71, 527.57, 1718.99 | 2629.27 | 69.4104 | 69.14 | 0.0055293 | 0.9186 |
| **Proposed IPSO** | **61, 11, 18** | 1718.97, 526.83, 380.05 | **2625.85** | **69.4100** | **69.15** | 0.0055754 | 0.9185 |

**Table 17**
Comparative results for active power loss minimisation only with optimal power factor DG (such as ICE-DG).

| Method | Bus No | DG capacity kVA (pf) | Total DG size (kVA) | RPL (kW) | % Loss Reduction | TVD (p.u) | Min (VSI) (p.u) |
|---|---|---|---|---|---|---|---|
| Base case | – | – | – | 224.961 | – | 0.099577 | 0.6833 |
| SOS-NNA [49] | 11, 18, 61 | 607.76(0.8120), 456.18(0.8330), 2059.41 (0.8130) | 3123.35 | 4.2676 | 98.10 | **0.000127** | 0.9772 |
| APSO [72] | 17, 61, 64 | 633.55(0.8302), 1633.57(0.7756), 485.45 (0.9051) | 2752.57 | 6.6000 | – | – | – |
| MGSA [72] | 17, 61, 64 | 761.29(0.7895), 1357.22(0.7153), 801.20 (0.9023) | 2919.71 | 8.6100 | – | – | – |
| IHHO [22] | 11, 18, 61 | 536.71(0.8500), 474.63(0.8200), 2066.02 (0.8300) | 3077.36 | 4.4400 | – | – | – |
| LSF-SCA [97] | 11, 18, 61 | 595.93(0.8200), 459.03(0.8300), 2063.68 (0.8100) | 3118.65 | 4.2700 | 98.10 | – | – |
| DE [48] | 61, 18, 11 | 2057.80(0.8140), 454.90(0.8340), 608.80 (0.8130) | 3121.50 | 4.2680 | 98.10 | – | – |
| TSO [102] | 12, 59, 61 | 871.69(0.8000), 930.10(0.9100), 1314.99 (0.8100) | 3115.78 | 11.890 | – | – | – |
| I-GWOPSO [104] | 11, 61, 21 | 636.47(0.8500), 2068.29(0.8200), 380.25 (0.8100) | 3085.01 | 4.2700 | 98.10 | 0.000203 | **0.9815** |
| I-GWO [104] | 21, 61, 11 | 355.29(0.8500), 1978.05(0.8200), 655.56 (0.8100) | 2988.90 | 4.2900 | 98.08 | 0.000757 | 0.9815 |
| BWO [8] | 12, 21, 61 | 707.06(0.8500), 329.41 (0.8500), 1885.88 (0.8500) | 2922.35 | 4.9800 | 97.97 | – | – |
| Standard PSO | 61, 11, 18 | 2069.17(0.8138), 638.89(0.8305), 390.27 (0.8397) | 3098.33 | 4.4010 | 98.04 | 0.000248 | 0.9773 |
| **Proposed IPSO** | **61, 11, 18** | 2057.17(**0.8139**), 607.93(**0.8135**), 454.54 **(0.8333)** | 3119.64 | **4.2667** | **98.10** | 0.000129 | 0.9773 |

Power factor (pf), p.u (per unit) Particle swarm optimisation (PSO), Symbiosis organism search and neural network algorithm (SOS-NNA), Adaptive particle swarm optimisation (APSO), Loss sensitivity factor based sine cosine algorithm (LSF-SCA), Improved particle swarm optimisation (IPSO), Modified gravitational search algorithm (MGSA), Opposition based chaotic differential evolution (OCDE), Analytical-Hybrid-particle swarm optimisation (Hybrid-PSO), Comprehensive teaching learning-based optimisation (CTLBO), Improved Harris hawks optimisation (IHHO), Whales optimisation algorithm (WOA), Differential Evolution (DE) algorithm, Ant lion optimisation (ALO). Hybrid Fuzzy Equilibrium Optimizer (HFEO), Black Widow Optimizer (BWO), improved grey wolf optimisation with particle swarm optimisation (I-GWOPSO), Opposition-based tuned-chaotic differential evolution (OTCDE).

*8.2.1.2. Scenario 2: CHP-DG placement for multi-objective minimisation.* In this scenario, simultaneous optimisation of power loss, voltage deviation and voltage stability index are carried out. The results of this multi-objective optimisation is depicted in Table 18. According to Table 18, optimal allocation of 3 FCs (i.e., Case 1) at buses (61, 11, and 18) causes a reduction in the total active power loss to 73.8032 kW (67.92%), reduction in the VD to 0.001216 p.u (98.78%) and improvement in total VSI to 67.0983 p.u (9.59%) in comparison with 224.9606 kW, 0.099577 p.u, and 61.2241 p.u from the base case, respectively. In Case 2, after determining the

**Table 18**
Results of optimal location, power factor and capacity of FC and ICE under constant load model for multi-objectives.

| Year | $PL^{DG}$ (kW) | $VSI^{DG}$ (p.u) | $VD^{DG}$ (p.u) | $V_{min}$ (bus) | Capacity/location | | |
|---|---|---|---|---|---|---|---|
| Case 1: Allocation of 3 FCs at unity power factor | | | | | FC (kW)/bus/pf | FC (kW)/bus/pf | FC (kW)/bus/pf |
| Base | 73.7928 | 67.1463 | 0.001246098 | 0.989294 (65) | 2029.0308/**61**/1.0 | 628.8287/**11**/1.0 | 447.5560/**18**/1.0 |
| 1 | 81.3770 | 67.1327 | 0.001308799 | 0.988873 (65) | 2135.1528/**61**/1.0 | 631.9793/**11**/1.0 | 488.2790/**18**/1.0 |
| 2 | 89.7398 | 67.1029 | 0.001408307 | 0.988493 (65) | 2247.0733/**61**/1.0 | 664.2318/**11**/1.0 | 511.5881/**18**/1.0 |
| 3 | 98.9745 | 67.0725 | 0.001515191 | 0.988103 (65) | 2365.0176/**61**/1.0 | 698.3019/**11**/1.0 | 535.9996/**18**/1.0 |
| 4 | 109.1733 | 67.0415 | 0.001630123 | 0.987699 (65) | 2489.3267/**61**/1.0 | 734.2409/**11**/1.0 | 561.5811/**18**/1.0 |
| 5 | 120.4439 | 67.0139 | 0.001738518 | 0.987276 (65) | 2620.4190/61/1.0 | 806.9219/11/1.0 | 640.3648/**18**/1.0 |
| Case 2: Allocation of 3 ICE @ optimal power factor | | | | | ICE (kVA)/bus/pf | ICE (kVA)/bus/pf | ICE (kVA)/bus/pf |
| Base | 4.4285 | 67.9859 | 0.000113785 | 0.994265 (50) | 2089.6638/**61**/0.8155 | 651.7211/**11**/0.8170 | 485.7999/**18**/0.8428 |
| 1 | 4.8818 | 67.9949 | 0.000128904 | 0.993986 (50) | 2191.8100/**61**/0.8156 | 685.0575/**11**/0.8172 | 510.5149/**18**/0.8431 |
| 2 | 5.3918 | 68.0116 | 0.000150084 | 0.993693 (50) | 2298.7898/**61**/0.8158 | 720.6134/**11**/0.8173 | 538.4134/**18**/0.8435 |
| 3 | 5.9376 | 68.0177 | 0.000167197 | 0.993391 (50) | 2411.8997/**61**/0.8157 | 757.4016/**11**/0.8175 | 563.9925/**18**/0.8438 |
| 4 | 7.1309 | 68.0447 | 0.000214941 | 0.993060 (50) | 2547.7837/**61**/0.8053 | 837.9143/**11**/0.8176 | 621.6031/**18**/0.8441 |
| 5 | 7.2315 | 68.0482 | 0.000220203 | 0.992726 (50) | 2654.2553/**61**/0.8159 | 849.9710/**11**/0.8177 | 623.4363/**18**/0.8446 |

optimal locations, sizes, and optimal pfs of 3ICEs, the network performance metrics improved with the total active power loss reducing to 4.4285 kW (98.03% reduction), VD reduces to 0.0001138 p.u and the total VSI improves to 67.9859 p.u when compared with the base case (without DG integration).

The comparison of the results of the proposed IPSO with the original PSO and other existing state-of-the-art methods found in literature is presented in Table 19 for Case 1 and Table 20 for Case 2, respectively. It should be noted that the results of the base year are adopted for this comparison purpose.

According to Table 19, for Case 1, the proposed IPSO dominates TSO [102], MOTEO [106] and MOLA [106] in terms of total active power loss minimisation. It performs better than SPBO [105] in VD minimisation and outweighs TSO [102] and SPBO [105] in VSI maximisation. It gives better results than SOS-NNA [49] in all the three comparative objectives and returns better performance than PSO in two out of the three comparing objectives. Similarly, for Case 2, as shown in Table 20, the proposed IPSO shows a better solution than TSO [102] and I-GWO [104] in all the compared objectives, and it gives better solutions than SOS-NNA [49], MOIHHO [22], ALO [108], MVO [108], MOLA [106], MOTEO [106], I-GWOPSO [104] and MVO [108] in two out of the three compared objectives. It also gives better results than PSO in all the compared objectives. This shows that the proposed IPSO outperforms the standard PSO and other comparing methods in terms of the solution quality.

### *8.2.2. Category 2: seasonal mixed voltage dependent load model*

In this category, the performance of the system before and after the installation of FCs and ICE-based CHP-DGs to the distribution network under seasonal voltage-dependent mixed load models with an estimated load growth of 4.83 % and different network loading conditions (levels) over a five-year operation horizon is investigated. The performance parameters of the test network before penetration of CHP-DGs over the operating time of five years are displayed in Table 21.

It is obvious from Table 21 that at different seasons and different loading conditions, the impact on the network is different. It is shown that the network experiences larger power loss in winter day while the lowest power loss is reported in autumn season. Other system parameters are equally affected. However, the penetration of DGs to the DN has been chosen by the DISCOs to ameliorate these effects, and impacts of which are investigated in the following section. It should be noted that only multiple objective optimisation scenario is applied in this scenario.

**Table 19**
Comparative results for multi-objective optimisation with unity power factor DG (such as FC-DG).

| Method | Bus No | DG capacity kW | Total DG size (kW) | $PL^{DG}$ (kW) | % Loss Reduction | VDI (p.u) | Min (VSI) (p.u) | Sum (VSI) p.u |
|---|---|---|---|---|---|---|---|---|
| Base case | – | – | – | 224.9606 | – | 0.099600 | 0.6833 | 61.2241 |
| TSO [102] | 7, 22, 62 | 977.40, 513.68, 1954.80 | 3445.88 | 76.280 | – | 0.001100 | 0.9632 | – |
| SPBO [105] | 11, 18, 61 | 559.93, 369.16, 1713.10 | 2642.19 | **69.450** | – | 0.005200 | 0.9182 | – |
| MOTEO [106] | 17, 61, 59 | 29.54, 1730.10, 447.96 | 2907.60 | 77.517 | – | 0.185200 | – | 67.278 |
| MOLA [106] | 13, 17, 61 | 306.44, 722.53, 1864.50 | 2893.47 | 76.616 | – | 0.287400 | – | **67.395** |
| SOS-NNA [49] | 20, 44, 63 | 1021.50,849.50, 1813.10 | 3684.10 | 91.378 | 59.38 | 0.004007 | 0.9430 | – |
| CTLBO [107] | 11, 18, 61 | 560.30, 427.40, 2153.40 | 3141.10 | 76.372 | 66.04 | 0.000800 | 0.9770 | – |
| I-DBEA [20] | 61, 19, 11 | 2148.70,471.70, 712.60 | 3320.00 | 78.347 | 65.17 | **0.000200** | **0.9772** | – |
| IPSO [21] | 61, 18, 66 | 2038.48, 487.99, 529.23 | 3055.57 | 74.104 | 67.06 | 0.0012497 | 0.9626 | 67.145 |
| Standard PSO | 18, 61, 50 | 649.64, 2099.18, 714.79 | 3373.61 | 74.601 | 66.84 | 0.0017292 | 0.9623 | 66.984 |
| **Proposed IPSO** | **61, 11, 18** | **2029.03, 628.83, 447.56** | **3105.42** | **73.793** | **67.20** | 0.0012460 | 0.9627 | 67.146 |

**Table 20**
Comparative results of multi-objective optimisation for optimal power factor DG (such as ICE-DG).

| Method | Bus No | DG capacity kVA (pf) | Total DG size (kVA) | $PL^{DG}$ (kW) | % Loss reduction | VDI (p.u) | VSI (p. u) | Sum VSI (p. u) |
|---|---|---|---|---|---|---|---|---|
| Base case | – | – | – | 224.9606 | – | 0.099600 | 0.6833 | 61.2241 |
| SOS-NNA [49] | 16, 49, 61 | 735.55(0.8270),1465.36(0.8140), 2260.96(0.8120) | 4461.87 | 6.593 | 97.06 | 0.000297 | 0.9879 | – |
| MOIHHO [22] | 13, 49, 62 | 1313.58(0.8100),1300.00(0.9500), 1987.65(0.8100) | 4601.23 | 13.900 | 93.82 | 0.000500 | 0.9910 | – |
| MVO [108] | 17, 11, 61 | 523.10(0.8200),827.50(0.8000), 2012.30(0.8100) | 3362.90 | 6.3600 | 67.17 | 0.000319 | 0.9929 | |
| ALO [108] | 21, 61, 11 | 467.20(0.8200),1999.80(0.8000), 860.90(0.8000) | 2927.90 | 6.3800 | 97.16 | 0.000329 | **0.9937** | – |
| MOLA [106] | 16, 54, 61 | 748.86(0.8501),589.94(0.8447), 2065.74(0.7880) | 3404.54 | 7.5257 | 96.66 | – | – | 68.3160 |
| MOTEO [106] | 11, 15, 61 | 638.23(0.8134),678.37(0.7733), 2130.69(0.8256) | 3447.29 | 7.0665 | 96.87 | – | – | **68.4990** |
| TSO [102] | 12, 58, 61 | 1140.85(0.8000),1211.33(0.8700), 1301.45(0.8000) | 3653.63 | 16.320 | 92.27 | 0.001500 | 0.9769 | – |
| I-GWOPSO [104] | 61, 11, 21 | 2037.80(0.8200),860.00(0.8000), 367.90(0.8100) | 3265.70 | 4.8667 | – | 0.000117 | 0.9774 | – |
| I-GWO [104] | 19, 61, 11 | 391.57(0.8300),2000.00(0.8500), 779.76(0.8400) | 3171.33 | 5.3273 | – | 0.000131 | 0.9773 | – |
| IPSO [21] | 15, 61, 49 | 714.95(0.9013),2165.29(0.8049), 961.21 (0.9087) | 3841.45 | 5.8040 | 97.42 | 0.000192 | 0.9850 | 67.7801 |
| Standard PSO | 12, 50, 61 | 720.70(0.8063),875.57(0.8090), 2096.23(0.8152) | 3692.50 | 6.3924 | 97.16 | 0.002190 | 0.9477 | 67.0801 |
| **Proposed IPSO** | **61, 11, 18** | **2089.66(0.8155), 651.73(0.8170), 485.80(0.8428)** | **3227.19** | **4.4285** | **98.03** | **0.000114** | 0.9774 | 67.9807 |

Multi-objective thermal exchange optimisation (MOTEO) and the multi-objective Lichtenberg algorithm (MOLA), Transient Search Optimisation (TSO) algorithm, Student psychology-based optimisation (SPBO), Multiverse optimisation (MVO), Comprehensive teaching learning-based optimisation (CTLBO).

### *8.3. CHP-DG placement for multi-objective optimisation*

In this scenario, multiple objectives are optimised simultaneously considering seasonal voltage-dependent mixed load models under two operating cases (Case 1 considering FC-CHP) and Case 2 considering ICE-CHP). The results of this multi-objective optimisation under seasonal voltage dependent mixed load models are depicted in Table 22 (Case 1) and Table 23 (Case 2).

#### *8.3.1. Allocation of FC-CHP-DGs under seasonal voltage dependent loads (case 1)*

According to Table 22, all the FC CHP-DGs are located at buses 61, 11 and 20 for all the years of operation. In the summer day, the total active power loss drastically reduces from 170.703579 kW (base case) to 41.2268728 kW (75.84 % reduction) in the base year. In the summer night, the power loss reduces to 20.7561844 kW in comparison to the daytime due to light loading of the network which is about 49.65 % reduction. In the winter day and night, the total active power loss reduces to 60.2408682 kW (77.14 % reduction) and 37.1952485 kW (76.50 % reduction), respectively in comparison to 263.504873 kW and 158.268892 kW in the base year when no CHP-DG was connected. In the spring season, the total active power loss reduces to 22.9593917 kW from 92.4493876 kW (75.17 % reduction) in the base case. In the autumn, the total active power loss reduces to 20.7243020 kW from 85.87011 kW (75.87 % reduction) in the base case.

#### *8.3.2. Allocation of ICE-CHP-DGs under seasonal voltage dependent loads (case 2)*

The results are depicted in Table 23. In this table it is revealed that the optimal locations of the DGs at buses (61, 11, and 18), sizes and optimal PFs substantially reduces the total power loss, improves the VSI and drastically reduces the VD of the network at all seasons and years. Specifically, in the summer day the power loss reduces to 4.015645 kW in the base year about 90.23 % and 97.65 % loss reduction when compared with the base case as well as summer day in Case 1. Similar results are obtained in all other years and seasons.

It could be seen that with load growth over the planning period in both cases, the power loss continues to increase but well improved when compared to the base case (no CHP-DGs). Also, other network performance parameters are equally improved in comparison with base case. Generally, in both cases, optimal integration of FCs and ICEs have remarkably ameliorated the impact of network loading due to load growth and at various seasons of the year with the application of the proposed method. It should be noted that with the load growth, the locations of the DGs remain the same while the capacities are increasing to trail the load growth. Again, it is observed that at night the capacities of the DGs decrease in comparison to the day-time. This will avail the DISCO opportunity to remove some DGs from the network and ensure optimal economic dispatch. This action will bring about economic saving in terms of fuel cost reduction.

To show the influence of the penetration of these DGs into the test network on the system voltage distribution, the voltage profiles

**Table 21**
Results for load demand and system performance parameters for seasonal mixed voltage-dependent load model before integrating CHP-DGs.

| Year | $P_{Di(t)}$ (MW) | $Q_{Di(t)}$ (MVar) | $PL^0$ (kW) | $VSI^0$ (pu) | $VD^0$ p.u | $V_{min}$(bus) |
|---|---|---|---|---|---|---|
| Summer day (loading co-efficient of 1.00) | | | | | | |
| (Base) | 3.660286 | 2.261802 | 170.703579 | 61.862439 | 0.0789082 | 0.9202803 (65) |
| 1 | 3.837099 | 2.371060 | 189.029352 | 61.568642 | 0.0873411 | 0.9160815 (65) |
| 2 | 4.022453 | 2.485596 | 209.422999 | 61.260824 | 0.0967188 | 0.9116386 (65) |
| 3 | 4.216759 | 2.605664 | 232.137157 | 60.938303 | 0.1071552 | 0.9069341 (65) |
| 4 | 4.420453 | 2.731532 | 257.459295 | 60.600365 | 0.1187800 | 0.9019494 (65) |
| 5 | 4.633986 | 2.863481 | 285.717410 | 60.246249 | 0.1317408 | 0.8966636 (65) |
| Summer night (loading co-efficient of 0.75) | | | | | | |
| (Base) | 2.742022 | 1.644488 | 89.758332 | 63.435991 | 0.0417908 | 0.9422339 (65) |
| 1 | 2.874474 | 1.723926 | 99.158729 | 63.217260 | 0.0461535 | 0.9392703 (65) |
| 2 | 3.013331 | 1.807202 | 109.577099 | 62.988118 | 0.0509861 | 0.9361441 (65) |
| 3 | 3.158892 | 1.894499 | 121.129659 | 62.748049 | 0.0563420 | 0.9328451 (65) |
| 4 | 3.311484 | 1.986014 | 133.947017 | 62.496542 | 0.0622808 | 0.9293623 (65) |
| 5 | 3.471447 | 2.081950 | 148.176173 | 62.233049 | 0.0688698 | 0.9256837 (65) |
| Spring (0.75 co-efficient of summer day) | | | | | | |
| (Base) | 2.745215 | 1.696352 | 92.4493876 | 63.386013 | 0.04282596 | 0.9414330 (65) |
| 1 | 2.877824 | 1.778295 | 102.1407420 | 63.164865 | 0.04730139 | 0.9384248 (65) |
| 2 | 3.016839 | 1.864197 | 112.8832030 | 62.933173 | 0.05225982 | 0.9352512 (65) |
| 3 | 3.162569 | 1.954248 | 124.797072 | 62.690434 | 0.05775609 | 0.9319016 (65) |
| 4 | 3.315339 | 2.048649 | 138.017609 | 62.436124 | 0.06385180 | 0.9283648 (65) |
| 5 | 3.475489 | 2.147611 | 152.697124 | 62.169689 | 0.07061621 | 0.9246287 (65) |
| Winter day (loading co-efficient of 1.25 co-efficient) | | | | | | |
| (Base) | 4.5237639 | 2.7623445 | 263.504873 | 60.494749 | 0.1221099 | 0.9008899 (65) |
| 1 | 4.7422871 | 2.8957813 | 292.457274 | 60.135730 | 0.1354459 | 0.8955411 (65) |
| 2 | 4.9713664 | 3.0356637 | 324.808679 | 59.759509 | 0.1503322 | 0.8898633 (65) |
| 3 | 5.2115112 | 3.1823034 | 361.002905 | 59.365225 | 0.1669687 | 0.8838309 (65) |
| 4 | 5.4632564 | 3.3360266 | 401.551783 | 58.951959 | 0.1855836 | 0.8774148 (65) |
| 5 | 5.7271623 | 3.4971754 | 447.048101 | 58.518732 | 0.2064429 | 0.8705826 (65) |
| Winter night (loading of 1.0 loading co-efficient) | | | | | | |
| (Base) | 3.5959110 | 2.1928427 | 158.268892 | 62.040664 | 0.0736465 | 0.9233913 (65) |
| 1 | 3.7696138 | 2.2987693 | 175.193558 | 61.755490 | 0.0814877 | 0.9193727 (65) |
| 2 | 3.9517073 | 2.4098128 | 194.015543 | 61.456725 | 0.0902016 | 0.9151226 (65) |
| 3 | 4.1425970 | 2.5262203 | 214.964148 | 61.143716 | 0.0998930 | 0.9106247 (65) |
| 4 | 4.3427077 | 2.6482509 | 238.299760 | 60.815772 | 0.1106798 | 0.9058616 (65) |
| 5 | 4.5524849 | 2.7761764 | 264.318796 | 60.472167 | 0.1226965 | 0.9008141 (65) |
| Autumn (0.75 co-efficient of winter night) | | | | | | |
| (Base) | 2.6969333 | 1.6446320 | 85.8701102 | 63.519755 | 0.0400397 | 0.9436638 (65) |
| 1 | 2.8272104 | 1.7240770 | 94.8482609 | 63.305043 | 0.0442134 | 0.9407781 (65) |
| 2 | 2.9637805 | 2.9637800 | 104.796009 | 63.080102 | 0.0488357 | 0.9377346 (65) |
| 3 | 3.1069478 | 1.8946654 | 115.823561 | 62.844443 | 0.0539572 | 0.9345235 (65) |
| 4 | 3.2570308 | 1.9861882 | 128.054672 | 62.597559 | 0.0596346 | 0.9311341 (65) |
| 5 | 3.4143637 | 2.0821322 | 141.628519 | 62.338915 | 0.0659317 | 0.9275550 (65) |

for each case in category 1 (i.e., constant load model) and category 2 (i.e., seasonal voltage dependent mixed load models) for the fifth year are presented in Figs. 5 and 6, respectively since this is the year when maximum load is connected to the system.

It is observed from Fig. 5 that before the integration of DGs to the distribution network the system voltage magnitude has been deteriorated and far below the acceptable limit of 0.95 p.u at buses 18–27 and 59–65. It means that the loads connected to these buses will experience poor power quality due to poor voltage profile. However, after the integration of FCs and ICEs, the voltage magnitudes at all buses improve to higher values far beyond the 0.95 p.u minimum voltage limit and less than 1.05 p.u of the maximum limit. The minimum voltage remains in bus 65 when FCs are integrated while it appears in bus 50 when ICE is penetrated. This means that the integration of DGs can improve the voltage profile of the system.

Similarly, Fig. 6(a–f), show the voltage profile of the network during different seasons for single and multiple objectives. Similar to what has been explained previously, prior to the integration of DGs, the voltage profile of the system at bus 65 in all seasons has deteriorated far below the acceptable limit. With the integration of DGs, the system voltage is substantially improved in all the seasons. It is noticed that there is more voltage drop in the day-time than the night-time due to increased load demand during the day hours which necessitates utilisation of larger DG capacity. The voltage drop is more pronounced in the winter day due to large power demand as a result of coldness when people use more of energy consuming heating equipment. Less voltage drop occurs in the spring season as the network is less congested. With the integration of DGs, the voltage profiles of the network are well improved compared to the base case.

## 9. Economic and environmental evaluation

In this section, the solutions obtained for the multi-objective optimisation by the proposed IPSO are further evaluated in economic and environmental aspects. Only the seasonal voltage dependent mixed load models are considered in this analysis.

**Table 22**
Results for optimal location and capacity of FC for seasonal mixed load model for multi-objective.

| Year | $PL^{DG}$ (kW) | $VSI^{DG}$ (p.u) | $VD^{DG}$ (p.u) | Vmin (bus) | Capacity/location | | |
|---|---|---|---|---|---|---|---|
| Allocation of 3 FC @ optimal power factor for Summer day | | | | | FC (kW)/bus/PF | FC (kW)/bus/PF | FC (kW)/bus/PF |
| Base | 41.226872 | 67.2473689 | 0.001048423 | 0.9891275999 | 1719.3131/**61**/1.0 | 610.0728/**11**/1.0 | 445.7084/**20**/1.0 |
| 1 | 45.394404 | 67.2200420 | 0.001139647 | 0.9886303229 | 1804.5819/**61**/1.0 | 652.6796/**11**/1.0 | 457.3421/**20**/1.0 |
| 2 | 49.989623 | 67.1915423 | 0.001238502 | 0.9881133148 | 1894.1835/**61**/1.0 | 686.9654/**11**/1.0 | 480.5833/**20**/1.0 |
| 3 | 55.056416 | 67.1626474 | 0.001345087 | 0.9875748899 | 1988.3674/**61**/1.0 | 723.2037/**11**/1.0 | 505.0728/**20**/1.0 |
| 4 | 60.644288 | 67.1334506 | 0.001459865 | 0.9870144472 | 2087.3828/**61**/1.0 | 761.5228/**11**/1.0 | 530.8859/**20**/1.0 |
| 5 | 66.808146 | 67.1040644 | 0.001583302 | 0.9864314156 | 2191.4941/**61**/1.0 | 802.0610/**11**/1.0 | 558.1035/**20**/1.0 |
| Allocation of 3 FC @ optimal power factor for Summer Night | | | | | FC (kW)/bus/PF | FC (kW)/bus/PF | FC (kW)/bus/PF |
| Base | 20.756184 | 67.4278826 | 0.000565836 | 0.9921662675 | 1272.0371/61/1.0 | 452.2333/11/1.0 | 320.3055/20/1.0 |
| 1 | 22.841541 | 67.4045863 | 0.000616891 | 0.9918038484 | 1334.5983/61/1.0 | 475.3526/11/1.0 | 336.3235/20/1.0 |
| 2 | 25.138273 | 67.3806136 | 0.000672265 | 0.9914256035 | 1400.2957/61/1.0 | 499.7213/11/1.0 | 353.1726/20/1.0 |
| 3 | 27.668114 | 67.3559795 | 0.000732279 | 0.9910309506 | 1469.2926/61/1.0 | 525.4143/11/1.0 | 370.8990/20/1.0 |
| 4 | 30.455084 | 67.3307060 | 0.000797268 | 0.9906193052 | 1541.7617/61/1.0 | 552.5114/11/1.0 | 389.5521/20/1.0 |
| 5 | 33.525741 | 67.3048217 | 0.000867585 | 0.9901900804 | 1617.8855/61/1.0 | 581.0980/11/1.0 | 409.1847/20/1.0 |
| Allocation of 3 ICE @ optimal power factor Spring | | | | | FC (kW)/bus/PF | FC (kW)/bus/PF | FC (kW)/bus/PF |
| Base | 22.959392 | 67.4059021 | 0.000622007 | 0.9917401890 | 1281.4557/61/1.0 | 456.1367/11/1.0 | 322.7146/20/1.0 |
| 1 | 25.267116 | 67.3817270 | 0.000678337 | 0.9913568224 | 1344.5674/61/1.0 | 479.5233/11/1.0 | 338.8630/20/1.0 |
| 2 | 27.807290 | 67.3540641 | 0.000743409 | 0.9909608712 | 1410.7914/61/1.0 | 481.9534/11/1.0 | 379.1845/20/1.0 |
| 3 | 30.607157 | 67.3283648 | 0.000810001 | 0.9905433487 | 1480.4115/61/1.0 | 506.8451/11/1.0 | 398.2262/20/1.0 |
| 4 | 33.693581 | 67.3050742 | 0.000877588 | 0.9901028501 | 1553.6075/61/1.0 | 557.6331/11/1.0 | 392.5281/20/1.0 |
| 5 | 37.092579 | 67.2782304 | 0.000955336 | 0.9896482779 | 1630.4499/61/1.0 | 586.5726/11/1.0 | 412.3304/20/1.0 |
| Allocation of 3 FC @ optimal power factor Winter Day | | | | | FC (kW)/**bus**/PF | FC(kW)/**bus**/PF | FC(kW)/**bus**/PF |
| Base | 60.240868 | 67.1255746 | 0.001459849 | 0.9871359101 | 2111.4874/61/1.0 | 739.7019/11/1.0 | 548.9988/20/1.0 |
| 1 | 66.375344 | 67.1011877 | 0.001571249 | 0.9865594819 | 2216.3291/61/1.0 | 807.3689/11/1.0 | 580.2591/20/1.0 |
| 2 | 73.013201 | 67.0382930 | 0.001752589 | 0.9859967730 | 2325.7599/61/1.0 | 896.2525/11/1.0 | 584.0387/20/1.0 |
| 3 | 80.591914 | 67.0426621 | 0.001841697 | 0.9853412527 | 2443.4147/61/1.0 | 928.9749/11/1.0 | 645.8034/20/1.0 |
| 4 | 88.823795 | 67.0148806 | 0.001991348 | 0.9846958568 | 2565.8981/61/1.0 | 960.1707/11/1.0 | 663.3979/20/1.0 |
| 5 | 97.913480 | 66.9811096 | 0.002159722 | 0.9840371354 | 2694.6487/61/1.0 | 968.8384/11/1.0 | 743.5781/20/1.0 |
| Allocation of 3 FC @ optimal power factor for Winter Night | | | | | FC (kW)/bus/PF | FC (kW)/bus/PF | FC (kW)/bus/PF |
| Base | 37.195249 | 67.2710393 | 0.000959729 | 0.9897111183 | 1657.7925/61/1.0 | 607.8710/11/1.0 | 426.1151/20/1.0 |
| 1 | 40.952165 | 67.2434785 | 0.001043758 | 0.9892417033 | 1739.8552/61/1.0 | 639.5146/11/1.0 | 447.6645/20/1.0 |
| 2 | 45.093224 | 67.2153955 | 0.001134487 | 0.9887526071 | 1826.0879/61/1.0 | 672.9295/11/1.0 | 470.3591/20/1.0 |
| 3 | 49.463851 | 67.1472068 | 0.001322222 | 0.9879806061 | 1911.2058/61/1.0 | 700.0263/11/1.0 | 488.5788/20/1.0 |
| 4 | 54.692400 | 67.1579394 | 0.001337763 | 0.9877129874 | 2011.9711/61/1.0 | 745.5324/11/1.0 | 519.4577/20/1.0 |
| 5 | 60.244145 | 67.1287427 | 0.001451185 | 0.9871613295 | 2112.1100/61/1.0 | 784.9731/11/1.0 | 546.0114/20/1.0 |
| Allocation of 3 FC @ optimal power factor for Autumn | | | | | FC (kW)/bus/PF | FC (kW)/bus/PF | FC (kW)/bus/PF |
| Base | 20.724302 | 67.4254279 | 0.000569155 | 0.9921835595 | 1236.0982/61/1.0 | 447.6244/11/1.0 | 316.0907/20/1.0 |
| 1 | 22.805848 | 67.4018553 | 0.000620761 | 0.9918208996 | 1296.8999/61/1.0 | 470.4878/11/1.0 | 331.8827/20/1.0 |
| 2 | 25.098277 | 67.3775754 | 0.000676775 | 0.9914422837 | 1360.7502/61/1.0 | 494.5848/11/1.0 | 348.4920/20/1.0 |
| 3 | 27.620975 | 67.3497360 | 0.000741695 | 0.9910514917 | 1427.7469/61/1.0 | 497.1094/11/1.0 | 389.9715/18/1.0 |
| 4 | 30.403403 | 67.3238424 | 0.000807997 | 0.9906395321 | 1498.1750/61/1.0 | 522.5816/11/1.0 | 409.7689/18/1.0 |
| 5 | 33.469534 | 67.2999934 | 0.000875061 | 0.9902056443 | 1572.2135/61/1.0 | 565.6133/11/1.0 | 413.3709/18/1.0 |

### 9.1. Economic assessment

The economic aspect is assessed based on two modes of system operation (i.e., CHP and power only) considering LCOE and NPV profit.

#### 9.1.1. The LCOE

The results for the LCOE for power only and CHP modes for the DGs are shown in Table 24.

As depicted in Table 24, the LCOEs for power only and CHP modes for both FC and ICE based DGs are highest at the base year. This could be attributed to huge investment costs of DGs at the base year of the planning. However, due to the dynamic planning approach adopted for the economic evaluation, the total cost falls in the following years, hence reduction in the LCOEs in the subsequent years compared to the base year. Due to load growth and the need to add new DGs in subsequent years, the LCOE begins to increase from first year till the end of planning period.

*9.1.1.1. Power only operation mode.* As shown in Table 22, for FC-DGs in power only mode, the LCOE increases from 0.07440 $/kWh to 0.0811 $/kWh in first year till the final year of planning horizon with an aggregated LCOE of 0.0918 $/kWh. In a similar manner for ICE-DG, LCOE increases from 0.0698 $/kWh in the first year to 0.0751 $/kWh in the last year of planning period while the aggregated LCOE is 0.0786 $/kWh. This value is less than that obtained for FC-DG operating power only mode. This implies that operating ICE-DGs in power only mode could be more economically viable than operating FC-DGs in power only mode.

**Table 23**
Results for optimal location, power factor and capacity of ICE for seasonal mixed load model for multi-objective.

| Year | $PL^{DG}$ (kW) | $VSI^{DG}$ (p.u) | $VD^{DG}$ (p.u) | Vmin (bus) | Capacity/location | | |
|---|---|---|---|---|---|---|---|
| Allocation of 3 ICE @ optimal power factor for Summer day | | | | | ICE (kW)/bus/pf | ICE (kW)/bus/pf | ICE (kW)/bus/pf |
| Base | 4.015645 | 67.951608 | 0.0000979072 | 0.99434844 | 1586.5917/**61**/0.8771 | 521.6560/**11**/0.8503 | 385.9342/**18**/0.8549 |
| 1 | 4.436946 | 67.961844 | 0.0001189051 | 0.99407351 | 1656.8433/**61**/0.8767 | 508.5197/**11**/0.8035 | 432.3001/**18**/0.8893 |
| 2 | 4.867556 | 67.964049 | 0.0001240987 | 0.99378481 | 1744.9415/**61**/0.8771 | 567.5407/**11**/0.8383 | 432.8834/**18**/0.8694 |
| 3 | 5.363503 | 67.971467 | 0.0001396553 | 0.99348209 | 1830.3599/**61**/0.8771 | 596.5074/**11**/0.8384 | 454.9419/**18**/0.8696 |
| 4 | 5.911318 | 67.980167 | 0.0001575413 | 0.99316449 | 1919.9754/**61**/0.8771 | 627.4890/**11**/0.8387 | 477.9778/**18**/0.8697 |
| 5 | 6.617017 | 68.043558 | 0.0002236104 | 0.99283127 | 2016.6666/**61**/0.8788 | 659.0051/**11**/0.8360 | 504.9960/**18**/0.8699 |
| Allocation of 3 ICE @ optimal power factor for Summer Night | | | | | ICE (kW)/bus/pf | ICE (kW)/bus/pf | ICE (kW)/bus/pf |
| Base | 2.4804204 | 67.917071 | 0.0000504262 | 0.99577644 | 1165.6808/**61**/0.8685 | 422.1706/**11**/0.9576 | 293.0859/**18**/0.9022 |
| 1 | 2.5316210 | 67.936731 | 0.0000567982 | 0.99557407 | 1240.9237/**61**/0.8888 | 399.2662/**11**/0.8424 | 304.6106/**18**/0.8737 |
| 2 | 2.6761657 | 67.937651 | 0.0000631757 | 0.99535910 | 1299.2131/**61**/0.8876 | 416.6355/**11**/0.8394 | 321.5442/**18**/0.8762 |
| 3 | 2.9457175 | 67.939853 | 0.0000698218 | 0.99513343 | 1364.8665/**61**/0.8888 | 440.3637/**11**/0.8425 | 335.9244/**18**/0.8740 |
| 4 | 3.2804650 | 67.933776 | 0.0000761101 | 0.99489621 | 1428.5667/**61**/0.8816 | 470.4607/**11**/0.8953 | 346.3857/**18**/0.8491 |
| 5 | 3.5703113 | 67.945352 | 0.0000863976 | 0.99464862 | 1501.3249/**61**/0.8888 | 485.8769/**11**/0.8426 | 370.5977/**18**/0.8743 |
| Allocation of 3 ICE @ optimal power factor for Autumn | | | | | ICE (kW)/bus/pf | ICE (kW)/bus/pf | ICE (kW)/bus/pf |
| Base | 3.4843247 | 67.897307 | 0.000080513 | 0.99465188 | 1450.6765/**61**/0.8829 | 472.9205/**11**/0.8393 | 359.4347/**18**/0.8700 |
| 1 | 3.4895003 | 67.904458 | 0.000080807 | 0.99465198 | 1451.5104/**61**/0.8829 | 474.1206/**11**/0.8399 | 360.3207/**18**/0.8703 |
| 2 | 3.4968978 | 67.912964 | 0.000081332 | 0.99465212 | 1450.5043/**61**/0.8816 | 478.0948/**11**/0.8458 | 360.2914/**18**/0.8684 |
| 3 | 3.5107931 | 67.930601 | 0.000083386 | 0.99465233 | 1454.5589/**61**/0.8329 | 479.5073/**11**/0.8401 | 363.5602/**18**/0.8710 |
| 4 | 3.5204500 | 67.941163 | 0.000085099 | 0.99465248 | 1455.7902/61/0.8830 | 480.2788/**11**/0.8402 | 364.8690/**18**/0.8713 |
| 5 | 3.6246778 | 67.958815 | 0.000086371 | 0.99465001 | 1449.5091/**61**/0.8784 | 511.2947/**11**/0.9393 | 355.2460/**18**/0.8266 |
| Allocation of 3 ICE @ optimal power factor Winter Day | | | | | ICE (kW)/**bus**/pf | ICE (kW)/**bus**/pf | ICE (kW)/**bus**/pf |
| Base | 6.2355312 | 67.978646 | 0.0001671942 | 0.99293879 | 1946.2403/61/0.8823 | 644.3044/11/0.8404 | 490.0498/18/0.8722 |
| 1 | 6.8766911 | 67.989027 | 0.0001892081 | 0.99259447 | 2041.6699/61/0.8823 | 677.1555/11/0.8405 | 515.4523/18/0.8724 |
| 2 | 7.0775401 | 67.964729 | 0.0002134486 | 0.99222149 | 2180.3760/61/0.8901 | 739.3198/11/0.9771 | 577.8073/18/0.9032 |
| 3 | 8.3628871 | 68.016799 | 0.0002463649 | 0.99185412 | 2247.1081/61/0.8823 | 745.4234/11/0.8386 | 571.5167/18/0.8741 |
| 4 | 9.2266539 | 68.032368 | 0.0002803371 | 0.99145631 | 2357.5805/61/0.8824 | 787.9483/11/0.8408 | 599.1324/18/0.8733 |
| 5 | 10.188869 | 68.051456 | 0.0003219287 | 0.99103888 | 2473.6287/61/0.8824 | 828.7202/11/0.8408 | 630.6416/18/0.8736 |
| Allocation of 3 ICE @ optimal power factor for Winter Night | | | | | ICE (kW)/bus/pf | ICE (kW)/bus/pf | ICE (kW)/bus/pf |
| Base | 3.9180865 | 67.946894 | 0.0000987767 | 0.99436607 | 1534.0965/61/0.8830 | 543.6666/11/0.8436 | 347.6464/21/0.8697 |
| 1 | 4.3091948 | 67.949175 | 0.0001069803 | 0.99409189 | 1609.0004/61/0.8830 | 532.6459/11/0.8404 | 404.6062/18/0.8717 |
| 2 | 4.7462730 | 67.954391 | 0.0001197112 | 0.99380423 | 1687.6689/61/0.8830 | 559.6759/11/0.8404 | 425.1142/18/0.8719 |
| 3 | 5.2286669 | 67.960681 | 0.0001342867 | 0.99350245 | 1770.2384/61/0.8830 | 588.1505/11/0.8405 | 446.7162/18/0.8721 |
| 4 | 5.7739344 | 67.970629 | 0.0001505574 | 0.99318582 | 1856.9743/61/0.8830 | 636.2951/11/0.8420 | 450.3509/19/0.8717 |
| 5 | 6.3495927 | 67.977083 | 0.0001703731 | 0.99285368 | 1947.8909/61/0.8830 | 649.7813/11/0.8407 | 493.4661/18/0.8726 |
| Allocation of 3 ICE @ optimal power factor Spring | | | | | ICE (kW)/bus/pf | ICE (kW)/bus/pf | ICE (kW)/bus/pf |
| Base | 2.2325725 | 67.937402 | 0.0000518001 | 0.99576894 | 1186.1790/61/0.8769 | 380.8743/11/0.8377 | 290.6629/18/0.8679 |
| 1 | 2.4936445 | 67.945236 | 0.0000585890 | 0.99556308 | 1239.7785/61/0.8751 | 406.0030/11/0.8300 | 314.8579/18/0.9080 |
| 2 | 2.7042264 | 67.939942 | 0.0000635749 | 0.99534781 | 1304.6238/61/0.8770 | 420.0422/11/0.8379 | 320.5159/18/0.8682 |
| 3 | 3.0252136 | 67.861101 | 0.0000740546 | 0.99512037 | 1334.9597/61/0.8601 | 410.8751/11/0.8741 | 344.0947/18/0.8671 |
| 4 | 3.2770977 | 67.944653 | 0.0000785122 | 0.99488451 | 1435.0242/61/0.8770 | 463.4108/11/0.8380 | 353.5635/18/0.8686 |
| 5 | 3.6083043 | 67.948020 | 0.0000874899 | 0.99463571 | 1505.0893/61/0.8770 | 486.8210/11/0.8380 | 371.3994/18/0.8687 |

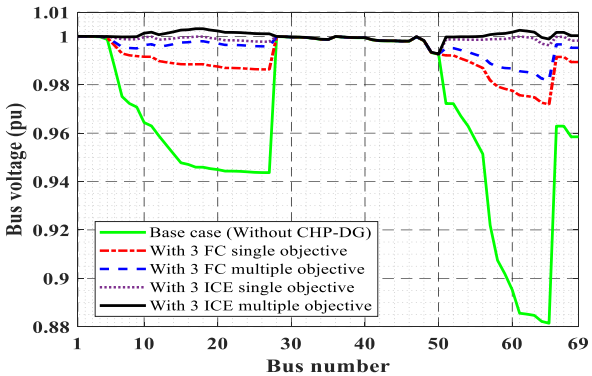


**Fig. 5.** Voltage profile for single and multiple objectives under constant load model.

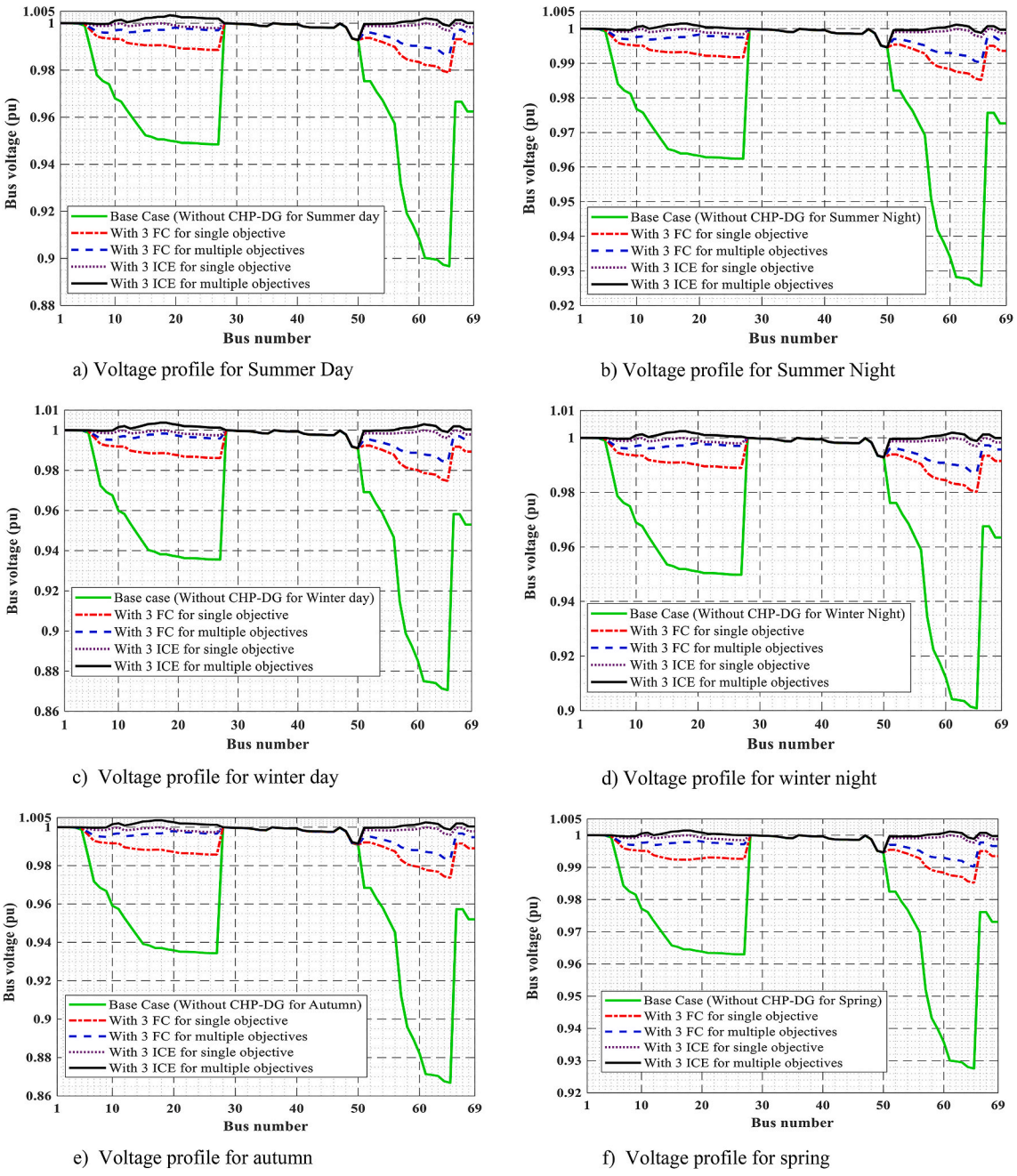


**Fig. 6.** Seasonal voltage profiles for the integration of FC and ICE-CHP-DG.

*9.1.1.2. CHP operation mode.* For the FC-DGs operating, the LCOE increases from 0.0399 $/kWh to 0.0435 $/kWh from the first year till the last year of system planning period. The aggregated LCOE for CHP mode is 0.0493 $/kWh. In the case of ICE-DGs, LCOE increases from 0.0443 kWh to 0.0478 kWh with an aggregated value of 0.0501 kWh. It should be observed that the LCOE for FC-CHP is far less than ICE-DGs operating in CHP mode. The implication of this is that FC-DGs are better operated in CHP mode.

*9.1.2. The NPV profit*

In this section the NPV profit of the system planning before and after the integration of DGs are assessed.

*9.1.2.1. NPV profit before DGs integration.* Table 25 depicts the NPV profit before connecting CHP-DG to the distribution network. In this case, the DISCO must either undergo load shedding or upgrade the network feeders and expand the size of the existing substation

**Table 24**
Results for LCOE.

| FC | Years | | | | | |
|---|---|---|---|---|---|---|
| ***Power only*** | Base (0) | 1 | 2 | 3 | 4 | 5 |
| Yearly net generated (x $10^6$ kWh) | 22.2572 | 26.2275 | 30.8863 | 36.35150 | 42.7232 | 50.2778 |
| Total net cost (M$) | 4.493820 | 1.951773 | 2.396904 | 2.902208 | 3.347117 | 4.077148 |
| Yearly LCOE($/kWh) | 0.2019 | 0.07440 | 0.0776 | 0.0798 | 0.0783 | 0.0811 |
| Aggregated LCOE ($/kWh) | **0.0918** | | | | | |
| ***CHP mode*** | | | | | | |
| Yearly net generated (x $10^6$ kWh) | 4.128650 | 4.865190 | 5.729490 | 6.743220 | 7.924980 | 9.326480 |
| Total net cost (M$) | 4.485509 | 1.941981 | 2.385372 | 2.888634 | 3.331166 | 4.058376 |
| Yearly LCOE($/kWh) | 0.1086 | 0.0399 | 0.0416 | 0.0428 | 0.0420 | 0.0435 |
| Aggregated LCOE ($/kWh) | **0.0493** | | | | | |
| **ICE** | **Years** | | | | | |
| ***Power only*** | Base (0) | 1 | 2 | 3 | 4 | 5 |
| Yearly net generated (x $10^6$ kWh) | 20.82950 | 24.20000 | 28.46830 | 32.99340 | 38.60190 | 45.15950 |
| Total net cost (M$) | 2.582631 | 1.688075 | 2.002952 | 2.418697 | 2.873898 | 3.393114 |
| Yearly LCOE($/kWh) | 0.1240 | 0.0698 | 0.0704 | 0.0733 | 0.0744 | 0.0751 |
| Aggregated LCOE ($/kWh) | **0.0786** | | | | | |
| ***CHP mode*** | | | | | | |
| Yearly net generated (x $10^6$ kWh) | 32.10830 | 37.30460 | 43.88380 | 50.85930 | 59.50580 | 69.61310 |
| Total net cost (M$) | 2.552636 | 1.653140 | 1.961928 | 2.371114 | 2.818388 | 3.328178 |
| Yearly LCOE($/kWh) | 0.0795 | 0.0443 | 0.0447 | 0.0466 | 0.0474 | 0.0478 |
| Aggregated LCOE ($/kWh) | **0.0501** | | | | | |

**Table 25**
Economic results before installing CHP system.

| Profit/cost (Million $) | Power only operation | | | | | |
|---|---|---|---|---|---|---|
| | Base (0) | 1 | 2 | 3 | 4 | 5 |
| Yearly net profit | 1.286796 | 1.350.711 | 1.528598 | 1.996824 | 2.205071 | 2.568720 |
| Yearly net revenue | 3.926690 | 4.610350 | 5.413040 | 6.355370 | 7.461860 | 8.761080 |
| Total net yearly cost | 2.639894 | 3.259639 | 3.884442 | 4.358546 | 5.256789 | 6.192360 |
| Cost of power purchase | 1.898770 | 2.235518 | 2.632370 | 3.100320 | 3.652160 | 4.303280 |
| Yearly environmental cost | 0.741124 | 0.872211 | 1.026642 | 1.208611 | 1.423089 | 1.675920 |
| Cost of system upgrade | 0 | 0.151910 | 0.225430 | 0.049615 | 0.181540 | 0.213160 |
| **NPV Profit** | **10.936720** | | | | | |

in order to take care of the yearly load growth. This cost (i.e., cost of system upgrade) in addition to other costs increases the total yearly cost and hence reduces the total profit. In this case the NPV profit of 10.936720 million $ is achieved over the planning horizon.

*9.1.2.2. NPV profit with integration of DGs in power-only operation.* For power only mode of operation, the FC based CHP returns less profit compared with ICE as observed in Tables 26 and 27. According to Tables 26 and it is seen that in the base year, the net profit is negative. This could be linked to the higher initial costs which are higher than the revenue made. It has been argued by Ref. [49] that a DG operating at unity PF (such as FC) is likely to be economically unviable due to increased total costs compared with the total revenue (benefit). In the subsequent years, it is obvious that due to the dynamic approach used for the incremental investment cost determination in this study, it is possible that the integration of FC based DG could be profitable in the medium to long term planning as shown in Table 26. As depicted in Table 27, ICE based DGs gives positive profit values all year round with higher value than FC based DGs.

*9.1.3. NPV profit with integration of DGs in combined heat and power operation*

Again, it is observed in Tables 26 and 27 that the sale of heat and electricity to consumers increases the revenue base for DISCO, hence an increase in total profit. It is noticed that the FC-based CHP produces slightly more profit than ICE-based CHP. The reason could be attributed to the higher power production capacity of FC due to its high electrical efficiency as well as its high heat-to-power ratio (HPR) which affords DISCO to sell more energy to the consumers Another possible reason is the decrease in the emission cost as FCs are virtually pollution free. However, the investment as well as operation costs of FCs are substantially higher compared to ICE. The cost of power purchase is also lower with ICE due to less power loss with ICE based CHP in comparison with FC making the total cost of FC more than that of ICE. Due to extensive research on the FCs, the cost of FC technology is likely to decline making FC a viable power and heat source of the future.

By and large, it could be inferred that the use of CHP-DG either in power-only mode or CHP makes a remarkable increase in the total profit over the planning period due to a rise in income and a fall in the total cost of the DISCO compared to the base case when no DER equipment is connected. The presence of CHP-DGs in the distribution network improves the voltage profile which consequently increases the active and reactive loads of the network due to voltage dependency. As a result of this, there is an opportunity for DISCO to

**Table 26**
Economic results of the two modes of operation for FC-based CHP.

| Profit/cost (Million $) | Combined heat and power operation | | | | | | Power only operation | | | | | |
|---|---|---|---|---|---|---|---|---|---|---|---|---|
| | Base (0) | 1 | 2 | 3 | 4 | 5 | Base | 1 | 2 | 3 | 4 | 5 |
| Yearly net profit | 0.702211 | 4.156359 | 4.781378 | 5.532476 | 6.555724 | 7.557194 | −0.567130 | 2.658577 | 3.016136 | 3.453162 | 4.114743 | 4.683932 |
| Yearly net revenue | 5.187720 | 6.098340 | 7.166750 | 8.421110 | 9.886890 | 11.615570 | 3.926690 | 4.610350 | 5.413040 | 6.355370 | 7.461860 | 8.761080 |
| Total net yearly cost | 4.485509 | 1.941981 | 2.385372 | 2.888634 | 3.331166 | 4.058376 | 4.493820 | 1.951773 | 2.396904 | 2.902208 | 3.347117 | 4.077148 |
| Yearly net investment cost | 2.959353 | 0.158278 | 0.297270 | 0.443461 | 0.452659 | 0.682578 | 2.959353 | 0.158278 | 0.297270 | 0.443461 | 0.452659 | 0.682578 |
| Yearly net operation cost | 0.033239 | 0.039167 | 0.046126 | 0.054286 | 0.063807 | 0.075090 | 0.041550 | 0.048960 | 0.057658 | 0.067860 | 0.079758 | 0.093861 |
| Yearly net upgrade cost | – | – | – | – | – | – | – | – | – | – | – | – |
| Yearly net power purchase | 0.470499 | 0.542836 | 0.629701 | 0.731540 | 0.865737 | 1.010746 | 0.470499 | 0.542836 | 0.629701 | 0.731540 | 0.865737 | 1.010746 |
| Yearly net environmental cost | 0.176644 | 0.205107 | 0.238606 | 0.278033 | 0.325449 | 0.379320 | 0.176644 | 0.205107 | 0.238606 | 0.278033 | 0.325449 | 0.379320 |
| Yearly net maintenance cost | 0.845774 | 0.996593 | 1.173668 | 1.381316 | 1.623514 | 1.910643 | 0.845774 | 0.996593 | 1.173668 | 1.381316 | 1.623514 | 1.910643 |
| **NPV Profit** | **29.285342** | | | | | | **17.359420** | | | | | |

**Table 27**
Economic results of the two modes of operation for ICE-based CHP.

| Profit/cost (Million $) | Combined heat and power operation | | | | | | Power only operation | | | | | |
|---|---|---|---|---|---|---|---|---|---|---|---|---|
| | Base (0) | 1 | 2 | 3 | 4 | 5 | Base | 1 | 2 | 3 | 4 | 5 |
| Yearly net profit | 2.089814 | 3.789880 | 4.435572 | 5.120946 | 5.973592 | 6.989372 | 1.319349 | 3.125425 | 3.376028 | 3.896683 | 4.541012 | 5.312846 |
| Yearly net revenue | 4.642450 | 5.443020 | 6.397500 | 7.492060 | 8.791980 | 10.31755 | 3.901980 | 4.813500 | 5.378980 | 6.315380 | 7.414910 | 8.705960 |
| Total net yearly cost | 2.552636 | 1.653140 | 1.961928 | 2.371114 | 2.818388 | 3.328178 | 2.582631 | 1.688075 | 2.002952 | 2.418697 | 2.873898 | 3.393114 |
| Yearly net investment cost | 1.196227 | 0.053259 | 0.107120 | 0.155327 | 0.212968 | 0.264974 | 1.196227 | 0.053259 | 0.107120 | 0.155327 | 0.212968 | 0.264974 |
| Yearly net operation cost | 0.036662 | 0.042593 | 0.050107 | 0.058070 | 0.067947 | 0.079488 | 0.066659 | 0.077442 | 0.091105 | 0.105584 | 0.123537 | 0.144524 |
| Yearly net upgrade cost | – | – | – | – | – | – | – | – | – | – | – | – |
| Yearly net power purchase | 0.547064 | 0.650900 | 0.740302 | 0.909320 | 1.072046 | 1.263613 | 0.547064 | 0.650900 | 0.740302 | 0.909320 | 1.072046 | 1.263613 |
| Yearly net environmental cost | 0.251945 | 0.301421 | 0.352698 | 0.423589 | 0.500340 | 0.591065 | 0.251945 | 0.301421 | 0.352698 | 0.423589 | 0.500340 | 0.591065 |
| Yearly maintenance cost | 0.520738 | 0.604967 | 0.711700 | 0.824808 | 0.965087 | 1.129038 | 0.520738 | 0.604967 | 0.711700 | 0.824808 | 0.965087 | 1.129038 |
| **NPV Profit** | **28.399176** | | | | | | **21.571343** | | | | | |

sell more energy to voltage-dependent loads. This assertion corroborates the use of voltage-dependent load models for distribution system studies.

### 9.2. Environmental assessment

Table 28 illustrates the possible outcomes for the environmental assessment of both types of CHP equipment and base case (no CHP connection).

According to Table 28, a large amount of pollutants is emitted when the CHP-DGs are not connected to the distribution network. As stated in Table 28 no pollutant emission value is recorded for FC based CHP since the only emission is water vapour [109] which portends no danger to the environment. Therefore, the environmental emission from FC is negligibly zero. In the case of ICE, combustion of biogas results in emission of some gaseous substances such as $CO_2$, $SO_2$ and $NO_X$. It has been argued that $CO_2$ emitted due to combustion of biogas is considered biogenic and regarded as carbon neutral, and of no environmental impact. The combined emissions of other pollutants are considered and the results of which are shown in Table 28.

## 10. Statistical analysis and convergence characteristic

To demonstrate the effectiveness of the proposed IPSO in comparison with the standard PSO, the two methods are applied to solve the same objective function defined in (28) with constraints (29)–(40) for all test cases in scenario 1 (constant load model) in the fifth year of the system planning. The choice of only scenario 1 for this analysis assumes that the performance of the proposed algorithm is not expected to change with whatever load models it is used for. Due to the stochastic nature of both algorithms, they are subjected to 20 independent runs from which the best, worst, average and standard deviation of the fitness values of the objective function are determined. Tables 29 and 30 depict results of the statistical values obtained by implementing the two methods.

According to these tables, the proposed IPSO algorithm is more efficient than the original PSO, since its best, worst, average and standard deviation of the objective function's fitness values are more promising than those of the original PSO. Again, the convergence characteristics of the two methods for base year are displayed in Fig. 7 which demonstrate the speed of convergence of both methods. Fig. 7a shows the convergence curve for single objective while Fig. 7b indicates the convergence curve for multiple objectives.

It is apparent that the proposed IPSO has better convergence capability than the PSO, as it reaches a better fitness value in fewer iterations than the standard PSO. This implies that fewer iterations are required for the proposed IPSO in comparison with standard PSO.

To further demonstrate the robustness and to show the solution quality of the proposed IPSO and standard PSO, the percentage deviation of the best and worst fitness values from the corresponding average result are determined according to Eqns. (80) and (81) [13,110] and the results are tabulated in Tables 31 and 32 for single and multi-objective optimisation.

$$A = \frac{|Best - Average|}{Average} \times 100 \tag{80}$$

$$B = \frac{|Worst - Average|}{Average} \times 100 \tag{81}$$

Where 'A' is the deviation of the best result from the average and 'B' is deviation of the worst result from the average.

According to Tables 31 and 32 and it could be observed that the solutions obtained by IPSO has lower deviations from the average result than the standard PSO. This smaller value of deviations for the proposed IPSO confirms the algorithm's robustness in finding the global minima solution. Therefore, the outcomes of Tables 29–32 and Fig. 7 show the efficiency, robustness, and stability of the results of the proposed IPSO in comparison with the standard PSO.

## 11. Conclusion

In this paper, an improved particle swarm optimisation (IPSO) algorithm has been applied for the dynamic planning of EDSEP in which the integration of biogas-fired CHP-based DGs (such as ICE and FC) are considered in order to respond to yearly load growth. It is assumed that only the DISCO is permitted to own and operate the CHP-DG with the aim to improve the technical performance of the network. The proposed optimisation algorithm aims to find the possible best size of the CHP-DG, optimal location, and power factors. In this study, different load models including constant and seasonal mixed voltage-dependent load modes under single and multi-objective scenarios are considered. The multi-objective problem is solved using weighted sum of three objectives such as total active power loss, voltage deviation, and total voltage stability index. Furthermore, assessments of the economic and environmental

**Table 28**
Environmental results with and without CHP equipment.

| Total yearly emission (Million kg) | Base (0) | 1 | 2 | 3 | 4 | 5 |
|---|---|---|---|---|---|---|
| Without CHP | 30.2333 | 31.7722 | 33.3950 | 35.1059 | 36.9119 | 38.8182 |
| ICE-CHP | 0.04228 | 0.04386 | 0.04607 | 0.04767 | 0.04980 | 0.05202 |
| FC-CHP | 0 | 0 | 0 | 0 | 0 | 0 |

**Table 29**
Statistical results for both methods under single-objective function.

| Statistical parameters | PSO | | IPSO | |
|---|---|---|---|---|
| | FC | ICE | FC | ICE |
| Average value | 0.318965 | 0.057683 | 0.312527 | 0.054729 |
| Best value | 0.297042 | 0.019489 | 0.295872 | 0.019455 |
| Worst value | 0.433068 | 0.280224 | 0.415348 | 0.260097 |
| Standard deviation | 0.006079 | 0.010223 | 0.005709 | 0.010011 |

**Table 30**
Statistical results for both methods under multi-objective function.

| Statistical parameters | PSO | | IPSO | |
|---|---|---|---|---|
| | FC | ICE | FC | ICE |
| Average value | 0.330834 | 0.268879 | 0.322799 | 0.189629 |
| Best value | 0.314345 | 0.247159 | 0.312752 | 0.178574 |
| Worst value | 0.455513 | 0.394208 | 0.432666 | 0.273989 |
| Standard deviation | 0.003638 | 0.004907 | 0.003406 | 0.004418 |

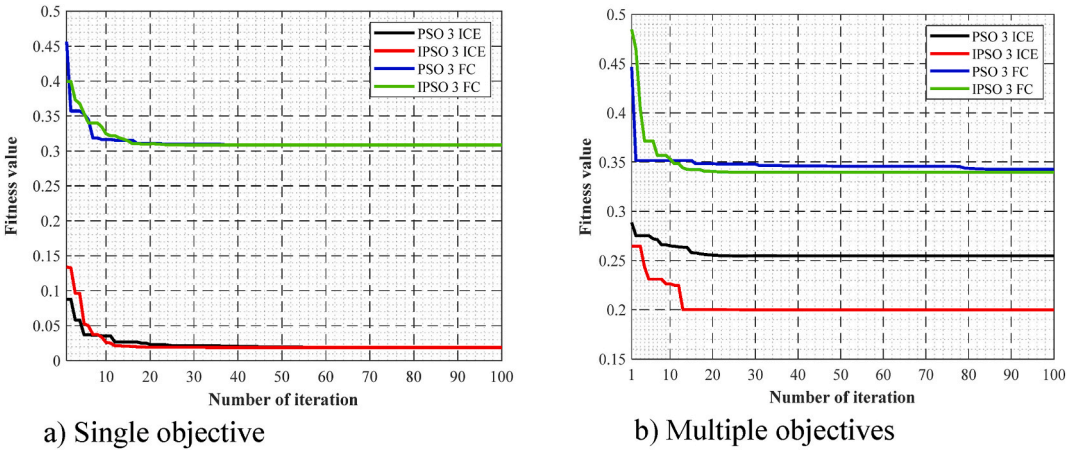


**Fig. 7.** Convergence characteristic of IPSO and PSO for single and multiple objectives.

**Table 31**
Percentage deviation from average for both methods for single objective.

| Deviations from average | PSO | | IPSO | |
|---|---|---|---|---|
| | FC | ICE | FC | ICE |
| A % | 6.8732 | 66.2136 | 5.3291 | 64.4521 |
| B % | 35.7729 | 385.7999 | 32.8999 | 375.2453 |

**Table 32**
Percentage deviation from average for both methods for multiple objective.

| Deviations from average | PSO | | IPSO | |
|---|---|---|---|---|
| | FC | ICE | FC | ICE |
| A % | 4.9840 | 8.0779 | 3.1125 | 5.8298 |
| B % | 37.6863 | 46.6117 | 34.0357 | 44.4869 |

impact of the CHP-DG integration are also carried out. The CHP-DG is modelled in two operation modes (i.e., power only and CHP) for economic assessment. The applicability and effectiveness of the proposed method have been tested on a well-known IEEE 69 bus benchmark distribution network. The outcomes of the proposed IPSO are compared with the standard PSO, other improved PSO as well as recent state-of-the art optimisation approaches found in literature for only constant load model. Main observations from the obtained results of this paper are enumerated below.

- The proposed method is able to find optimal size, location and power factor of CHP-DG while improving the network performance parameters. It is found that ICE based CHP modelled to operate at optimal power factor returns better network performance than unity power factor CHP-DG such as FC in all cases and scenarios considered. To be specific, for constant load model, ICE-based CHP reduces the active power loss to 4.2667 kW (98.10 % loss reduction) and 4.4285 kW (98.03 % loss reduction) for single and multi-objective optimisation respectively in comparison with 69.4100 kW (69.15 % loss reduction) and 73.7928 kW (67.20 % reduction) for FC-based CHP-DG, respectively. Similar improved results are obtained for mixed seasonal voltage-dependent load models.
- It is deduced that yearly load growth causes an increase in the size of the DG but not on the locations. This is quite reasonable as it may be practically and economically unwise to move DGs from one location to another as a result of load growth.
- The use of seasonal mixed load models including daytime and night-time of the season has revealed that lower DG capacities are needed in the night-time compared to the daytime hence, allowing the DISCO to disengage some DG units in the night-time thereby reducing the cost of fuel and ensuring optimal economic dispatch of the DGs. This will also give room for maintaining any ailing equipment and ensure year round operation of the system.
- One of the greatest advantages of integrating CHP-DG is that the need for feeder upgrade or substation expansion due to load growth is mitigated. It also reduces power flow in the feeder which subsequently lessens the stress on the feeder as well as the power loss in the network, which may contribute to elongating the lifespan of the feeder. The less dependence on the grid due to integration of the DG reduces the cost of power purchase as well as environmental cost incurred due to power purchase from the grid. An aggregate of all of these brings about a significant reduction in the total cost, and therefore a substantial increase in the total profit over the planning period for the DISCO.
- When operating the DGs (ICE and FC) in CHP mode, FC returns NPV profit of 29.29 million $ and LCOE of 0.0493 $/kWh while ICE based CHP achieves NPV profit of 28.40 million $ and LCOE of 0.0501 $/kWh. This shows that FC is more economically viable than ICE based DGs when operated in CHP mode. The reason could be due to the higher electrical efficiency and HPR of FC than ICE. However, in power-only mode, ICE gives a profit of 21.57 million $ and LCOE of 0.0786 $/kWh while FC-based DG achieves a profit of 17.36 million $ and LCOE of 0.0918 $/kWh over the planning horizon. This makes ICE-based DG to be more economically viable than FC when operating in power only mode.
- In comparison to base case, operating ICE-DG in power only mode could achieve a profit margin of 49.28 % while FC-based DGs achieves 36.98 % profit margin.
- For the environmental assessment, FC-CHP is more environmentally friendly than ICE since the FC is a non-combustion-based equipment in which the main emission during its operation is water vapour which has no health or harmful effect on humans and the environment. Also, ICE is able to reduce emission by 99.860%–99.866 % over the planning period in comparison to base case scenario.
- The proposed IPSO algorithm outperforms the original PSO in terms of quality solution, convergence capability and statistical outputs in all the studied cases.
- Based on comparison with some recent works, the proposed IPSO is perceived to produce better outcomes in most of the studied cases.

### *11.1. Future work*

Since the DER used in the present work is CHP and only power distribution network is considered, the future work will consider both power and heat distribution networks in the optimal planning of the system. Moreover, the impact of network reconfiguration as well as the addition (combination) of capacitor bank (CB) with FC based CHP-DG will be investigated. Also, methodology to get Pareto-optimal solutions for the multi-objective allocation of FC and ICE under mixed seasonal voltage dependent load models can be further researched. Finally, future work exercises will consider private investors and the society in the EDSEP as each of them has different objectives. Larger networks such as IEEE 85 bus and IEEE 118 bus networks are also to be applied for future work. This study has direct and indirect advantages to both the electricity utility such as ESKOM (local electricity producer in South Africa), the community and the Department of Energy and other stakeholders in the energy and environment sectors. The practicality of this study could shift the attention of the utilities using waste as a renewable source of power and also will assist in allocating the right capacity of FC and ICE-based DGs during different seasonal periods for economic dispatch of the DGs.

## Data availability statement

Data will be made available on request.

## CRediT authorship contribution statement

**Moshood Akanni Alao:** Writing – original draft, Methodology, Conceptualization. **Olawale Mohammed Popoola:** Validation, Supervision.

## Declaration of competing interest

The authors declare that they have no known competing financial interests or personal relationships that could have appeared to influence the work reported in this paper.

## Acknowledgement

This work is based on the research supported wholly/in part by the National Research Foundation of South Africa (Grant Numbers: 150574 & 145900); and Tshwane University of Technology - Faculty of Engineering and Built Environment and Centre for Energy and Electric Power.

## References

[1] F. Borousan, M.A. Hamidan, Distributed power generation planning for distribution network using chimp optimization algorithm in order to reliability improvement, Elec. Power Syst. Res. 217 (2023) 109109.
[2] A. Bayat, A. Bagheri, Optimal active and reactive power allocation in distribution networks using a novel heuristic approach, Appl. Energy 233 (2019) 71–85.
[3] T.E. Gümüs, S. Emiroglu, M.A. Yalcin, Optimal DG allocation and sizing in distribution systems with Thevenin based impedance stability index, Electrical Power and Energy Systems (2023) 144.
[4] C.H. Prasad, K. Subbaramaiah, P. Sujatha, Optimal DG unit placement in distribution networks by multi-objective whale optimization algorithm & its techno-economic analysis Electric Power Systems Research 214 (2023) 108869.
[5] A. Rathore, N.P. Patidar, Optimal sizing and allocation of renewable based distribution generationwith gravity energy storage considering stochastic nature using particle swarm optimization in radial distribution network, J. Energy Storage 35 (2021).
[6] B. Arandian, M.M. Ardehali, Effects of environmental emissions on optimal combination and allocation of renewable and non-renewable CHP technologies in heat and electricity distribution networks based on improved particle swarm optimization algorithm, Energy 140 (2017) 466–480.
[7] R. Ebrahimi, M. Ehsan, H. Nouri, A profit-centric strategy for distributed generation planning considering time varying voltage dependent load demand, Electrcal Power and Energy Systems 44 (2013) 168–178.
[8] S.A. Salimon, et al., Comparative assessment of techno-economic and environmental benefits in optimal allocation of distributed generators in distribution networks, Scientific African 19 (2023).
[9] V.V.S.N. Murty, A. Kumar, Optimal placement of DG in radial distribution systems based on new voltage stability index under load growth, Electrical Power and Energy Systems 69 (2015) 246–256.
[10] N. Khalesi, N. Rezaei, M.R. Haghifam, DG allocation with application of dynamic programming for loss reduction and reliability improvement, Electrical Power and Energy Systems 33 (2011) 288–295.
[11] H. HassanzadehFarda, A. Jalilian, Optimal sizing and location of renewable energy based DG units in distribution systems considering load growth, Electrical Power and Energy Systems 101 (2018) 356–370.
[12] H.M. Bakr, et al., Optimal allocation of distributed generation considering protection, Energies 13 (2402) (2020) 1–18.
[13] B. Jeddi, et al., Robust optimization framework for dynamic distributed energy resources planning in distribution networks, Electrical Power and Energy Systems 110 (2019) 419–433.
[14] S.F. Santos, et al., Novel multi-stage stochastic DG investment planning with recourse, IEEE Trans. Sustain. Energy 8 (1) (2017) 164–178.
[15] N. Acharya, P. Mahat, N. Mithulananthan, An analytical approach for DG allocation in primary distribution network, Int. J. Electr. Power Energy Syst. 28 (10) (2006) 669–678.
[16] R. Viral, D.K. Khatod, An analytical approach for sizing and siting of DGs in balanced radial distribution networks for loss minimisation, Electrcal Power and Energy Systems 67 (2015) 191–201.
[17] S. Boljevic, M.F. Conlon, Optimal sising of combined heat & power (CHP) generation in urban distribution network (UDN), in: 46th International Universities Power Engineering Conference (UPEC), IEEE, Soest Germany, 2011.
[18] S. Yadegari, H. Abdi, S. Nikkhah, Risk-averse multi-objective optimal combined heat and power planning considering voltage security constraints, Energy 212 (2020) 1–13.
[19] M.H.A. Pesaran, et al., A hybrid genetic particle swarm optimization for distributed generation allocation in power distribution networks, Energy (2020) 209.
[20] A. Ali, M.U. Keerio, J.A. Laghari, Optimal site and size of distributed generation allocation in radial distribution network using multi-objective optimization, Journal of Modern Power Systems and Clean Energy 9 (2) (2021) 404–415.
[21] R. Sellami, F. Sher, R. Neji, An improved MOPSO algorithm for optimal sizing & placement of distributed generation: a case study of the Tunisian offshore distribution network (ASHTART), Energy Rep. 8 (2022) 6960–6975.
[22] A. Selim, et al., Optimal placement of DGs in distribution system using an improved Harris hawks optimizer based on single- and multi-objective approaches, IEEE Access 8 (2020) 52815–52829.
[23] M.A. Mejia, et al., Medium-term planning of active distribution systems considering voltage-dependent loads, network reconfiguration, and CO2 emissions Electrcal Power and Energy Systems 135 (2022) 107541.
[24] M. Kumar, P. Nallagownden, I. Elamvazuthi, Optimal placement and sizing of distributed generators for voltage-dependent load model in radial distribution system, Renewable Energy Focus 19–20 (2017) 23–37.
[25] A. Ahmed, et al., An improved hybrid approach for the simultaneous allocation of distributed generators and time varying loads in distribution systems, Energy Rep. 9 (2023) 1549–1560.
[26] A. Ahmed, et al., A novel framework to determine the impact of time varying load models on wind DG planning, IEEE Access 9 (2021) 11342–11357.
[27] K.D. Mistry, R. Roy, Enhancement of loading capacity of distribution system through distributed generator placement considering techno-economic benefits with load growth, Electrical Power and Energy Systems 54 (2014) 505–515.
[28] M. Kia, et al., Short-term operation of microgrids with thermal and electrical loads under different uncertainties using information gap decision theory, Energy (2020) 208.
[29] H. Latifi, et al., Optimal sizing of combined heat and power generation units using of MPSO in the Besat Industrial Zone, International Journal of Energy and Statistics 4 (2016).
[30] A. Gimelli, et al., Optimal configuration of modular cogeneration plants integrated by a battery energy storage system providing peak shaving service, Appl. Energy 242 (2019) 974–993.

[31] O. Mahian, et al., Optimal sizing and performance assessment of a hybrid combined heat and power system with energy storage for residential buildings, Energy Convers. Manag. 211 (2020).
[32] M.A. Meybodi, M. Behnia, Impact of carbon tax on internal combustion engine size selection in a medium scale CHP system, Appl. Energy 88 (2011).
[33] Z. Beihong, L. Weiding, An optimal sizing method for cogeneration plants, Energy Build. 38 (2006) 189–195.
[34] P. Benalcazar, Optimal sizing of thermal energy storage systems for CHP plants considering specific investment costs: a case study, Energy 24 (2021).
[35] S. Azad, M.M. Amiri, M.T. Ameli, Optimal placement of combined heat and power (CHP) systems considering the cost of environmental pollutants, in: V. Vahidinasab, B. Mohammadi-Ivatloo (Eds.), Whole Energy Systems . Power Systems, Springer, Cham, 2022, pp. 153–168.
[36] S.M. Hosseini, et al., Stochastic placement and sizing of combined heat and power systems considering cost/benefit analysis, Res. J. Appl. Sci. Eng. Technol. 5 (2) (2013) 498–506.
[37] M. Addisu, A.O. Salau, H. Takele, Fuzzy logic based optimal placement of voltage regulators and capacitors for distribution systems efficiency improvement, Heliyon 7 (2021) 12345.
[38] S. Pazouki, et al., Optimal place, size, and operation of combined heat and power in multi carrier energy networks considering network reliability, power loss, and voltage profile, IET Gener., Transm. Distrib. 10 (7) (2016) 1615–1621.
[39] A. Hussain, et al., Optimal siting and sizing of tri-generation equipment for developing an autonomous community microgrid considering uncertainties, Sustain. Cities Soc. 32 (2017) 318–330.
[40] T. Niknam, M. Bornapour, A. Gheisari, Combined heat, power and hydrogen production optimal planning of fuel cell power plants in distribution networks, Energy Convers. Manag. 66 (11–25) (2013).
[41] P. Sedaghatmanesh, M. Taghipour, Reduction of losses and capacity release of distribution system by distributed production systems of combined heat and power by graph methods, Am. J. Electr. Power Energy Syst. 4 (6) (2015) 84–99.
[42] A. Naderipour, et al., Optimal allocation for combined heat and power system with respect to maximum allowable capacity for reduced losses and improved voltage profile and reliability of microgrids considering loading condition, Energy 196 (2020).
[43] P. Ahmadi, H. Rastegar, CHP systems optimal allocation in the interconnected heatand electricity distribution network based on minimizing electrical and heat transfer losses, IET Gener. Transm. Distrib. 16 (2022) 2701–2715.
[44] A.O. Salau, Y. Gebru, D. Bitew, Optimal network reconfiguration for power loss minimization and voltage profile enhancement in distribution systems, Heliyon 6 (2020) 12345.
[45] Y. Chen, et al., Multi-objective sequential CHP placement based on flexible demand in heat and electricity integrated energy system, IOP Conf. Ser. Mater. Sci. Eng. 486 (2019) 1–10.
[46] M.T. Mouwafi, R.A. El-Sehiemy, A.A.A. El-Ela, A two-stage method for optimal placement of distributed generation units and capacitors in distribution systems, Appl. Energy (2022) 307.
[47] A.F. Raj, G.A. Saravanan, An optimization approach for optimal location & size of DSTATCOM and DG, Appl. Energy 336 (2023).
[48] P.D. Huy, et al., Optimal placement, sizing and power factor of distributed generation: a comprehensive study spanning from the planning stage to the operation stage, Energy (2020) 195.
[49] T.P. Nguyen, et al., A comprehensive analysis for multi-objective distributed generations and capacitor banks placement in radial distribution networks using hybrid neural network algorithm, Knowl. Base Syst. (2021) 231.
[50] S. Boljevic, M.F. Conlon, Optimal sizing of combined heat & power (CHP) generation in urban distribution network (UDN), in: 2011 46th International Universities' Power Engineering Conference (UPEC), VDE, Soest, Germany, 2011, pp. 1–6.
[51] Injeti, S. K, N.P. Kumar, A novel approach to identify optimal access point and capacity of multiple DGs in a small, medium and large scale radial distribution systems, Int. J. Electr. Power Energy Syst. 45 (1) (2013) 142–151.
[52] N.M. Isa, C.W. Tan, A.H.M. Yatim, A comprehensive review of cogeneration system in a microgrid: a perspective from architecture and operating system, Renew. Sustain. Energy Rev. 81 (2018) 2236–2263.
[53] M.A. Alao, O.M. Popoola, T.R. Ayodele, Sustainable prime movers selection for biogas-based combined heat and power for a community microgrid: a hybrid fuzzy multi criteria decision-making approach with consolidated ranking strategies, Energy Convers. Manag. X (2022) 16.
[54] T.R. Ayodele, et al., Electricity generation prospective of hydrogen derived from biogas using food waste in south-western Nigeria, Biomass Bioenergy 127 (2019).
[55] M.A. Alao, O.M. Popoola, T.R. Ayodele, Biogas-to-hydrogen for fuel cell distributed generation using food wastes of the Cities of Johannesburg and Cape Town, South Africa, in: 2022 IEEE PES/IAS PowerAfrica, IEEE, Kigali, Rwanda, 2022, pp. 1–5.
[56] G. Saur, A. Milbrandt, Renewable Hydrogen Potential from Biogas in the United States, National Renewable Energy Laboratory, USA, 2014.
[57] M.A. Alao, O.M. Popoola, T.R. Ayodele, Projecting the energetic potential and economic viability of renewable power generation from municipal solid waste: indication from South African Provinces, Energy for Sustainable Development 71 (2022) 352–367.
[58] L.B. Braga, et al., Hydrogen production by biogas steam reforming: a technical, economic and ecological analysis, Renew. Sustain. Energy Rev. 28 (2013) 166–173.
[59] T.R. Ayodele, J.L. Munda, Potential and economic viability of green hydrogen production by water electrolysis using wind energy resources in South Africa, Int. J. Hydrogen Energy 44 (2019) 17669–17687.
[60] R. Folkson, Alternative fuels and advanced vehicle technologies for improved environmental performance, in: Hydrogen as an Energy Vector for Transportation Vehicles, second ed., Elsevier, 2022.
[61] P. Muthukumar, et al., Review on large-scale hydrogen storage systems for better sustainability, Int. J. Hydrogen Energy 48 (2023) 33223–33259.
[62] A.M. Elberry, et al., Large-scale compressed hydrogen storage as part of renewable electricity storage systems, Int. J. Hydrogen Energy 46 (2021) 15671–15690.
[63] I. Dincer, C. Acar, Review and evaluation of hydrogen production methods for better sustainability, Int. J. Hydrogen Energy 40 (2015) 11094–11111.
[64] T.R. Ayodele, A.S.O. Ogunjuyigbe, N.O. Oyelowo, Hybridisation of battery/flywheel energy storage system to improve ageing of lead-acid batteries in PV-powered applications, Int. J. Sustain. Eng. 13 (5) (2020) 337–359.
[65] A.S.O. Ogunjuyigbe, T.R. Ayodele, M.A. Alao, Electricity generation from municipal solid waste in some selected cities of Nigeria: an assessment of feasibility, potential and technologies, Renew. Sustain. Energy Rev. 80 (2017) 149–162.
[66] A. Zeinalzadeh, Y. Mohammadi, M.H. Moradi, Optimal multi objective placement and sizing of multiple DGs and shunt capacitor banks simultaneously considering load uncertainty via MOPSO approach, Electrical Power and Energy Systems 67 (2015) 336–349.
[67] V.A. Evangelopoulos, P.S. Georgilakis, Probabilistic spatial load forecasting for assessing the impact of electric load growth in power distribution networks, Elec. Power Syst. Res. 207 (2022).
[68] M.J. Hadidian-Moghaddam, et al., A multi-objective optimal sizing and siting of distributed generation using ant lion optimization technique, Ain Shams Eng. J. 9 (2018) 2101–2109.
[69] J.S. kumar, et al., Hybrid renewable energy-based distribution system for seasonal load variations, Int. J. Energy Res. 42 (2018) 1066–1087.
[70] J.H. Teng, A direct approach for distribution system power fow solution, IEEE Trans. Power Deliv. 18 (3) (2003) 882–887.
[71] S.S. Parihar, N. Malik, Interval arithmetic power flow analysis of radial distribution system with probabilistic load model and distributed generation, Process Integration and Optimization for Sustainability 6 (2022) 3–15.
[72] A. Eid, Allocation of distributed generations in radial distribution systems using adaptive PSO and modified GSA multi-objective optimizations, Alex. Eng. J. 59 (2020) 4771–4786.
[73] S. Devi, M. Geethanjali, Optimal location and sizing determination of distributed generation and DSTATCOM using particle swarm optimization algorithm, Electrcal Power and Energy Systems 62 (2014) 562–570.
[74] S. Barik, D. Das, A novel Q & PQV bus pair method of biomass DGs placement in distribution networks to maintain the voltage of remotely located buses, Energy (2020) 194.

[75] M. Hashem, et al., Optimal placement and sizing of wind turbine generators and superconducting magnetic energy storages in a distribution system, J. Energy Storage 38 (2021).
[76] P.M. Cuce, S. Riffat, A comprehensive review of heat recovery systems for building applications, Renew. Sustain. Energy Rev. 47 (2015) 665–682.
[77] S. Alishahi, et al., Placement and sizing of combined heat and power systems considering cost/benefit analysis, in: CIRED 2012 Workshop: Integration of Renewables into the Distribution Grid, IET, Lisbon, 2012, pp. 1–4.
[78] M. Casisi, P. Pinamonti, M. Reini, Optimal lay-out and operation of combined heat & power (CHP) distributed generation systems, Energy 34 (2009) 2175–2183.
[79] M. Farshad, Distributed generation planning from the investor's viewpoint considering pool-based electricity markets, Elec. Power Syst. Res. (2020) 187.
[80] A.A.A. El-Ela, R.A. El-Sehiemy, A.S. Abbas, Optimal placement and sizing of distributed generation and capacitor banks in distribution systems using water cycle algorithm, IEEE Syst. J. 12 (2018) 3629–3636.
[81] V. Paolini, et al., Environmental impact of biogas: a short review of current knowledge, Journal of Environmental Science and Health 53 (10) (2018) 899–906.
[82] J. Kennedy, R. Eberhart, Particle swarm optimization, in: IEEE International Conference on Neural Networks, IEEE, 1995.
[83] D. Tian, X. Zhao, Z. Shi, Chaotic particle swarm optimization with sigmoid-based acceleration coefficients for numerical function optimization, Swarm Evol. Comput. (2019) 51.
[84] D. Zhou, et al., Randomization in particle swarm optimization for global search ability, Expert Syst. Appl. 38 (2011) 15356–15364.
[85] A. Alanazi, T.I. Alanazi, Multi-objective framework for optimal placement of distributed generations and switches in reconfigurable distribution networks: an improved particle swarm optimization approach, Sustainability 9034 (15) (2023) 1–25.
[86] I. Fister, et al., A comprehensive review of firefly algorithms, Swarm Evol. Comput. 13 (2013) 34–46.
[87] M. Clerc, J. Kennedy, The particle swarm—explosion, stability, and convergence in a multidimensional complex space, IEEE Trans. Evol. Comput. 6 (1) (2002) 58–73.
[88] N. Hantash, T. Khatib, M. Khammash, An improved particle swarm optimization algorithm for optimal allocation of distributed generation units in radial power systems, Hindawi Applied Computational Intelligence and Soft Computing 2020 (2020) 1–8.
[89] A. Nickabadi, M.M. Ebadzadeh, R. Safabakhsh, A novel particle swarm optimization algorithm with adaptive inertia weight, Appl. Soft Comput. 11 (2011) 3658–3670.
[90] O.O. Ayeleru, F.N. Okonta, F. Ntuli, Cost benefit analysis of a municipal solid waste recycling facility in Soweto, South Africa, Waste Manag. 134 (2021) 263–269.
[91] M.A. Alao, O.M. Popoola, T.R. Ayodele, Selection of waste-to-energy technology for distributed generation using IDOCRIW-Weighted TOPSIS method: a case study of the City of Johannesburg, South Africa, Renew. Energy 178 (2021) 162–183.
[92] S. Oelofse, A. Muswema, F. Ramukhwatho, Household food waste disposal in South Africa: a case study of Johannesburg and Ekurhuleni, South Afr. J. Sci. 114 (2018) 1–6.
[93] M.M. Aman, et al., A new approach for optimum simultaneous multi-DG distributed generation units placement and sizing based on maximization of system loadability using HPSO (hybrd particle swarm optimization) algorithm, Energy 66 (2014) 202–215.
[94] A.J. van der Walt, J.M. Fitchett, Statistical classification of South African seasonal divisions on the basis of daily temperature data, South Afr. J. Sci. 116 (9) (2020) 1–15.
[95] NERSA, Approved Municipal Electricity Tariffs, National Energy Regulator of South Africa: South Africa, 2023, pp. 1–138.
[96] ESKOM, Eskom Retail Tariff Plan for the Restructuring of Eskom Tariffs, ESKOM, South Africa, 2022, pp. 1–118.
[97] A. Selim, et al., Optimal allocation of multiple types of distributed generations in radial distribution systems using a hybrid technique, Sustainability 6644 (13) (2021) 1–31.
[98] S. Kumar, K.K. Mandal, N. Chakraborty, Optimal DG placement by multi-objective opposition based chaotic differential evolution for techno-economic analysis, Applied Soft Computing Journal 78 (2019) 70–83.
[99] S. Kansal, V. Kumar, B. Tyagi, Hybrid approach for optimal placement of multiple DGs of multiple types in distribution networks, Electrical Power and Energy Systems 75 (2016) 226–235.
[100] R. Palanisamy, S.K. Muthusamy, Optimal siting and sizing of multiple distributed generation units in radial distribution system using ant lion optimization algorithm, Journal of Electrical Engineering & Technology 16 (2021) 79–89.
[101] M. Yehia, D. Allam, A.F. Zobaa, A novel hybrid fuzzy-metaheuristic strategy for estimation of optimal size and location of the distributed generators, Energy Rep. 8 (2022) 12408–12425.
[102] J.S. Bhadoriya, A.R. Gupta, A novel transient search optimization for optimal allocation of multiple distributed generator in the radial electrical distribution network, Int. J. Emerg. Elec. Power Syst. 23 (1) (2022) 23–45.
[103] S. Kumar, K.K. Mandal, N. Chakraborty, A novel opposition-based tuned-chaotic differential evolution technique for techno economic analysis by optimal placement of distributed generation, Eng. Optim. (2019) 1–23.
[104] M.I. Akbar, et al., A novel hybrid optimization-based algorithm for the single and multi-objective achievement with optimal DG allocations in distribution network, IEEE Access 10 (2022) 25669–25687.
[105] K. Balu, V. Mukherjee, Optimal siting and sizing of distributed generation in radial distribution system using a novel student psychology-based optimization algorithm, Neural Comput. Appl. (2021) 1–29.
[106] M.A. Elseify, et al., Multi-objective optimal allocation of multiple capacitors and distributed generators considering different load models using Lichtenberg and thermal exchange optimization techniques, Neural Comput. Appl. 35 (2023) 11867–11899.
[107] I.A. Quadri, S. Bhowmick, D. Joshi, A comprehensive technique for optimal allocation of distributed energy resources in radial distribution systems, Appl. Energy 211 (2018) 1245–1260.
[108] M.S. Sultan, et al., Multi-objective optimization-based approach for optimal allocation of distributed generation considering techno-economic and environmental indices, Sustainability 4306 (15) (2023) 1–30.
[109] A.B. Stambouli, E. Traversa, Fuel cells, an alternative to standard sources of energy, Renew. Sustain. Energy Rev. 6 (2002) 297–306.
[110] H. Doagou-Mojarrad, et al., Optimal placement and sizing of DG (distributed generation) units in distribution networks by novel hybrid evolutionary algorithm, Energy 54 (2013) 129–138.